[redacted]

STAT

TECHNICAL REPORT NO. 2

STAT

TO THE

CHEMISTRY DIVISION

OFFICE OF SCIENTIFIC RESEARCH

U. S. AIR FORCE

[redacted]

FUNDAMENTAL ASPECTS OF PHOTOSENSITIZATION. INTERCOMBINATIONS IN MOLECULES

JUNE 15, 1958

[redacted]

STAT

Technical Report No. 2

to the Chemistry Division U. S. Air Force Office of Scientific Research

[redacted] STAT

FUNDAMENTAL ASPECTS OF PHOTOSENSITIZATION. INTERCOMBINATIONS IN MOLECULES

STAT

Technical Report No. 2, to the U. S. Air Force Office of Scientific Research, Air Research and Development Command.

[redacted] June 15, 1958 STAT

FUNDAMENTAL ASPECTS OF PHOTOSENSITIZATION. INTERCOMBINATIONS IN MOLECULES.

[redacted]

Table of Contents

1. Solvent Effects in Merocyanine Spectra, E. G. McRae [redacted] STAT (Spectrochimica Acta).*
2. Intramolecular Twisting Effects in Substituted Benzenes.
   I. Electronic Spectra, Eion G. McRae and Lionel Goodman. (J. Molecular Spectroscopy).*
3. Intramolecular Twisting Effects in Substituted Benzenes.
   II. Ground State Properties. (J. Chemical Physics).*
4. Energy Transfer in Molecular Complexes of Sym-Trinitrobenzene with Polyacenes. I. General Considerations, S. P. McGlynn and J. D. Boggus. (J. American Chemical Society).*

[redacted] STAT

SOLVENT EFFECTS ON MEROCYANINE SPECTRA[1,2]

by E. G. McRae[3]

Department of Chemistry, University of Western Australia, Nedlands, Western Australia, and Department of Chemistry, Florida State University, Tallahassee, Florida.

---

(1) Taken in part from a thesis submitted by E.-G. McRae for the degree of M. Sc. at the University of Western Australia.

(2) Part of the work was carried out under a contract between the U. S. Air Force, Office of Scientific Research, ARDC, and the Florida State University.

(3) Present address: Department of Chemistry, Indiana University, Bloomington, Indiana.

(Abstract)

Solvent effects on the visible absorption spectra of three merocyanine dyes are described. The dyes comprise two (I and II) of exceedingly high polarity, and a third (III) less polar than I and II but still highly polar by ordinary standards.

I.

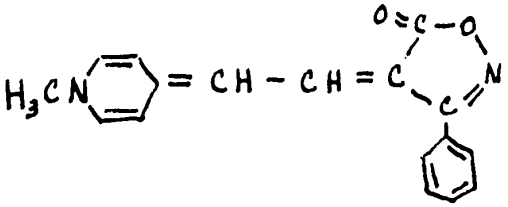

II.

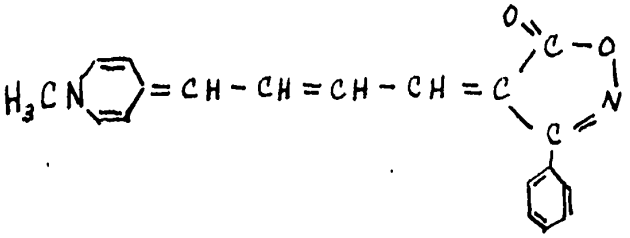

III.

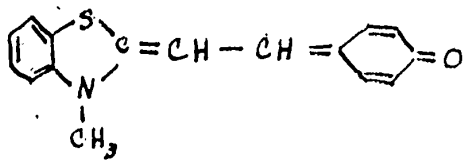

The absorption curves, values of the extinction coefficient and frequency at the absorption maxima (ϵ_{max} and ν_{max} respectively) and oscillator strengths are given for I dissolved in pure solvents, and for dyes II and III in a variety of both pure and mixed solvents. For each dye, ϵ_{max} and ν_{max} undergo pronounced solvent effects, but the oscillator strengths are insensitive to solvent perturbations. The results are discussed in terms of a simple theory in which the combining states are considered as superpositions of a polar and a non-polar resonance structure. A more detailed theory is applied in the interpretation of the frequency shifts induced by non-hydrogen bonding solvents.

I. INTRODUCTION

The visible absorption spectra of highly polar merocyanine dyes undergo extraordinary solvent effects. The phenomena were first reported by Brooker and his collaborators,[4,5] who studied

(4) L.G.S. Brooker, G. H. Keyes, R. H. Sprague, R. H. Van Dyke, E. Van Lare, G. Van Zandt, F. L. White, H.W.J. Cressman and S. G. Dent, J. Am. Chem. Soc., 73, 5332 (1951).

(5) L.G.S. Brooker, G. H. Keyes and D. W. Heseltine, J. Am. Chem. Soc., 73, 5350 (1951).

the spectra of several merocyanines dissolved in pyridine - water mixed solvents. It was found that variation of the percentage water content of the solvent gives rise to pronounced changes of both the maximum extinction coefficients, ϵ_{max}, and the corresponding frequencies, ν_{max}, at the visible absorption maxima.

The main qualitative features of the solvent effects have been described in a recent review by Brooker.[6] For an exceedingly highly polar dye in a pyridine - water or lutidine - water mixed solvent, the progressive addition of water to the solvent leads to a shift of ν_{max} to higher frequencies, with a concomitant diminution of ϵ_{max}. The curve of ϵ_{max} vs. ν_{max} has the shape of the "highly polar" branch of the curve shown in Fig. 1. The arrow indicates the effect of adding water to the solvent. The opposite behavior is exhibited in the case of a dye which is comparatively weakly polar (but which may still be fairly highly polar by ordinary standards). Here, the plot of ϵ_{max} vs. ν_{max} resembles the "weakly polar" branch (Fig. 1). For dyes of intermediate polarity, the initial addition of water to a pure pyridine or lutidine solvent has an effect qualitatively similar to that observed with weakly polar dyes. Upon further progressive addition of water to the solvent, ϵ_{max} and ν_{max} pass through extreme values, and the subsequent differential solvent effect is qualitatively similar to that observed with exceedingly highly polar dyes.

For convenience in a subsequent discussion, we shall refer to points on the ϵ_{max} vs. ν_{max} plot as "solvent representative points" for the dye in question. The point on the plot at which ϵ_{max} attains its maximum value will be called the "reversal point", and will be thought of as the junction of the two branches.[7]

---

(6) L. G. S. Brooker, Experientia Supplementum II (XIV the International Congress of Pure and Applied Chemistry), 229 (1955).

(7) Fig. 1 is slightly idealized in that the minimum of ν_{max} is shown to coincide with the reversal point. Actually, the two extremes do not exactly coincide, although in most but not all cases they lie quite close together.

With this nomenclature, the above description of merocyanine solvent effects may be summarized as follows: for exceedingly highly polar dyes, the representative points for pyridine - water or lutidine - water solvents lie on the highly polar branch, for relatively weakly polar dyes they lie on the weakly polar branch, and for dyes of intermediate polarity they straddle the reversal point.

The work reviewed by Brooker[6] is extensive in that it encompasses the spectra of dyes covering a wide range of polarity. However, the published data pertain only to the absorption maxima, and the solvents used were limited largely to pyridine - water and lutidine - water mixtures. In this paper, we give a more detailed description of solvent effects on the visible absorption spectra of three of the merocyanines previously studied by Brooker et al.[4,5] Of the three dyes, I and II, which have the same pair of end-groups, are exceedingly highly polar, while III has intermediate polarity.[8] The absorption curves of II

(8) I and II are labeled XII (n = 1 and n = 2 respectively) in ref. 4, and III is labeled V in ref. 5.

in pure solvents have been given by Bayliss and McRae, in a preliminary report on the present work.[9]

(9) N. S. Bayliss and E. G. McRae, J. Am. Chem. Soc., 74, 5803 (1952).

I 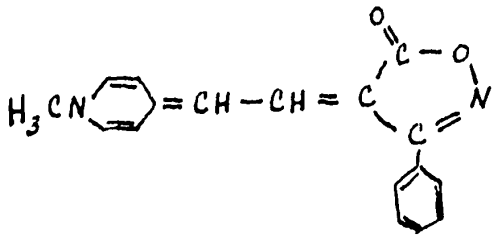

II 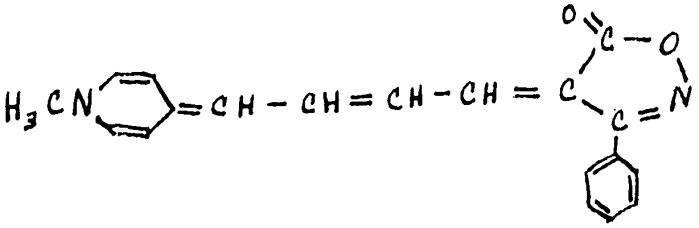

III 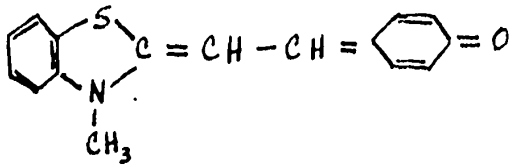

Taken together with the data previously published by Brooker et al,[4,5] our results provide an overall picture of solvent effects on merocyanine band frequencies, intensities (oscillator strengths) and band shapes. This information is thought to be of particular interest in view of several recent discussions of the origins of solvent effects on merocyanine spectra.[6,9,10-12]

---

(10) W. T. Simpson, J. Am. Chem. Soc., 73, 5359 (1951).

(11) J. R. Platt, J. Chem. Phys., 25, 80 (1956).

(12) E. G. McRae, J. Phys. Chem., 61, 562 (1957).

II. EXPERIMENTAL.

Solvents: - Most of the solvents used in this work have been described in a previous paper,[13] and the remaining solvents are described below. Except where other references are given, the physical constants in parentheses are those quoted by Timmermans.[14]

(13) N. S. Bayliss and E. G. McRae, J. Phys. Chem., 58, 1006 (1954).

(14) J. Timmermans, "Physico-chemical Constants of Pure Organic Compounds", Elsevier Publishing Co., Amsterdam, 1950.

Aniline of a technical grade was dissolved in hydrochloric acid, and the main impurity, nitrobenzene, was removed by steam distillation. The aniline hydrochloride was neutralized, and steam distilled. The distillate was dried with potassium hydroxide, and fractionated twice under reduced pressure. It was stored in the dark over potassium hydroxide pellets, and fractionated again immediately before use. B. P. 94°C/35mm. $(94/35)^{15}$; n_D^{20} 1.5860 (1.5863).

(15) Landolt-Bornstein, "Physikalisch-Chemische Tabellan", 5th Ed., Eg. III C, Springer, Berlin, 1935, p. 2462.

Dioxane of British Drug Houses Technical grade was refluxed for ten hours with 1/10 its volume of 0.1N hydrochloric acid. It was then allowed to stand for one day over sodium hydroxide sticks, and fractionated. It was kept in the dark and used within one week of purification. B. P. 101.6°C (101.4); n_D^{20} 1.4215 (1.4214).

Formamide was prepared from ethyl formate by the method of Slobodin et al,[16] and the product was fractionated under reduced pressure. The formamide was again fractionated immediately before use. B. P. 116°C/39.2 mm.; n_D^{20} 1.4482 (1.4475).

(16) Ya. M. Slobodin, M. S. Zigel and M. V. Yanishevska, J. Applied Chem. (U.S.S.R.) 16, 280 (1943). See Chem. Abstr. 39, 702 (1945).

Pyridine of a grade conforming to British Drug Houses Analar standards (Judex analytical reagent) was allowed to stand for one week over sodium hydroxide sticks, refluxed for ten hours over freshly burned calcium oxide, and fractionated. B. P. 115.2°C (115.4); $n_D^{18.7}$ 1.5106 (1.5106).

Buffer solutions: For the pH range 5.0 - 8.0, McIlvaine's standard buffer solutions[17] were prepared, using Analar grade reagents. The solvent of pH 9 was a 0.05 molar solution of Analar grade borax.

(17) "Handbook of Chemistry and Physics", 24th Ed., Chemical Rubber Publishing Co., 1940, p. 1374.

Merocyanine Dyes: Pure merocyanine dye samples were supplied by Dr. L. G. S. Brooker.

Solutions: In so far as permitted by the dye solubilities, the dye solutions were prepared to give a minimum transmission reading between 20 and 70%. This corresponds to a dye concentration in the vicinity of 5×10^{-6} M. Where practicable, solutions of known dye concentration were prepared. Weighed 1 mg. dye samples were dissolved, and the resulting solutions diluted either by volume or by weight. The latter method was

used for most of the solutions in mixed solvents. Volume dilutions were carried out with a standardized 5 ml. pipette and standardized 25 ml. flasks. Where weight dilution was employed, the dye molarity was calculated with the aid of the tabulated densities of the mixed solvents in question.[18]

(18) Landolt-Bornstein, "Physikalisch-Chemische Tabellen", 5th ed., Springer, Berlin, 1935.

Spectra: Except in the tests of Beer's law (see below), all spectra were measured with a Beckman spectrophotometer, model DU, using matched 1 cm. Corex cells.

Frequencies, ν (cm^{-1}), were obtained from the wavelength settings, no vacuum corrections being applied. The molar extinction coefficients, ϵ, were calculated according to the formula:

$$\epsilon = (1/cd) \log_{10} (100/T),$$

where c denotes the molarity, d the path length in cm., and T the percentage transmission reading. Oscillator strengths, f, were calculated from the absorption curves according to the formula[19]

(19) R. S. Mulliken and C. A. Rieke, Rep. Prog. Physics 8, 231 (1941).

$$f = 4.32 \times 10^{-9} \int \epsilon \, d\nu$$

Errors: The errors in the determination of ν_{max} ranged from 20 to 50 cm^{-1}, depending on the band width.

The errors in the measurement of absolute extinction coefficients, which were essentially concentration errors, did

not exceed 5%. In several cases it was not possible to measure extinction coefficients, because of sparing dye solubility. In these cases, ϵ_{max} was estimated by adjusting the area under the absorption curve to correspond to the oscillator strength of the dye dissolved in water. The justification of the procedure rests on a particular result of the present work, namely that the oscillator strengths are rather insensitive to solvent perturbations. The percentage error of ϵ_{max} determined in this way is considered not greater than the total percentage variation of oscillator strength, viz. 20% (Sec. III).

In merocyanine spectra, the visible absorption band is not overlapped appreciably by bands at higher frequencies; consequently the same errors in the oscillator strengths were only slightly greater than those in the extinction coefficients.

In a few cases, which are noted individually in the next section, the errors were probably greater than indicated above.

In the cases in which a comparison is possible, our results agreed with those of Brooker et al,[4,5] within the limits of error quoted above.

Tests of Beer's Law: Beer's law tests were carried out using a Beckman spectrophotometer, model DK, with 0.1, 2.0 and 10.00 cm. cells. The spectra of dyes I and III were measured in the concentration range 3×10^{-7} to 3×10^{-5} M. Most of the measurements were carried out at concentrations near the middle of this range ($\sim 5 \times 10^{-6}$ M). The solvents in each case were pyridine - water mixtures. The solvent for dye I contained 90 mole % pyridine, and that for dye III, 80 mole % pyridine. In

both cases, Beer's law was obeyed well within the dilution error, and there was no detectable change of band shape throughout the hundred-fold range of concentration.

III. RESULTS.

The solvents used in this research are listed in Table 1, together with their designations in the figures, their relevant physical properties, and the values of some derived properties thought to be of importance in the interpretation of the solvent effects (Sec. IV).

Dyes I and II: The results obtained with dyes I and II dissolved in pure solvents (Table 2, Figs. 2,3) are qualitatively similar, the solvent effects being somewhat less pronounced in the case of I. In the case of dye II, the results include the effects of mixed as well as pure solvents (Table 3, Fig. 4).

The absorption bands of dyes I and II in 0.26N hydrochloric acid lie at higher frequencies than the corresponding curves for water solvent. The absorption curves obtained at lower acid concentration passed through a well-defined isosbestic point, indicating that the higher-frequency absorption is due to the protonated dye in each case.

Frequencies: The pure solvents induce increasing shifts to higher frequencies in the order: dioxane, chloroform, nitrobenzene, pyridine, acetone, aniline, ethanol, formamide, water. As has been pointed out previously,[9] there is a sharp distinction between the effects of the hydrogen bonding solvents (last four

members of the above sequence) and the non-hydrogen bonding solvents (first five members).[20]

(20 It is not clear whether or not chloroform should be classified as a hydrogen bonding solvent. Presumably it can form hydrogen bonds with the dyes, yet its solvent effect is intermediate between those of dioxane and pyridine. A similar result appeared in the writer's analysis of solvent effects on the spectrum of phenol blue;[12] there, it was found that the frequency shift produced by chloroform was close to that predicted for a non-hydrogen bonding solvent having the same macroscopic properties. In this paper, chloroform will be considered provisionally as a non-hydrogen bonding solvent.

In each case, the absorption of the protonated dye lies at a higher frequency than that of the dye itself dissolved in water.

Intensities: The band intensities do not undergo pronounced solvent effects, nor do they show any progressive variation with the band frequency. Yet, for each dye, some of the observed oscillator strengths differ significantly from the mean observed oscillator strength. For example, acetone, and to a smaller extent, pyridine, appear to cause a relative intensification. It is noteworthy that the intensity of absorption of the protonated dye is nearly the same as that of the dye itself dissolved in water.

Band Shapes: The absorption curves for dyes I and II in dioxane each display a definite shoulder on the high-frequency side. In the case of dye II, further structure may be discerned at still higher frequencies. With dye II, the vibrational structure is developed even more strongly in benzene-rich benzene-acetone and benzene-pyridine mixed solvents, a second

peak appearing in each case. The separation of the peaks is 1030 ± 100 cm^{-1}.[21]

(21) The absorption curves obtained with benzene-rich mixed solvents changed slowly with time, probably because of the dye crystallizing out. They are less accurate than the other curves, but the frequencies were reproducible within the quoted limits of error.

The structureless absorption curves become progressively broader with increasing shift to higher frequencies. On plotting the corresponding solvent representative points for dye II, it is found that within the limits of error in the determination of ϵ_{max}, they all lie close to a curve corresponding to the highly polar branch. (Fig. 5. The values of ϵ_{max} for dioxane-water solvents were determined on the assumption of a constant oscillator strength. The actual values may be as much as 20% higher). It is interesting that the point for the protonated dye lies near the extrapolated curve. The representative points corresponding to the absorption curves with structure lie close to a curve corresponding to the weakly polar branch, between the reversal point and the minimum of ν_{max}.

Dye III: At first sight the absorption curves for dye III in pure solvents (Table 2, Fig. 6) appear to bear no relation to those obtained with dyes I and II. However, the results are readily rationalized with reference to the absorption curves obtained with mixed solvents (Table 4, Fig. 7), and the ϵ_{max} vs. ν_{max} plot showing points for both pure and mixed solvents (Fig. 8). Again, the solvent representative points all lie close to a curve having the general shape of that shown in Fig. 1.

The visible absorption of dye III in water is the superposition of the absorption of the dye itself and a higher-frequency absorption attributed to the protonated dye. The absorption curves for the separate components (Fig. 6) were obtained in buffer solutions of pH 9 and pH 6 respectively. At intermediate pH, the composite absorption curves were found to pass through a definite isosbestic point. A similar result was obtained with the solvent ethanol, in which the composite absorption curve varied slowly with time. By observing the absorption over a period of a few hours, it was resolved into the two curves shown in Fig. 6, the higher-frequency absorption being attributed to the protonated dye. The curves obtained with ethanol solvent are somewhat less accurate than the other curves shown in Fig. 6. The absorption observed with the solvent formamide is thought to be due to the protonated dye.

Frequencies: Of the pure solvents, ethanol has a representative point closest to the reversal point. The representative point for water definitely lies on the highly polar branch of the ϵ_{max} vs. ν_{max} curve, while the points for the non-hydrogen bonding solvents all appear to belong to the weakly polar branch. However, on the weakly polar branch the solvent order of increasing shift to higher frequencies is not the reverse of that observed with dyes I and II, as would be expected if there were a perfectly regular relationship between ϵ_{max} and ν_{max}.

The consideration of band frequencies alone affords no definite distinction between the effects of hydrogen bonding

and non-hydrogen bonding solvents. Perhaps the most concise description of the effect of hydrogen bonding, in terms of experimentally observed quantities, is that it causes a displacement of the solvent representative point in the arrow direction along the ϵ_{max} vs. ν_{max} curve (Fig. 1). This does not necessarily imply a large frequency shift.

Intensities: Again, the band intensities appear to be rather insensitive to solvent perturbations, although the variation of oscillator strength from solvent to solvent slightly exceeds the experimental error in a few cases.

Band Shapes: The absorption curves correspondong to representative points lying on the weakly polar branch display definite vibrational structure. A high-frequency shoulder or second peak is observed in every case, together with some less pronounced structure at still higher frequencies. As the solvent representative point moves away from the reversal point, the second peak grows up at the expense of the first, actually surpassing it in intensity in the case of a benzene-pyridine solvent.[21] (Throughout, ϵ_{max} and ν_{max} refer to the lower-frequency peak). The separation of the peaks is 1100 $\pm$ 100 cm^{-1} (average of observed separations).

On the high-frequency side of the reversal point, the absorption curves undergo progressive broadening similar to that observed with dyes I and II. The trend extends to the absorption curves of the protonated dye, the corresponding points lying near the extrapolated ϵ_{max} vs. ν_{max} curve (Fig. 8).

Gross Features of the Solvent Effects: Inasmuch as the dyes I-III are typical members of the series of dyes studied by Brooker et al,[4,5] the gross features of the solvent effects reported here are probably common to all merocyanine spectra. They are as follows:

(1) For a given dye, all solvent representative points lie near part of a curve having the general shape shown in Fig. 1. The particular part of the curve traced out by the points for a given series of solvents depends on the dye polarity, as indicated in Sec. I.

(2) The representative points for hydrogen bonding solvents tend to be displaced in the arrow direction along the ϵ max vs. ν max curve (Fig. 1), compared with non-hydrogen bonding solvents.

(3) Band intensities (oscillator strengths) are almost independent of the solvent.

(4) As the solvent representative point moves away from the reversal point on the weakly polar branch, at least one new absorption peak grows up on the high-frequency side, at the expense of the lowest-frequency peak. The peak separation is 1000-1100 cm^{-1}.

IV. DISCUSSION

Frequency Shifts: The gross features of the frequency shifts have been explained by Brooker[6] in terms of the relative solvent stabilization of the extreme polar and the non-polar

resonance structures. (IVa and IVb respectively).

IV

(a) $\overset{+}{N} = (C - C =)_n C - O^-$

(b) $N - (C = C -)_n C = O$

Brooker has identified the reversal point with the isoenergetic point, i.e., the point at which the two structures have the same energy. The situation in which the polar structure is the more stable corresponds to the highly polar branch of the ϵ max vs. ν max curve, and the opposite situation corresponds to the weakly polar branch.

Brooker's interpretation has been elaborated by Simpson,[10] who has taken into account the interactions between many resonance structure functions. However, the results of Simpson's treatment are not in agreement with experiment,[9] and the treatment itself has been adversely criticized on the ground that it is based on an over-simplified representation of the solvent-solute interaction energy.[22] Platt[11] has pointed out the relationship between Brooker's interpretation and an alternative scheme in which the frequency shift is related to the relative magnitudes of the dipole moment of the solute in its ground and excited states.[23]

(22) Y. Ooshika, J. Phys. Soc. Japan, 9, 594 (1954).

(23) Platt has attributed the latter method of interpretation to McConnell[24] and to Bayliss and McRae.[25] Actually, Platt's discussion represents an advance on the earlier work, which was based implicitly on the assumption of a rigid solute dipole.

(24) H. McConnell, J. Chem. Phys., 20, 700 (1952).

(25) N. S. Bayliss and E. G. McRae, J. Phys. Chem., 58, 1002 (1954).

Recently, the writer[12] has given a general treatment of frequency shifts arising from dipole interactions. It was shown that the frequency shift may be expressed in terms of contributions to the environmental electric field at the solute dipole (all molecular dipoles being treated as point dipoles). In the case of a merocyanine dye dissolved in a polar solvent, it was proposed that as far as the relative frequency shifts induced by different solvents are concerned, the most important contribution to the environmental field is the field arising from the oriented permanent dipoles of the solvent molecules. Denoting the latter field by $\underline{R}$, and neglecting all other contributions to the environmental field, the following expression was derived for the frequency shift:

$$\nu - \nu_{ref} = (1/\underline{h}\,\underline{c})\,(\underline{M}_g - \underline{M}_e)\cdot\underline{R} + (3/2\,\underline{h}\,\underline{c})\,(\alpha_g - \alpha_e)\,\underline{R}^2 \qquad (1)$$

Here, ν and ν_{ref} denote the band frequencies for the dye dissolved respectively in the solvent under consideration, and in a non-polar reference solvent. On the right, $\underline{h}$ and $\underline{c}$ have the usual meanings, $\underline{M}_g$ and α_g respectively signify the permanent dipole moment and isotropic polarizability of the isolated solute molecule in its ground electronic state, and $\underline{M}_e$, α_e stand for the corresponding quantities for the excited state. The term involving $\underline{R}^2$ represents the quadratic Stark effect.

It has been shown that, with $\alpha_g > \alpha_e$ and M_e assumed parallel to M_g, Eq. 1 provides a satisfactory interpretation of the gross features of the frequency shifts in merocyanine spectra, including the order of magnitude of the shifts.[12] From a purely qualitative viewpoint, the description is exactly the same as that given previously by Platt.[11] The important new feature of the approach based on (1) is the introduction of the field intensity, R, as a parameter to which the frequency shifts may advantageously be referred.

Probably the most serious errors inherent in (1) are those incurred through the neglect of environmental field contributions other than R. This implies the neglect of dispersive interactions and interactions of the solute permanent dipole-solvent induced dipole type. In most cases apart from merocyanine spectra, these interactions make an important if not dominant contribution to the frequency shift. However, they may be expected to play a relatively small part in the case of merocyanine spectra, because of the high polarity of the merocyanines compared with ordinary molecules. The extent to which this expectation is realized is indicated in the following discussion of the results of the present work; this discussion is based at first on Eq. 1.

Non-hydrogen Bonding Solvents: In the absence of hydrogen bonding, the field intensity may be related to macroscopic properties of the solvent. On the basis of the simplest possible model for the solute in solution (point dipole at the center of a spherical cavity in a homogeneous dielectric medium), together

with certain other simplifying assumptions, there results[12]

$$R = \frac{2\,M_g}{a^3}\left[\frac{D-1}{D+2} - \frac{n_o^2-1}{n_o^2+2}\right], \qquad (2)$$

where a denotes the cavity radium, D the solvent dielectric constant and n_o the refractive index of the solvent at zero frequency. Combining (1) and (2), assuming M_e parallel to M_g in (1) and denoting the expression in brackets (Eq. 2) by $F(D, n_o)$, we obtain:

$$\nu - \nu_{ref} = (2/h\,c\,a^3)\,M_g\,(M_g - M_e)\,F + (6/h\,c\,a^6)M_g^2\,(\alpha_g - \alpha_e)\,F^2 . \qquad (3)$$

According to (3), the band frequencies should vary regularly, though not necessarily linearly, with F.

Figs. 9 and 10 show graphically the relationship between F and the observed band frequencies for dyes II and III dissolved in non-hydrogen bonding solvents. The corresponding plot for dye I is similar to that for dye II. The values of F for the pure solvents are taken from Table 1 (here and elsewhere in this paper, all refractive indices are replaced by n_D for the purpose of numerical calculation). For the benzene-pyridine mixed solvents, the dielectric constants are interpolated from the data of Lange.[26] It is seen that there is a definite though

(26) L. Lange, Z. Physik 33, 169 (1925).

imperfect correlation between the frequency shifts and the corresponding values of F. The points obtained for dye II lie near

a curve having the shape expected from (1) and (2), with $M_g > M_e$ and $\alpha_g > \alpha_e$.

The irregularities in the relationship between band frequency and solvent F may be discussed in terms of the superposed effects of dispersive interactions and of interactions of the dipole-induced dipole type; as noted above, both types of interaction were neglected in the derivation of (1).

Dispersive interactions invariably give rise to a shift to lower frequencies, relative to the vapor frequency (the "general red shift"). The general red shift is expected to be particularly large for strong bands such as appear in the visible spectra of dyes, and the relative magnitudes of the red shifts produced by different solvents are known to depend primarily on the solvent refractive index.[12,22,26,27]

---

(27) The general red shift was called the "polarization red shift" in ref. 25.

Dipole-induced dipole interactions are expected to produce a shift to lower frequencies relative to the vapor frequency if the solute dipole moment of the dissolved dye molecule is greater in the excited state than in the ground state; otherwise, a shift to higher frequencies is expected. For a particular solute, the magnitudes of the shifts induced by different solvents are expected to depend on the solvent refractive index.[12,22,25]

Accepting the above description of the dispersive and dipole-induced dipole effects, we conclude that the dipole-induced dipole shift augments the general red shift in the case

of dye III and opposes it in the case of dye II. Upon reference to Figs. 9 and 10, we find that the most noticeable irregularities occur with dye III in nitrobenzene and acetone. Now these two solvents have respectively the highest and the lowest refractive indices of the series. By virtue of the superposed effects of dispersive and dipole-induced dipole interactions, the two solvents are expected respectively to produce larger and smaller red shifts, compared with a reference solvent of intermediate refractive index, than predicted on the basis of the solvent F alone. The corresponding irregularities in the case of dye II in nitrobenzene and acetone are much less pronounced, as is expected in view of the partial cancellation of the dispersive and dipole-induced dipole shifts. A similar explanation can be advanced for most of the remaining irregularities; however, it is most likely that those irregularities reflect the limitations of the simple theory in which the solvent is treated as a homogeneous dielectric medium.

It is readily shown that the above discussion involves quantities of the correct order of magnitude. The curves superposed on Figs. 9 and 10 represent the behavior predicted by (3), with $\underline{M}_{\underline{g}} = 10$ Debye, $\underline{a} = 4$ Å, and $\alpha_{\underline{g}} - \alpha_{\underline{e}} = 0.4 \times 10^{-23}$ cm^3 for each of the two dyes, $\underline{M}_{\underline{g}} - \underline{M}_{\underline{e}} = 0.05$ Debye for dye II and $\underline{M}_{\underline{g}} - \underline{M}_{\underline{e}} = -1.7$ Debye for dye III. It may be noticed that the curves are drawn on the assumption that the value of $(\alpha_{\underline{g}} - \alpha_{\underline{e}})/\underline{a}^3$ is the same for both dyes; this is to be expected in view of the general similarity of the spectra of the two dyes.

It is noteworthy that the difference between the ground and excited state polarizabilities need not be particularly large to account for the observed trends. The chosen value of the difference is about one-quarter of the contribution of a strong visible transition to the ground state polarizability.

For strong transitions, such as those considered here, the general red shift is given approximately by[12]

$$\Delta \nu \text{ (dispersive)} = -2.14 \times 10^{-14} \frac{L f}{a^3} \frac{n^2 - 1}{2n^2 + 1},$$

where L and n respectively denote the "weighted mean wavelength" and refractive index of the solvent at the band frequency, f denotes the oscillator strength of the transition in question, and a again denotes the cavity radius. The minus sign indicates that the shift is to lower frequencies, relative to the vapor frequency. Adopting $L = 1250$ Å, $a = 4$ Å and $f = 0.8$, we obtain

$$\Delta \nu \text{ (dispersive)} \approx 3300 \frac{n_D^2 - 1}{2n_D + 1} \qquad (4)$$

as a rough estimate (cm^{-1}) of the general red shift. The literal application of the above formula (refractive indices from Table 1) accounts for a little over half the frequency separation of the points on Fig. 10 for dye III in nitrobenzene and acetone.

According to a formula given previously,[12] the dipole-induced dipole shift, relative to the vapor frequency, is

given by

$$\Delta\nu \text{ (dipole-induced dipole)} = \frac{M_g^2 - M_e^2}{hca^3} \quad \frac{n_o^2 - 1}{2n_o^2 + 1} \; .$$

Actually, the above formula does not apply accurately to the merocyanines, because it is based on the assumption of a rigid solute dipole. In a more elaborate discussion, we would have to replace M_g and M_e by appropriate expressions for the dipole moments of the dissolved dye. Bearing that in mind, the above formula suffices to show that if, for the dissolved dye, the ground and excited state dipole moments differ by less than 2 Debye, then the magnitude of the dipole-induced dipole shift is approximately equal to or less than that of the general red shift.

We have shown, first, that the observed frequency shifts display a definite though imperfect correlation with the solvent F, which has been defined with a reference to Eq. 2; second, that the observed behavior conforms approximately to that predicted by (3), with plausible values for the dipole moments and polarizabilities of the dyes; third, that the most noticeable discrepancies which do occur are of the nature and approximate magnitude to be expected from the superposition of dispersive and dipole-induced dipole effects. The evidence leaves little cause to doubt that the frequency shifts are caused primarily by dipole-dipole interactions, with the quadratic Stark effect playing an important or dominant role.

Hydrogen Bonding Solvents: Although the order in which the hydrogen bonding solvents induce shifts to higher frequencies is the same as that of increasing F, it is clear from the magnitudes of the shifts that they correspond, in a formal sense, to values of R much larger than those calculated from (2). It appears that the quadratic Stark effect makes a dominant contribution to the frequency shift.

Even when the quadratic Stark effect has been taken into account, there seems to be no simple explanation of the results in terms of hydrogen bonding. To take an extreme example, in the spectrum of dye II, the solvent water induces a shift of about 4500 cm^{-1} to higher frequencies, referred to acetone. If we allow 500 cm^{-1} for the change of F, there remains 4000 cm^{-1}, or about 12 Kcal/mole, to be accounted for by hydrogen bonding. This appears to be too large a shift to be attributable to the formation of a single hydrogen bond. Again the case of dye II the shift induced by water is about twice as great as that induced by formamide, and about four times as great as that induced by ethanol (all referred to acetone), though the three solvents presumably form hydrogen bonds of about the same strength. On the other hand, the band frequencies for dye II in ethanol and aniline exceed by about the same amount ($\sim$1200 cm^{-1}) those expected on the basis of the solvent F alone.

We suggest that in the case of the solvent water, and possibly formamide, two or more solvent molecules simultaneously form strong hydrogen bonds with one dye molecule to form a complex of structure V. In each of the dyes I-III only one dye

atom can be strongly hydrogen bonded, namely the carbonyl

V. 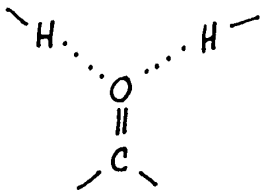

oxygen. The formation of two or more strong hydrogen bonds would therefore be sterically hindered or prohibited in ethanol and aniline solvents.

This possibility has been considered previously for another solute by Professor G. Pimentel in a discussion of solvent spectral shifts.[28]

(28) G. Pimentel, University of California, private communication to M. Kasha.

Intensities: A simple theory of solvent effects on merocyanine band intensities has been proposed by McConnell.[29]

(29) H. McConnell, quoted by Platt.[11]

The theory is based on the assumption that the ground and excited electronic state functions for the strong visible transition may be considered as linear combinations of the electronic state functions appropriate to the isoenergetic point. This assumption differs only formally from that upon which Brooker based his interpretation of the frequency shifts. There results

$$f/f_I = \nu_I/\nu, \qquad (5)$$

where f and ν respectively denote the oscillator strength and frequency of a band, and the subscript refers to the isoenergetic point.

The theory is not supported by the results of the present work. Whereas the frequencies of the bands of known intensity undergo a total variation of 20% and 30% for dyes I and II respectively, the oscillator strengths show no progressive variation with band frequency beyond the experimental error of 5%. With dye III, the band frequencies do not cover a sufficiently large range to permit a valid test of the theory.

Band Shapes: Platt[11] has shown that Brooker's interpretation of the frequency shifts can be extended to explain the concomitant changes of band width. At the isoenergetic point, the equilibrium nuclear configuration of the dye does not change upon excitation, so that only the 0-0 vibronic band appears strongly. As the solvent representative point moves away from the isoenergetic point, the equilibrium length of each bond in the C-C chain suffers a progressively more pronounced change upon excitation. According to the Franck-Condon principle, this should lead to the growing up of higher-frequency vibronic bands at the expense of the 0-0 band, with frequency separations corresponding to the C-C stretching frequency.

The above interpretation is strongly supported by the results of the present work. The absorption curves corresponding to representative points near the reversal point and

on the weakly polar branch show definite vibrational structure, which changes in the predicted manner as the representative point moves away from the reversal point. The separation of the vibronic peaks (1000-1100 cm^{-1}) is in satisfactory agreememt with the C-C stretching frequency. Vibrational structure does not appear in the absorption curves corresponding to points on the highly-polar branch, probably because of the blurring of structure normally associated with strong solvent-solute interaction. Nevertheless, the broadening may be attributed to changes of the relative intensity of the underlying vibronic transitions. It can be seen from the absorption curves that if it were possible to plot ϵ_{max} against the 0-0 frequency rather than against ν_{max}, the highly-polar and weakly-polar branches would be nearly superposed. This tends further to substantiate Platt's interpretation, since the ground and excited-state potential energy curves for C-C stretching are presumably nearly symmetrical near their respective minima.

Acknowledgements: Most of the work described above was carried out under the supervision of Professor N. S. Bayliss, to whom the writer is indebted for encouragement and helpful criticism. The writer is glad to thank Dr. L. G. S. Brooker for the gift of the merocyanine dye samples, and Professors N. S. Bayliss and M. Kasha for reading this paper prior to publication. Financial assistance provided by the University Research Fund (University of Western Australia), including the award of a studentship, is gratefully acknowledged, as is also the award of a Hackett Studentship by the University of Western Australia.

TABLE 1

SOLVENT DESIGNATIONS AND PROPERTIES

Solvent	Designation	$\underline{D}^a$	$\underline{n}_D{}^b$	$\underline{F}(\underline{D},\underline{n}_D)^c$	$\frac{\underline{n}^2_D - 1}{2\underline{n}^2_D + 1}$
Benzene	B	2.3	1.498	0	0.23
Dioxane	D	2.2	1.421	0.03	0.20
Chloroform	CF	5.2	1.446	0.32	0.21
Nitrobenzene	NB	35	1.555	0.60	0.24
Pyridine	P	12.4	1.511	0.49	0.23
Acetone	Ac	21	1.359	0.65	0.18
Aniline	An	7.3	1.586	0.34	0.25
Ethanol	E	28	1.363	0.68	0.18
Formamide	F	109	1.448	0.71	0.21
Water	W	79	1.333	0.76	0.17

(a) Dielectric constant
(b) Refractive index (sodium D line)
(c) $\underline{F}(\underline{D},\underline{n}_D) = (\underline{D} - 1)/(\underline{D} + 2) - (\underline{n}_D{}^2 - 1)/(\underline{n}_D{}^2 + 2)$

TABLE 2

DYES I-III IN PURE SOLVENTS

Solvent	ν_{max} x 10^{-4} (cm^{-1})			ϵ_{max} x 10^{-3}			f		
	I	II	III	I	II	III	I	II	III
Dioxane	1.864	1.559	1.838 1.947[b]	58.0[a]	82.5[a]	53.0[a] 52.6[a,b]	--	--	--
Chloroform	1.883	1.570	1.773 1.888[b]	74.0	103.5	90.4 50.4[b]	0.65	0.74	0.82
Nitrobenzene	1.920	1.629	1.753 1.853[b]	66.5	92.9	89.0 49.7[b]	0.63	0.79	0.80
Pyridine	1.935	1.638	1.768 1.883[b]	80.5	112.8	98.0 58.0[b]	0.70	0.91	0.81
Acetone	1.970	1.681	1.804 1.920[b]	78.0	103.6	76.0 50.5[b]	0.74	0.94	0.74
Aniline	1.986	1.690	---	67.5	79.3	--	0.64	0.82	--
Ethanol	2.071	1.805	1.811 2.333[d]	51.0	50.7	113.0 41.4[d]	0.62	0.85	0.90 0.82[d]
Formamide	2.115	1.890	2.351[d]	46.0	42.5	35.9[d]	0.62	0.82	0.73[d]
Water	2.292 2.615[c]	2.132 2.480[c]	2.028[e] 2.463[f]	37.5 29.0[c]	36.7 26.0[c]	43.3[e] 33.5[f]	0.63 0.62[c]	0.80 0.80[c]	0.74[e] 0.72[f]

(a) Adjusted to conform to an oscillator strength equal to that for the same dye in water.
(b) Refers to a second maximum.
(c) Protonated dye. Solvent: 0.26N HCL.
(d) Protonated dye.
(e) Solvent: buffer solution, pH 9.
(f) Protonated dye. Solvent: buffer solution, pH 6.

TABLE 3

DYE II IN MIXED SOLVENTS

Solvent	Mole%[a]	ν_{max} x 10^{-4} (cm^{-1})	ϵ_{max} x 10^{-3}[b]	f
Dioxane-water	95.0	1.570	90.0	-
	90.0	1.590	85.5	-
	78.4	1.660	62.0	-
	64.2	1.713	59.0	-
	44.6	1.770	49.8	-
	20.0	1.885	43.0	-
	11.7	1.958	40.4	-
Benzene-pyridine	98.1	1.533	76.2	-
		1.636[c]	56.4[c]	
	78.2	1.554	90.7	-
	52.7	1.589	102.0	-
	24.6	1.618	90.0	-
Benzene-acetone	98.3	1.534	75.2	-
		1.631[c]	53.7[c]	
	94.9	1.542	81.4	-
	91.7	1.549	100.0	-
	78.9	1.573	105.2	0.84
	49.3	1.618	117.7	0.93
	37.0	1.632	109.0	0.89
	12.4	1.661	105.0	0.94
Acetone-water	99.0	1.682	106.5	0.96
	95.4	1.695	103.8	0.99
	72.4	1.750	66.4	0.89
	57.9	1.776	63.8	0.91
	35.6	1.870	47.0	0.82
	22.2	1.927	46.0	0.86
	9.4	2.010	38.4	0.77

(a) Refers to first-named solvent component.
(b) Where no oscillator strengths are given, the extinction coefficients are adjusted to conform to an oscillator strength equal to that for the same dye in water.
(c) Refers to a second maximum.

TABLE 4

DYE III IN MIXED SOLVENTS

Solvent	Mole%[a]	ν_{max} x 10^{-4} (cm^{-1})	ϵ_{max} x 10^{-2}[b]	f
Dioxane-water	96.3	1.813 1.925[c]	58.0 50.0[c]	-
	88.7	1.791 1.908[c]	75.5 49.0[c]	-
	77.7	1.785	103.5	-
	61.1	1.791	107.0	-
	42.2	1.803	96.0	-
	23.1	1.835	70.0	-
	12.0	1.892	55.5	-
Benzene-pyridine	98.9	1.835 1.930[c]	52.0 52.4[c]	-
	70.3	1.798 1.914[c]	70.5 60.5[c]	0.83
	46.3	1.784 1.895[c]	84.0 60.5[c]	0.86
	22.4	1.775 1.890[c]	93.0 60.0[c]	0.86
Pyridine-water	92.3	1.766 1.876[c]	112.0 56.5[c]	0.84
	82.0	1.764	125.5	0.85
	48.4	1.785	104.5	0.80
	34.5	1.801	77.0	0.72
	4.2	1.913	55.4	0.82
	0.8	1.992	45.5	0.78

(a) Refers to first-named solvent component.
(b) Where no oscillator strengths are given, the extinction coefficients are adjusted to an oscillator strength equal to that for the same dye in water.
(c) Refers to a second maximum.

(Captions for Figures)

Fig. 1. ϵ_{max} vs. ν_{max} plot (schematic).

Fig. 2. Absorption curves for dye I in pure solvents. For solvent designations, see Table I. A prime indicates an absorption curve for the protonated dye.

Fig. 3. Absorption curves for dye II in pure solvents.

Fig. 4. Absorption curves for dye II in acetone-water and benzene-acetone mixed solvents. The numbers denote mole percentages of the first-named solvent component. The curve for pyridine-water solvents is redrawn from the data of Brooker et al.[4]

Fig. 5. ϵ_{max} vs. ν_{max} plot for dye II.

Fig. 6. Absorption curves for dye III in pure solvents.

Fig. 7. Absorption curves for dye III in benzene-pyridine and pyridine-water mixed solvents.

Fig. 8. ϵ_{max} vs. ν_{max} plot for dye III.

Fig. 9. (No caption).

Fig. 10. (No caption).

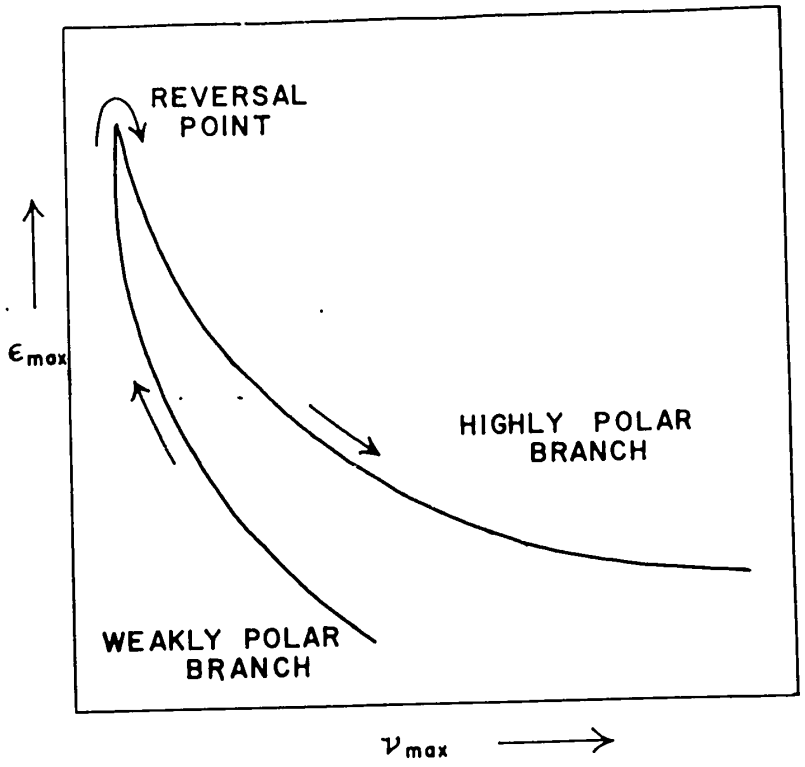

Fig 1

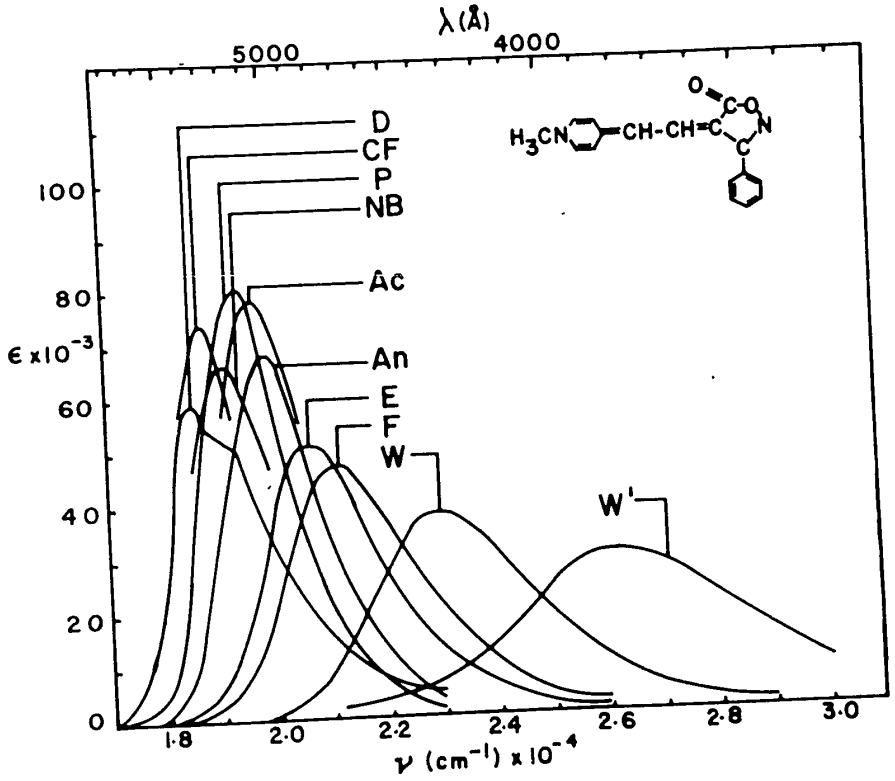

Fig. 2

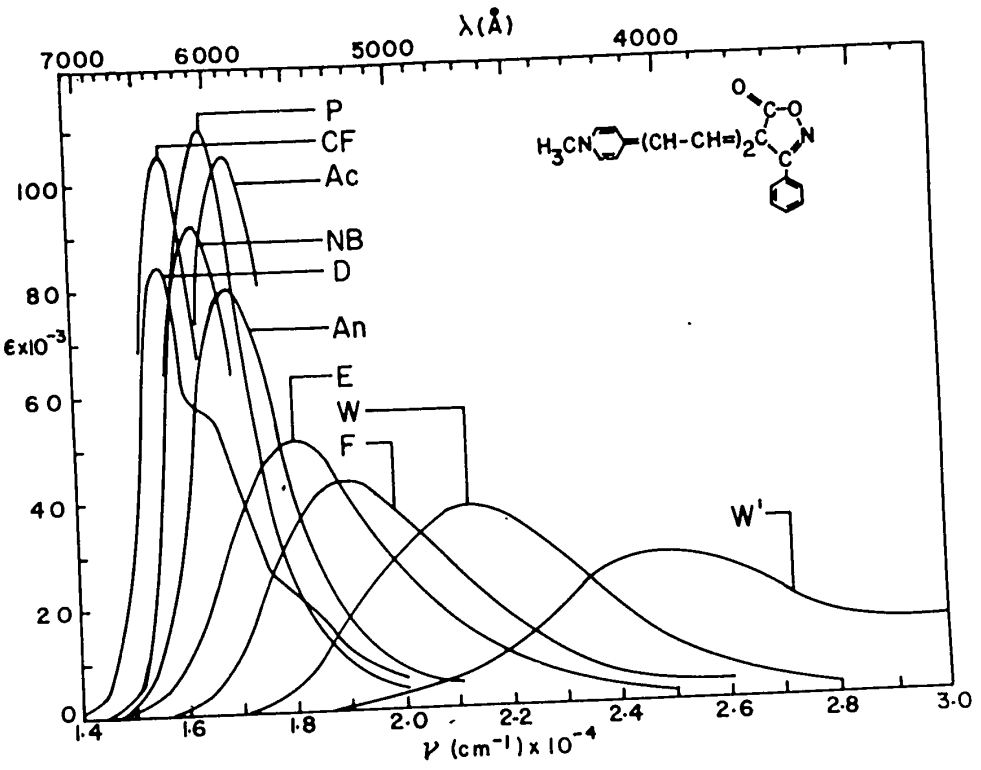

Fig. 3

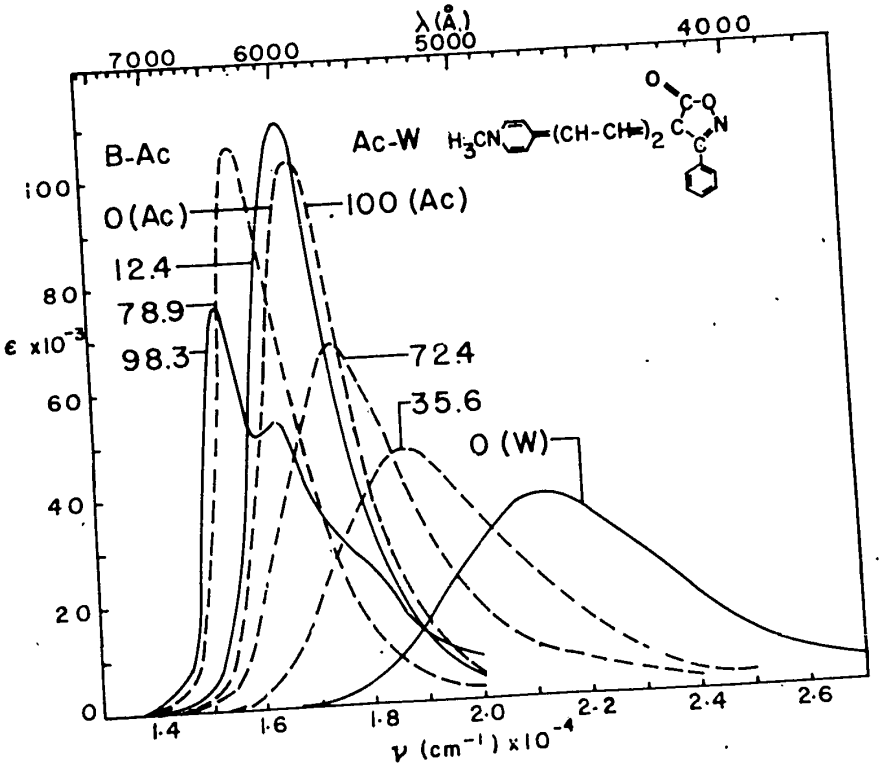

Fig. 4

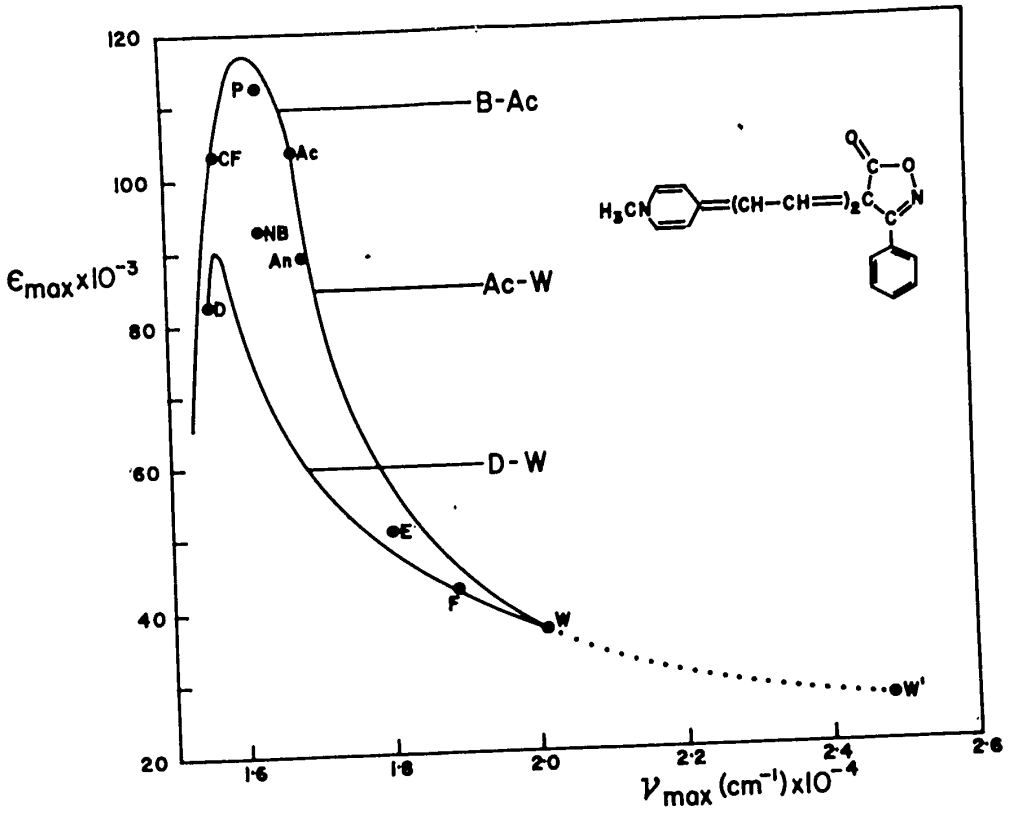

Fig. 5

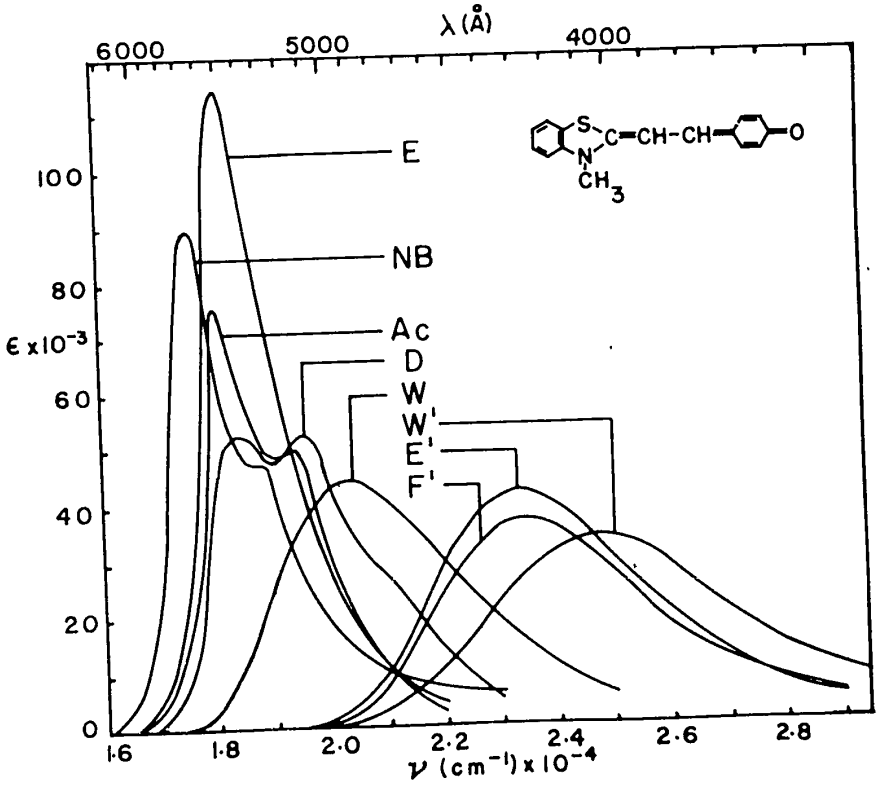

Fig. 6

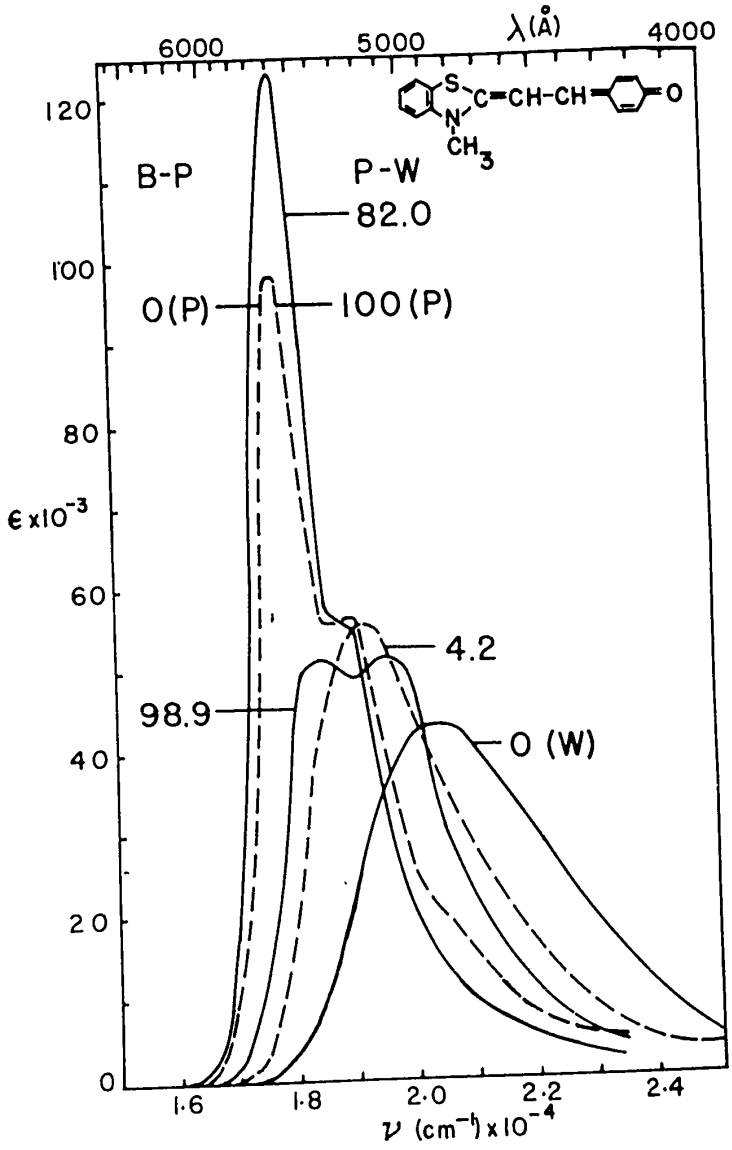

Fig. 7

Fig. 8

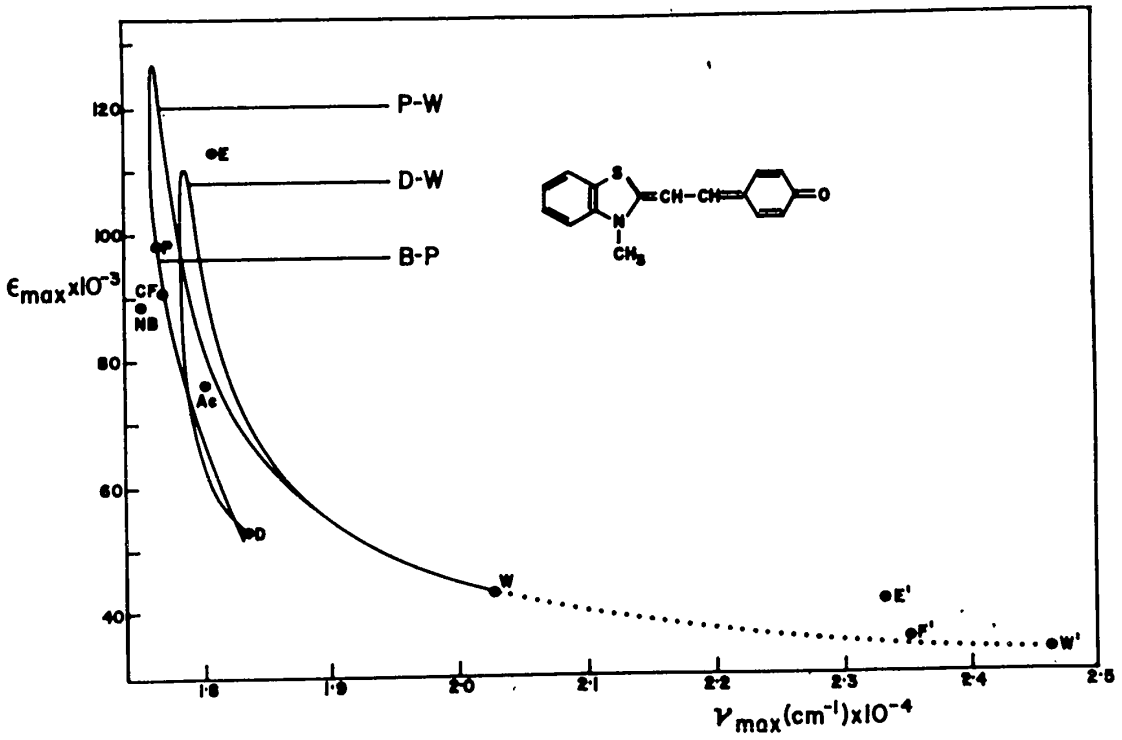

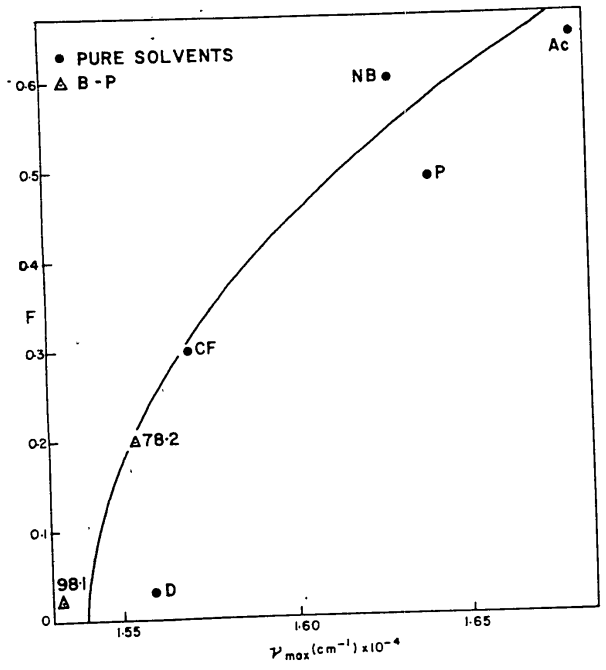

Fig. 9

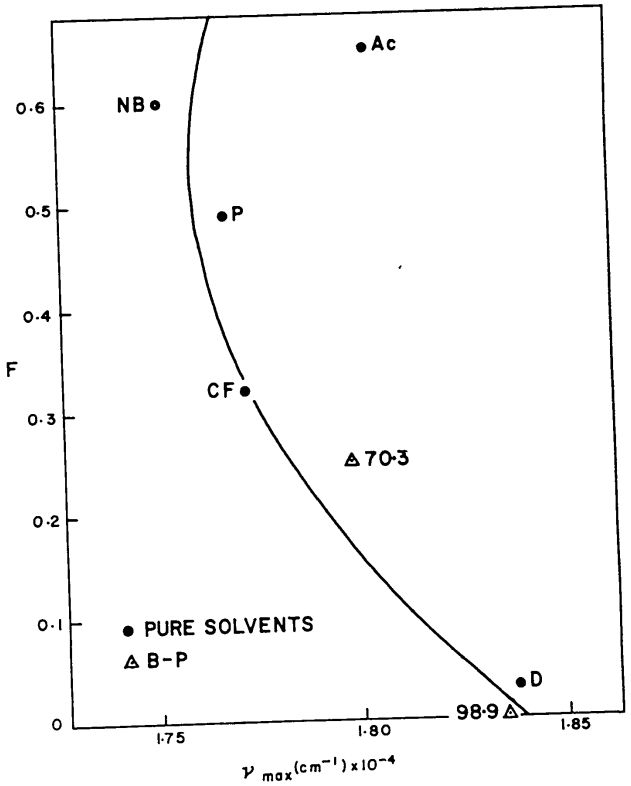

Fig. 10

INTRAMOLECULAR TWISTING EFFECTS IN SUBSTITUTED BENZENES. I. ELECTRONIC SPECTRA.[1,2]

By Eion G. McRae and Lionel Goodman[3]

Departments of Chemistry, Florida State University, Tallahassee, Florida and The Pennsylvania State University, University Park, Pennsylvania.

---

[1] Taken from a dissertation submitted by E. G. McRae for the degree of Ph.D. at Florida State University, 1957. Presented in part at the symposium on Molecular Structure and Spectroscopy, Columbus, Ohio, June 1955.

[2] The work was carried out under a contract between the U. S. Air Force, Office of Scientific Research, ARDC, and the Florida State University. Supported in part by a grant from Research Corporation.

[3] Present addresses: E. G. M. - Chemical Physics Section, C.S.I.R.O., Melbourne, Australia; L. G. (to whom reprint requests should be addressed) - Department of Chemistry, Pennsylvania State University, University Park, Pennsylvania.

(Abstract)

The electronic spectral effects of twisting a substituent group about the substituent-ring bond in substituted benzenes are analyzed from the viewpoint of semi-empirical MO theory including zeroth and first order configuration interaction. The substituent orbital ϕ_s° is expressed as a linear combination of two functions, ϕ_x and ϕ_y, which are respectively anti-symmetric and symmetric with respect to reflection in the ring plane: $\phi_s^{\circ} = \cos\theta\,\phi_x + \sin\theta\,\phi_y$. Transition energies and intensities are discussed with reference to the twisting parameter θ. Ordinarily, θ increases as the substituent is twisted, and can

be evaluated explicitly when the molecular geometry is known. The treatment is carried through both with and without cognizance of the nearest-neighbor overlap integrals, and the inductive effect of the substituent is discussed. Particular attention is given to the question of self-consistency.

The theory applies especially to those transitions which correspond to transitions observed in the spectrum of benzene ("benzene-analogue" transitions). Three possible types of θ-dependence of transition energies are distinguished, and the conditions under which each might be realized are specified. Of the four benzene-analogue singlet-singlet transitions considered, the two of lowest energy are ordinarily predicted to suffer a decrease of intensity as θ increases, while the intensities of the remaining two transitions are predicted to be insensitive to twisting perturbations. "Charge transfer" transitions are also considered, though in less detail.

The theory is applied in a detailed discussion of the ultraviolet absorption spectra of N,N-dimethylaniline and related molecules in which the dimethylamino substituent is twisted as a result of ortho substitution or intramolecular bridge formation.

1. INTRODUCTION

In several series of substituted benzenes, the twisting of the substituent group about the substituent-ring bond leads to pronounced changes in electronic properties. For example, the effect of twisting is revealed particularly clearly in the spectra and some ground-state properties of N,N-dimethylaniline and related molecules.[4-8] In this and other series of substituted benzenes, twisting may be produced either as a steric effect of ortho-substitution, or as a result of intramolecular bridge formation.

This paper is devoted to an analysis, from the molecular orbital (MO) viewpoint, of the effects of twisting perturbations on substituted benzene spectra. In the following paper[9], we apply a similar theory to ground-state properties such as dipole moment and resonance energy.

---

4 B. M. Wepster, Rec. Trav. Chim. 67, 411 (1948); 71, 1159 (1952); 76, 335 (1957); 76, 357 (1957).

5 B. M. Wepster, Rec. Trav. Chim. 73, 661 (1953).

6 H. B. Klevens and J. R. Platt, J. Am. Chem. Soc., 71, 1714 (1949).

7 W. R. Remington, J. Am. Chem. Soc., 67, 1838 (1945).

8 Ref. 4-7 are to literature on spectra. Further references, including references to the literature on ground-state properties, are given in the following paper (paper II).[9]

9 E. G. McRae and L. Goodman, J. Chem. Phys. 28, 0000 (1958).

2. GENERAL APPROACH

We consider a substituted benzene in which a particular substituent group is attached to the ring by a bond between the substituent atom, 7, and the adjacent ring carbon atom, 1. The other ring carbon atoms are numbered consecutively around the ring (See Fig. 1b). The 1-7 bond is assumed to lie on the projection of the line joining carbon atoms 1 and 4, but the substituent group itself is supposed not to be axially symmetric with respect to the 1-4 line.

Let us suppose that the substituent interacts conjugatively with the ring <u>via</u> the single atomic orbital (AO) ϕ_s^o, centered on 7. We assume that in the ground configuration there are formally two electrons in ϕ_s^o. In a future publication we shall consider the case of a substituent with several AO's capable of interacting with the ring carbon $2p\pi$ AO's.[10]

[10] L. Frolen and L. Goodman, work in progress.

We wish to discuss the spectral effects of twisting the substituent group about the 1-7 bond. The effect of twisting is observed experimentally as a regular relationship between the spectra and the twist angle[11,12]. In order to discuss twisting

[11] The observed spectra should be corrected, if necessary, to allow for the direct influence of the substituent or substituents responsible for twisting. For an example, see Table 6, footnote (b).

[12] The definition of the twist angle is arbitrary to some extent, as there are in general various ways of incorporating the part of the twist angle corresponding to the change of shape of the substituent as it is twisted.

effects from the theoretical viewpoint, we express ϕ_s^o as a linear combination of two normalized functions, ϕ_x and ϕ_y, which are respectively anti-symmetric and symmetric with respect to reflection in the ring plane:

$$\phi_s^o = \cos\theta\ \phi_x + \sin\theta\ \phi_y. \qquad (1)$$

We require that ϕ_x remain effectively unchanged during the twisting of the substituent. However, we place no such restriction on ϕ_y.

Because of its symmetry, the function ϕ_y in Eq. 1 may be assumed not to interact appreciably with the ring π-MO's. Consequently, the parameter θ enters into the theory in a particularly simple way. For this reason, and also because the twisting of the substituent ordinarily corresponds to an increase of θ, it is convenient to break the problem into two parts: First, to deduce the θ-dependence of the spectra, and, second, to relate θ to the angle of twist. In this paper, except where otherwise mentioned, we will be concerned with the first part of this program. The second part is difficult to treat generally; it could easily be carried through for any particular substituted benzene if its geometry were known. If ϕ_s^o is a pure 2p AO, the parameter θ takes on an especially simple meaning; it is the angle of twist of ϕ_s^o, and hence of the substituent group, with respect to the ring plane (Fig. 1c).

For the substituted benzene, we anticipate four low-energy singlet excited states, corresponding respectively to the

following states in benzene: $^1B_{2u}$ (energy 4.9 e. v. above ground state, $^1B_{1u}$ (6.2 e. v.) and the components of $^1E_{1u}$ (7.0 e. v.). In the foregoing, the benzene state energies refer to the absorption band centers, the symmetry designations pertain to the D_{6h} group, and the assumed assignments are those fairly generally accepted at the present time.[13] We shall refer to the above states of the substituted benzene as "benzene analogue" (BA) states. In addition to the BA states, we anticipate at least two low energy singlet "charge transfer" (CT) states, arising formally from the excitation of one of the substituent electrons to a vacant benzene π-MO. For each of the above states, we naturally anticipate a corresponding low-energy triplet state. In particular, we expect a lowest-energy triplet corresponding to $^3B_{1u}$ in benzene (absorption band center 3.8 e. v.).[13]

[13] D. P. Craig, Revs. Pure and Applied Chem. (Roy. Australian Chem. Inst.) 3, 207 (1953).

The treatment of CT transitions is rendered comparatively difficult by a number of factors, among which may be mentioned the possible inapplicability of the approximation in which the same effective Hamiltonian is deemed appropriate to both the ground and the excited states. A detailed discussion of that question is beyond the scope of the present work. Accordingly, only the BA states are treated in detail in this paper. The CT states, and the possible importance of BA-CT configuration interaction are also discussed, but in a purely qualitative way.

3. TREATMENT OF BENZENE ANALOGUE TRANSITIONS

The method of treatment adopted in this paper is based on the semi-empirical MO procedure developed by Goodman and Shull[14],

[14] L. Goodman and H. Shull, J. Chem. Phys. 23, 33 (1955).

and applied by them in a systematic interpretation of the spectra of substituted benzenes.[15] The above two papers should be consulted for those details of the method which are omitted in the present paper; to facilitate reference, the notation in the present paper has been made to conform as closely as practicable to that of Goodman and Shull.

[15] L. Goodman and H. Shull, J. Chem. Phys. 27, 1388 (1957).

Zeroth Order: - In the zeroth order of approximation, in which the substituent is considered not to interact with the ring, (Fig. 1a) the orbitals for the substituted benzene comprise the substituent AO ϕ_s°, and the benzene π-MO's. We denote the latter by ϕ_i° ($i = 0, 1, \bar{1}, 2, \bar{2}, 3$), and express them as linear combinations of AO's (ICAO):

$$\phi_i^{\circ} = \sum_{\mu=1}^{6} c_{i\mu}\, \phi_\mu \quad , \tag{2}$$

where ϕ_μ denotes the $2p\pi$ AO belonging to atom μ, all AO's having positive lobes on the same side of the ring plane.

The value of the carbon AO Coulomb integral, , is chosen as the zero of MO energy, and the orbital energies are expressed throughout in terms of the semi-empirical C-C resonance integral, β.

In the zeroth order, let e_i^o denote the energy of the orbital Φ_i^o. We write

$$e_i^o = n_i^o \beta \ ,$$

where n_i^o is the orbital energy factor for Φ_i^o. The AC coefficients and energy factors for the benzene MO's, either with or without nearest-neighbor overlap integrals included, may be obtained from the formulas given by Wheland.[16] For the C-C overlap integral in benzene, the value 1/4 is adopted for calculations with overlap included. The barred and unbarred MO subscripts respectively signify MO's belonging to A and B reps (irreducible representations)[17] of the C_2 group (see below).

16 G. W. Wheland, "Resonance in Organic Chemistry", John Wiley and Sons, New York, 1955, p. 666.

17 M. A. Melvin, Revs. Mod. Phys. 28, 18 (1956).

Intramolecular twisting destroys the C_{2v} symmetry of a substituted benzene, and in this paper we assume that the effective Hamiltonian has C_2 symmetry. Accordingly, we adopt the C_2 symmetry classification of wave functions, and consider only those interactions which are between functions of the same C2 symmetry type. As a particular consequence of the destruction of the C_{2v} symmetry by intramolecular twisting, it is no longer strictly meaningful to draw a distinction between π - and σ-electrons, because a molecule with a twisted substituent group no longer has a plane of symmetry containing the conjugated atoms. However, the ring carbon AO's which are anti-

symmetric with respect to reflection in the ring plane may be distinguished from the other ring carbon AO's, and it is convenient to refer to them still as $2p\pi$ AO's and to the occupying electrons as π-electrons. Similarly the two electrons in the substituent AO ϕ_s remain sharply differentiated from the other substituent electrons. For similar reasons, the π-electron approximation is no longer strictly applicable. We retain it in the sense that we consider interactions between only those AO's which are anti-symmetric with respect to reflection in the ring plane---viz. ϕ_x and the ring carbon $2p\pi$ AO's.

The ground state function is approximated throughout by a single (closed shell) configuration function, and the zeroth-order ground state function is denoted by Ψ_o^o. The zeroth-order state functions for the substituted benzene must be built up from the orbitals with due cognizance of zeroth-order configuration interaction (CI). There results, for the four low-energy singlet excited states,

$$\begin{aligned}
\Psi_I^o &= 2^{-1/2}\,(x_{12}^o - x_{\bar{1}\bar{2}}^o),\\
\Psi_{\bar{2}}^o &= 2^{-1/2}\,(x_{12}^o + x_{\bar{1}\bar{2}}^o),\\
\Psi_{\bar{1}}^o &= 2^{-1/2}\,(x_{12}^o + x_{\bar{1}2}^o),\\
\Psi_{\bar{2}}^o &= 2^{-1/2}\,(x_{1\bar{2}}^o - x_{\bar{1}2}^o),
\end{aligned} \qquad (3)$$

where x_{12}^o, for example, denotes the zeroth-order singlet configuration function arising from the configuration $s)^2\,0)^2\,1)^1\,\bar{1})^2\,2)^1$. Similar expressions can of course be

written down for the triplet state functions. In the notation for the state functions, as in that for the MO's, a barred subscript signifies an A-type function and an unbarred subscript a B-type function. The correspondence between the benzene states and the above functions is as follows: $\bar{0} \sim A_{1g}$; $1 \sim B_{2u}$; $\bar{1} \sim B_{1u}$; $\bar{2}$, $2 \sim E_{1u}$.

Interactions: - When the interactions between substituent and ring are taken into account, the new MO's are given in LCMO form,

$$\phi_i = \sum_{j = s,o}^{3} A_{ij} \phi_j^o \quad , (i,j = s, 0, \bar{1}, 1, \bar{2}, 2, 3)$$

by solution of the MO secular equation

$$\det \left\{ H_{ij} - e\, S_{ij} \right\} = 0. \tag{4}$$

Here,

$$H_{ij} = \int \phi_i^o \; H_{eff} \; \phi_j^o \, d\, v,$$

H_{eff} denoting the effective Hamiltonian, and

$$S_{ij} = \int \phi_i^o \, \phi_j^o \, d\, v.$$

In solving the secular equation, we follow Goodman and Shull[14], who have described a method for solving Eq. 4 under the following conditions:

$$\begin{aligned}
S_{is} &= c_{il}\, \rho_s, && (i \neq s) \\
H_{ij} &= c_{il}\, c_{jl}\, \delta_1 \beta, && (i \neq j,\ i \neq s,\ j \neq s) \\
H_{ii} &= n^o_i \beta + c_{il}\, \delta_1 \beta && (i \neq s) \\
H_{is} &= c_{il}\, \rho \beta && (i \neq s) \\
H_{ss} &= \delta \beta
\end{aligned} \tag{5}$$

Here, s denotes the C-C overlap integral, and

$$\rho = s_{17}/s \tag{6}$$

where s_{17} denotes the 1-7 overlap integral. The assumption

$$\beta_{17}/\beta = \rho \tag{7}$$

is implicit in the expression for H_{is} in (5). $\delta\beta$ means the Coulomb integral at atom 7, and $\delta_1\beta$ represents the increment of the Coulomb integral at atom 1, due to the substituent. Thus, δ_1 represents the inductive effect of the substituent.

The conditions (5) embody the approximation, frequently introduced, of neglecting interactions between non-nearest neighbor atoms. Two other common approximations, namely the neglect of overlap and the neglect of the inductive effect, may be brought in through (5). The neglect of overlap corresponds to putting $s = s_{17} = 0$. This implies that the benzene MO's and MO energy factors are to be taken without overlap. The neglect of the inductive effect corresponds to putting $\delta_1 = 0$.

The present problem is characterized by the condition that ρ varies approximately as cos θ, while δ remains approximately constant as the substituent is twisted. Therefore, we may appropriately specialize the conditions (5) by superposing the following conditions:

$$\rho = \rho_o \cos\theta, \tag{8a}$$

$$\delta \text{ independent of } \theta, \tag{8b}$$

where ρ_o is independent of θ. From Eqs. 7 and 8a,[18] we have

[18] The parameter β is assigned different values for the A-type as distinct from the B-type states. Therefore, in principle, ρ in 8c should be assigned different values so as to give β_{17} the same value in all states for any particular value of θ. However, in this paper, we adopt for simplicity a single parameter ρ_o.

$$\beta_{17} = \rho_o \beta \cos\theta. \tag{8c}$$

The configuration functions are altered as a result of the orbital perturbations. Also, the mixing of configurations is no longer symmetrical, the new state functions being determined by solution of the state secular equations.[15] The new state functions are of the form

$$\begin{aligned}
\Psi_{\bar{1}} &= \cos(\pi/4 - \Lambda_A)\, x_{12} - \sin(\pi/4 - \Lambda_A)\, x_{\bar{1}\bar{2}}, \\
\Psi_{\bar{2}} &= \sin(\pi/4 - \Lambda_A)\, x_{12} + \cos(\pi/4 - \Lambda_A)\, x_{\bar{1}\bar{2}}, \\
\Psi_{1} &= \cos(\pi/4 - \Lambda_B)\, x_{1\bar{2}} + \sin(\pi/4 - \Lambda_B)\, x_{\bar{1}2}, \\
\Psi_{2} &= \sin(\pi/4 - \Lambda_B)\, x_{1\bar{2}} - \cos(\pi/4 - \Lambda_B)\, x_{\bar{1}2},
\end{aligned} \tag{9}$$

where Λ_A and Λ_B are numbers measuring the asymmetry of mixing between the respective pairs of configurations.

In order to evaluate Λ_A, Λ_B and the BA state energies from (9), it is necessary first to evaluate the configuration energies and CI integrals. The former are given in the semi-empirical method as orbital energy differences, i.e.

$$E_{ij} = e_j - e_i = (n_j - n_i)\beta, \tag{10}$$

where the MO energy factors are obtained from (4), and β is evaluated empirically. The CI integrals may be evaluated with

the aid of the approximation[15]

$$M_{ij,k\ell} \approx a_{ii}\, a_{jj}\, a_{kk}\, a_{\ell\ell}\, M_{ij,k\ell}{}^{o} \tag{11}$$

where $M_{ij,k\ell}$ is a general MO electron repulsion integral and $M_{ij,k\ell}{}^{o}$ denotes the corresponding integral for benzene. Then H_A and H_B can be expressed in terms of the zeroth-order integrals (benzene integrals), $H^{o}{}_{A}$ and $H^{o}{}_{B}$ respectively, and the latter may be evaluated empirically. A similar method applied to triplet states. The empirical parameters are evaluated from the spectrum of benzene, as described in Ref. 15. The values of the parameters used in the present work are shown in Table 1.

From Eq. 9 the transition moments governing the BA transition intensities are given by

$$\begin{aligned}
\underline{M}_{\bar{1}} &= \cos \Lambda_A\, \underline{M}'_1 + \sin \Lambda_A\, \underline{M}'_2 \\
\underline{M}_{\bar{2}} &= -\sin \Lambda_A\, \underline{M}'_1 + \cos \Lambda_A\, \underline{M}'_2 \\
\underline{M}_1 &= \cos \Lambda_B\, \underline{M}'_1 + \sin \Lambda_B\, \underline{M}'_2 \\
\underline{M}_2 &= -\sin \Lambda_B\, \underline{M}'_1 + \cos \Lambda_B\, \underline{M}'_2
\end{aligned} \tag{12}$$

Here $\underline{M}_1$, for example, denotes the integral

$$\int \Psi_o\, \underline{M}\, \Psi_{\bar{1}}\, d\tau ,$$

where Ψ_o is the perturbed ground state (one-configuration) function and $\underline{M}$ denotes the classical dipole moment vector. $\underline{M}'_2$ and $\underline{M}'_1$ correspond to the allowed components of the $A_{1g} \rightarrow E_{1u}$ transition in benzene, but are modified by the orbital perturbations.

Thus, for example

$$\underline{M}_2' = 2^{-1/2} \int \Psi_o \underline{M} \quad (x_{12} + x_{\bar{1}\bar{2}}) \, d\,v.$$

$\underline{M}_1'$ and $\underline{M}_1$ similarly correspond respectively to the forbidden $A_{1g} \longrightarrow B_{1u}$ and $A_{1g} \longrightarrow B_{2u}$ transitions in benzene.

The orbitally perturbed transition moments, $\underline{M}_2'$, etc., can be evaluated in terms of the C-C distance in benzene. The method used in this paper is to express the transition moments in terms of the appropriate integrals involving MO's, to expand those integrals in terms of AO integrals, and to evaluate the AO integrals by the formulas

$$\begin{aligned} \int \phi_\mu \, \underline{M} \, \phi_\mu \quad dv &= \epsilon \underline{r}_\mu \\ \int \phi_\mu \, \underline{M} \, \phi_\nu \quad dv &= (1/2)\, \epsilon \, (\underline{r}_\mu + \underline{r}_\nu) \, s_{\mu\nu}, \quad (\mu \neq \nu) \end{aligned} \tag{13}$$

where $\underline{r}_\mu$ denotes the position vector of the μ^{th} atom, $s = \int \phi_\mu \phi_\nu \, dv$, and ϵ stands for the electronic charge. For simplicity, the 1-7 bond length is assumed equal to the C-C distance. For the purpose of calculating BA transition intensities, we choose the C-C distance to be 1.0 Å; with that value, Eq. 13 reproduces the observed oscillator strength, f = 1.2, for the $A_{1g} \longrightarrow E_{1u}$ transition in benzene vapor.[19]

---

19 L. W. Pickett, M. Muntz, and E. M. McPherson, J. Am. Chem. Soc. 73, 4862 (1951).
J. Romand and B. Vodiar, Compt. rend. 223, 930 (1951).

---

4. FOUNDATION OF THE METHOD

We describe the foundation of the semi-empirical method with reference to a formal LCAO SCF treatment of intramolecular

twisting perturbations in substituted benzenes. We pay special attention to the conditions (8), which for the purpose of the present problem are superposed on Goodman and Shull's conditions (5). Also, we discuss the constancy of the important empirical parameter β. Where feasible, the discussion is supported by numerical calculations.

SCF Method:--Following a procedure similar to that described by Roothaan,[20] we consider the derivation of the "best possible" LCAO MO for the ground configuration of a substituted benzene represented by Fig. 1c. We begin with the same orbitals as before, namely the benzene MO and the substituent AO $\phi_7 (\phi_7 \equiv \phi_s^o)$. For ϕ_7, we adopt the form (1). The ground configuration MO energies and MO are found by the iterative solution of the secular equation

$$\det \left\{ F_{ij} - \epsilon S_{ij} \right\} = 0,$$

where $F_{ij} = \int \phi^o_i \, F \, \phi^o_j \, dv$ is an MO interaction integral involving the Hartree-Fock Hamiltonian, F.

In the first cycle of the iterative process, the Hartree-Fock Hamiltonian is constructed with the zeroth-order MO's (Eq. 2). In a given subsequent cycle, the Hartree-Fock Hamiltonian is constructed with the MO's resulting from the previous cycle. Let ϕ_k (k = s, 0, $\bar{1}$, $\bar{2}$, 2, 3) denote these MO's and let $\sum_k^{occ}$ denote summation over the subscripts of the

---

20 C. C. J. Roothaan, Revs. Mod. Phys. 23, 69 (1951).

MO ϕ_k occupied in the ground configuration. Then the MO interaction integrals of the cycle in question are given in conventional notation by

$$F_{ij} = \int \phi_i^{\circ} T \phi^{\circ}_j \, dv + \sum_{\mu=1}^{7} (U_{c\mu}: \phi^{\circ}_i \phi^{\circ}_j)$$
$$+ \sum_{k}^{occ} 2(\phi_k \phi_k; \phi^{\circ}_i \phi^{\circ}_j) - (\phi_k \phi^{\circ}_j; \phi_k \phi^{\circ}_i)$$

where T denotes the electronic kinetic energy operation, $U_{c\mu}$ the electrostatic potential due to the μ th core, and in the notations for the electron repulsion integrals, the functions of one electron are written on the left and those of the other electron on the right.

The above MO interaction integrals may be expanded in terms of the changes in the AO interaction integrals $L_{\mu\nu} = \int \phi_\mu F \phi_\nu \, dv$ resulting from the interaction between ring and substituent. Let F° denote the Hartree-Fock Hamiltonian for the situation represented by Fig. 1a. The change in $L_{\mu\nu}$ is given by

$$\Delta L_{\mu\nu} = \int \phi_\mu F \phi_\nu \, dv - \int \phi_\mu F^{\circ} \phi_\nu \, dv.$$

Then we have

$$F_{ij} = \sum_{\mu=1}^{6} \sum_{\nu=1}^{6} c_{i\mu} c_{j\nu} \Delta L_{\mu\nu}, \quad (i \neq j;\ i, j \neq s)$$
$$F_{ii} = \varepsilon^{\circ}_i + \sum_{\mu=1}^{6} \sum_{\nu=1}^{6} c_{i\mu} c_{i\nu} \Delta L_{\mu\nu}, \quad (i \neq s) \qquad (14)$$
$$F_{is} = \sum_{\mu=1}^{6} c_{i\mu} \Delta L_{\mu 7}, \quad (i \neq s)$$

and $F_{ss} = \varepsilon^{\circ}_s + \Delta L_{77}$.

Comparison of Semi-empirical and SCF Methods:--We shall assume for the moment that all bond lengths are independent of θ, in which case condition 8(a) is automatically satisfied. On comparing corresponding semi-empirical and SCF MO integrals in Eqs. 5 and 14, we see that in order to substantiate conditions 8(b) and 8(c) we must have respectively:

$$\Delta L_{77} \text{ independent of } \theta,$$

$$\Delta L_{\mu 7} \equiv L_{\mu 7} \cos\theta, \quad (\mu \neq 7).$$

Also, in order that β be independent of θ, we must have:

$$\Delta L_{\mu\nu} \text{ independent of } \theta, \quad (\mu, \nu \neq 7).$$

As explained later in this section, the above condition is necessary but not sufficient for the constancy of β.

We first consider the θ-dependences of the SCF AO integrals in the first cycle of the iterative process. We have

$$\begin{aligned}
\Delta L_{\mu\nu} &= (U_{c7}:\phi_\mu\phi_\nu) + 2(\phi_7\phi_7;\phi_\mu\phi_\nu)-(\phi_7\phi_\mu;\phi_7\phi_\nu), (\mu,\nu \neq 7) \\
L_{\mu 7} &= \varepsilon^{\circ}_7 s_{\mu 7} + \sum_{\mu=1}^{6}(U_{c\mu}:\phi_\mu\phi_7) \qquad (15) \\
&+ \sum_{k}^{occ}\left[2(\Phi^{\circ}_k\Phi^{\circ}_k;\phi_\mu\phi_7)-(\Phi^{\circ}_k\phi_\mu;\Phi^{\circ}_k\phi_7), \quad (\mu \neq 7)\right. \\
\Delta L_{77} &= \sum_{\mu=1}^{6}(U_{c\mu}:\phi_7\phi_7) + \sum_{k}^{occ}\left[2\Phi^{\circ}_k\Phi^{\circ}_k;\phi_7\phi_7)-(\Phi^{\circ}_k\phi_7;\Phi^{\circ}_k\phi_7)\right] \\
&- (\phi_7\phi_7;\phi_7\phi_7).
\end{aligned}$$

We may express each core integral as the sum of a penetration integral and an AO electron repulsion integral,[21] e.g.

---

21 M. Goeppert-Mayer and A. L. Sklar, J. Chem. Phys. 6, 645 (1938).

$$(U_{c\mu} : \phi_1 \phi_2) = (U_\mu : \phi_1 \phi_2) - (\phi_\mu \phi_\mu : \phi_1 \phi_2),$$

where U_μ denotes the electrostatic potential due to neutral atom μ. On expressing ϕ_7, where appropriate, in the form (1), we obtain

$$\begin{aligned}
\Delta L_{\mu\nu} &= (U_7 : \phi_\mu \phi_\nu) \\
&+ (\phi_x\phi_x;\phi_\mu \phi_\nu) - (\phi_x\phi_\mu;\phi_x\phi_\nu) \cos^2\theta \\
&+ 2\,(\phi_x\phi_y;\phi_\mu \phi_\nu) - (\phi_x\phi_\mu;\phi_y\phi_\nu) \cos\theta \sin\theta \\
&+ (\phi_y\phi_y;\phi_\mu \phi_\nu) - (\phi_y\phi_\mu;\phi_y\phi_\nu) \sin^2\theta \qquad (\mu, \nu \neq s)
\end{aligned}$$

$$\begin{aligned}
L_{\mu 7} &= \Big\{ \underline{e}^{\circ}_{s}\, s_{\mu x} + \sum_{\mu=1}^{6} (U_\mu : \phi_\mu \phi_x) \\
&+ \sum_{k}^{occ} \left[2(\Phi^{\circ}_k \Phi^{\circ}_k; \phi_\mu \phi_x) - (\Phi^{\circ}_k \phi_\mu; \Phi^{\circ}_k \phi_x) \right] \\
&- \sum_{\mu=s,1}^{occ} (\phi_\mu \phi_\mu ; \phi_\mu \phi_x) \Big\} \cos\theta \qquad (\mu \neq s)
\end{aligned}$$

$$\begin{aligned}
\Delta L_{77} &= \sum_{\mu=1}^{6} (U_\mu : \phi_7 \phi_7) \\
&+ \Big\{ \sum_{k}^{occ} \left[2(\Phi^{\circ}_k \Phi^{\circ}_k;\phi_x \phi_x) - (\Phi^{\circ}_k \phi_x; \Phi^{\circ}_k \phi_x) \right] \\
&- \sum_{\mu=1}^{6} (\phi_\mu \phi_\mu ; \phi_x \phi_x) \Big\} \cos^2\theta \\
&+ 2\Big\{ \sum_{k}^{occ} \left[2(\Phi^{\circ}_k \Phi^{\circ}_k;\phi_x \phi_y) - (\Phi^{\circ}_k \phi_x; \Phi^{\circ}_k \phi_y) \right] \\
&- \sum_{\mu=1}^{6} (\phi_\mu \phi_\mu ; \phi_x \phi_y) \Big\} \cos\theta \sin\theta \\
&+ \Big\{ \sum_{k}^{occ} \left[2(\Phi^{\circ}_k \Phi^{\circ}_k; \phi_y \phi_y) - (\Phi^{\circ}_k \phi_y; \Phi^{\circ}_k \phi_y) \right] \\
&- \sum_{\mu=1}^{6} (\phi_\mu \phi_\mu ; \phi_y \phi_y) \Big\} \sin^2\theta \\
&- (\phi_7 \phi_7; \phi_7 \phi_7).
\end{aligned}$$

In the expression for $L_{\mu 7}$ the notation $s_{\mu x} = \phi_\mu \phi_x \, dv$ has been introduced, and we have taken note of the vanishing of all

integrals in which ϕ_y appears only once.

It is seen that in the approximation we are considering (first SCF cycle, bond lengths fixed), the integrals $L_{\mu 7}$ are strictly proportional to cos θ. A detailed discussion of the θ-dependence of the integrals $L_{\mu\nu}$ ($\mu, \nu \neq 7$) and L_{77} would require the knowledge of all the relevant penetration and AO electron repulsion integrals; however, some general conclusions can be drawn by referring to tables of two-center AO Coulomb integrals[22,23] (we neglect three- and four-center integrals,

---

22 R. G. Parrand and B. L. Crawford, J. Chem. Phys. 11, 1049 (1948).

23 C. C. J. Roothaan, "Tables of Two-center Coulomb Integrals between 1s, 2s, and 2p Orbitals", Special Technical Report, University of Chicago, 1955.

---

which are relatively small). If we take ϕ_x to be a 2p AO with axis perpendicular to the ring plane, and assume in turn that ϕ_y is a 2s AO and either of the two 2p AO's orthogonal to ϕ_x, in no case do we find $(\phi_x \phi_x; \phi_\mu \phi_\mu)$ and $(\phi_y \phi_y; \phi_\mu \phi_\mu)$ to differ by more than about ten per cent. Also, these integrals are at least an order of magnitude greater than the largest integrals involving both ϕ_x and ϕ_y. It follows that, in the first cycle of the iterative process, $L_{\mu\nu}$ ($\mu\nu \neq 7$) and L_{77} are nearly independent of θ.

We now discuss the more realistic case in which the Hartree-Fock Hamiltonian is constructed with MO's of the general form $\phi_k = \sum_i a_{ki} \phi^o_k$ ($k = s, 0, \pm 1$). Retaining only the one-center and two-center Coulomb electron repulsion integrals,

we find

$$\Delta L_{\mu\nu} = (U_{c7};\phi_\mu \phi_\nu) - 1/2\ \Delta P_{\mu\nu}\ (\phi_\mu \phi_\mu ;\phi_\nu \phi_\nu),\ (\mu \neq \nu;\ \mu, \nu \neq 7)$$

$$\Delta L_{\mu\mu} = (U_{c7}:\phi_\mu \phi_\mu) + 1/2\ \Delta Q_\mu\ (\phi_\mu \phi_\mu ;\phi_\mu \phi_\mu) + \sum_{\nu=1}^{6} \Delta Q_\nu\ (\phi_\mu \phi_\mu ;\phi_\nu \phi_\nu) + Q_7(\phi_\mu \phi_\mu ;\phi_7\phi_7),\ (\mu \neq 7)$$

$$L_{\mu 7} = \beta^{o}_{7}\, s_{\mu 7} + \sum_{\mu=1}^{6} (U_{c\mu}:\phi_\mu \phi_7) - 1/2\ P_{\mu 7}(\phi_\mu \phi_\mu ;\phi_7\phi_7),\ (\mu \neq 7)$$

and $$\Delta L_{77} = \sum_{\mu=1}^{6} (U_{c\mu}:\phi_7\phi_7) + 1/2\ \Delta Q_7\ (\phi_7\phi_7;\ \phi_7\phi_7) + \sum_{\mu=1}^{6} Q_\mu\ (\phi_\mu \phi_\mu ;\ \phi_7\phi_7), \qquad (15')$$

where

$$Q_\mu = 2 \sum_{k}^{occ} \sum_i a_{ki}\, c_{i\mu} \sum_j a_{kj}\, c_{j\mu},$$

$$P_{\mu\nu} = 2 \sum_{k}^{occ} \sum_i a_{ki}\, c_{i\mu} \sum_j a_{kj},\ c_{j\nu},$$

and $\Delta Q_\mu = Q_\mu - Q^{o}_{\mu}$, $\Delta P_{\mu\nu} = P_{\mu\nu} - P^{o}_{\mu\nu}$ (superscripts denote zeroth-order quantities).

If the MO's are derived with neglect of overlap, Q_μ, represents the π-charge density at the μ^{th} atom, and $P_{\mu\nu}$ represents the order of the π-bond joining atoms μ and ν. Since the semi-empirical MO integrals H_{ij} have been shown to be of approximately the correct form as judged by comparison with the first-cycle SCF integrals F_{ij}, it is not inappropriate to invoke semi-empirical charge densities and bond orders in order to discuss more fully the foundation of the semi-empirical method. Utilizing the semi-empirical MO's of Table 2 (overlap neglected),

tabulated values of the appropriate AO electron repulsion integrals[22,24] and again assuming all bond lengths fixed, we

---

[24] The adopted values were those for an effective nuclear charge of 3.2 a.u. and a nearest-neighbor internuclear distance of 1.4 Å (these are the parameters appropriate to benzene itself).

---

find that the integrals $L_{\mu 7}$ ($\mu \neq 7$) vary ($\pm$ 0.01 e.v.) as cos θ:

$$L_{\mu 7} = k_{\mu 7} \cos \theta, \tag{16a}$$

while the integrals $L_{\mu\nu}$ ($\mu, \nu \neq 7$) and L_{77} contain additive parts which vary approximately ($\pm$0.05 e.v.) as $\cos^2 \theta$:

$$L_{\mu\nu}(\theta) = L_{\mu\nu}(\pi/2) + k_{\mu\nu} \cos^2 \theta; \ (\mu, \nu \neq 7) \tag{16b}$$

$$L_{77}(\theta) = L_{77}(\pi/2) + k_{77} \cos^2 \theta. \tag{16c}$$

The constants $k_{\mu\nu}$ are easily evaluated if it is assumed that the integrals $L_{\mu\nu}$ are exactly constant in the first cycle; in that case, the values of the constants measure the θ-dependence of the integrals, resulting from the redistribution of charge accompanying twisting of the substituent. For the integrals $L_{\mu\mu}$ ($\mu \neq 7$) we find (e.v.)[24]: $k_{11} = -0.17$, $k_{22} = -0.03$, $k_{33} = +0.65$, $k_{44} = +0.57$. A positive sign indicates that the amount of electron repulsion decreases as θ increases; i.e., the electrons become more tightly bound as θ increases. For the integrals $L_{\mu\nu}$ (μ, ν denoting adjacent carbon atoms), we find (e.v.)[24] $k_{12} = +0.21$, $k_{23} = -0.04$, $k_{34} = +0.03$. A positive sign indicates that the magnitude of $L_{\mu\nu}$ increases as θ increases; i.e., the bond between atoms μ and ν becomes stronger

as θ increases. The integral L_{77} has a slightly greater θ-dependence; we find[24] $k_{77} = +0.78$ e.v. If the substituent atom 7 were more electronegative than carbon, the value of k_{77} would be greater. For example, for nitrogen we have[25]

---

[25] The integral $(\phi_7\,\phi_7;\ \phi_7\,\phi_7)$ was assigned the value appropriate to an effective nuclear charge of 3.9 a. u. The other AO electron repulsion integrals were assigned the same values as before.

$k_{77} = +1.02$ e.v. It is noteworthy that the sum $\sum_{\mu=1}^{6} Q_\mu\,(\phi_\mu\phi_\mu;\phi_7\phi_7)$ is almost independent of θ, so that most of the θ-depencence of L_{77} comes from $(1/2)\ \Delta Q_7\ (\phi_7\phi_7;\ \phi_7\phi_7)$.

We now consider the effect of the θ-dependence of the 7-1 bond length. Changes in the other bond lengths are relatively small, and are therefore not discussed. Assuming a linear relationship between bond length and MO bond order,[26] and assuming L_{17} inversely proportional to the bond length, we obtain

---

[26] C. A. Coulson, "Valence", Oxford University Press, London, 1952, p. 253.

$$L_{17} = k_{17}\cos\theta + k_{17}\,\frac{d_1-d_2}{d_1}\,P_{17}\cos^2\theta + \ldots.$$

Here, d_1 and d_2 respectively denote the lengths of single and double 7-1 bonds, and k_{17} is the value of $L_{17}(\theta)/\cos\theta$ for a fixed bond length equal to d_1. A similar formula applies for s_{17}. We note that P_{17} is almost exactly proportional to $\cos\theta^9$ (the order of the 7-1 π-bond is of course proportional to $P_{17}\cos\theta$, in view of Eq. 1). Therefore the second term is

really proportional to $\cos^3 \theta$. If we take $(d_1-d_2)/d_1 \approx 0.2/1.5$, and P_{17} ($\theta = 0$) ≈ 0.3, we see that the second term is not more than five per cent of the first.

We return now to discuss the conditions (8). We assume for the moment the is really a constant (see below). Condition 8c holds with an error in θ-dependence not greater than five per cent, the error arising almost entirely from the lengthening of the 7-1 bond as θ increases. A similar remark applies to 8a, but in this case the error arises solely from the bond lengthening. The applicability of 8b may be judged from the θ-dependence of the integral L_{77}. Changes in L_{77} arise mainly from charge redistribution, although the slight θ-dependence of the AO electron repulsion integrals such as $(\phi_\mu \phi_\mu ; \phi_s \phi_s)$ could also play a part. The calculated change in L_{77} throughout the range of θ, $\sim$ 1 e.v., implies a change of δ of about 0.3 ($\beta \approx -3$ e.v.). Previous experience[15] indicates that this change, while by no means negligible, is not sufficient to upset qualitative conclusions drawn by assuming δ constant.

The question that remains to be discussed is that of the constancy of β. We have stated that a necessary condition for the constancy of β is that the integrals $L_{\mu\nu}$ ($\mu, \nu \neq 7$) be independent of θ, and the foregoing discussion shows that this condition is approximately satisfied. To complete the discussion, we note that in the semi-empirical method the configuration energies are taken to be orbital energy differences (Eq. 10),

whereas in the SCF method the configuration energies are given by

$$E_{ij} = \underline{e}_j - \underline{e}_i - (J_{ij} - K_{ij}) \mp K_{ij} , \qquad (10')$$

where the $\underline{e}$'s are SCF orbital energies and J_{ij} and K_{ij} are respectively Coulomb and exchange MO electron repulsion integrals (the upper sign applies to singlet, the lower to triplet configurations). Now the semi-empirical and SCF orbital energies may be assumed to vary proportionately under perturbations, so that the assumption of a constant β is justified to the extent that the electron repulsion integrals vary in proportion to the corresponding semi-empirical configuration energies.

The θ-dependences of the electron repulsion integrals have been introduced through Eq. 11. With the aid of the MO's and MO energies of Table 2 (overlap neglected), we find that the ratios $(a_{11}\ a_{22})^2/(e_2-e_1)$, $(a_{11})^2/(e_2^- - e_1)$ and $(a_{22})^2/(e_2-e_1^-)$ respectively undergo variations of 30%, 20% and 10% throughout the entire range of θ. The errors come in mainly at values of θ approaching 90°. In the range of θ between 0 and 45°, the variations in these ratios do not exceed 5%. The semi-empirical procedure for the configuration energies is thus seen to be securely founded on the SCF method, especially at lower values of θ.

5. GENERAL CONCLUSIONS

Benzene-analogue Transitions:--In order to arrive quickly at the qualitative conclusions of the theory, we handle the orbital perturbations by means of second-order perturbation

theory. The MO energy factors are given by an expression of the form

$$n_i - n_i^o = A_i + B_i \cos^2 \theta, \qquad (17)$$

where for the constant A_i and B_i we adopt expressions conforming to conditions (5) and (8):

$$A_i = c_{il}^2 \, \delta_1 \; ; \; B_i = \beta_o^2 \, c_{il}^2 \, (1 - s \, n_i^o)^2/(n_i^o - \delta).$$

A term involving δ_1^2 has been neglected in the above expression for A_1. The effect of overlap on the MO energies is illustrated in Fig. 2.

For the BA state energies, three possible types of behavior under twisting perturbations may be classified and interpreted in terms of the relative magnitudes of B_1 and B_2 (Note that B_1^- and B_2^- are always zero under the conditions specified in this paper). Let us consider either of the two pairs of interacting configurations, and the states arising from them. Where $|B_1| >> |B_2|$, both state energies increase initially upon twist (increase of θ). We designate that behavior as Type i. Where the lower state energy initially increases and the higher state energy initially decreases upon twist, we speak of Type ii behavior; it would appear if $|B_1| \approx |B_2|$. Finally, where $|B_1| << |B_2|$, both the state energies would initially decrease upon twisting, and we refer to that behavior as belonging to Type iii. The three types of behavior are illustrated in Fig. 3.

The above classification is based on the <u>initial</u> behavior as θ is increased. The theory does not necessarily imply that the state energies should vary monotonically with θ. Non-

monotonic behavior could result from the variation of the CI integral. Also any non-monotonic trend in the mean configuration energy, such as might arise as a result of deviations from (17), could be reflected in a similar trend in one or both state energies.

Twisting effects on the BA singlet-singlet intensities depend primarily on the variation of the Λ's in Eq. 12 rather than on the much less marked variation of the orbitally perturbed transition moments. Now for either pair of interacting configurations, the appropriate Λ (Λ_A or Λ_B) approaches zero as the configuration functions become more nearly degenerate. Keeping that in mind, the qualitative intensity predictions of the theory may be inferred by inspection of Eq. 12.

Let us first consider the case where both the inductive effect and the overlap integrals are neglected. We have

$$A_1 = A_2 = 0 \tag{18a}$$

$$|B_1| > |B_2| \tag{18b}$$

In view of (18b), each pair of transition energies must conform either to Type i or Type ii behavior. Because of (18a), the configuration energies become degenerate at $\theta = \pi/2$. The theory thus predicts that the $\bar{0} \longrightarrow \bar{1}$ and $\bar{0} \longrightarrow 1$ transitions should each shift initially to the blue upon twisting, with a progressive diminution of intensity. The intensities of the other two transitions should be relatively insensitive to twisting.[27] As

---

[27] In speaking of intensity changes, we refer to percentage changes of the oscillator strength.

θ approaches $\pi/2$, the frequencies and intensities of all four transitions should approach those of the corresponding benzene transitions.

Next, we take up the case where the inductive effect is included but the overlap integrals are neglected. In place of (18a), we now have

$$A_1 = A_2 > 0,$$

and the B configuration energies become degenerate at a value of θ less than $\pi/2$. The intensity of the $\bar{0} \longrightarrow 1$ transition should initially decrease upon twisting, the transition should become accidentally forbidden at an intermediate value of θ (cf. Fig 5b), and subsequently the intensity should increase until θ becomes $\pi/2$. No other new features are brought in, except in that, when $\theta = \pi/2$, the transition frequencies are no longer expected to revert exactly to the corresponding benzene frequencies.

Finally, we consider the case where the inductive effect is again neglected, but the overlap integrals are taken into account. The effect of overlap is to decrease by a substantial amount the numerator of B_1, and at the same time to increase that of B_2 by about the same amount. Therefore, where overlap is included, the predicted behavior of the band frequencies tends more nearly to conform to Type iii than to where overlap is neglected. Type i behavior might still be predicted, however, if δ were sufficiently close to n_1^o. As the configurational interaction integrals depend only slightly on the AO overlap integrals, it follows that the calculated electronic state

energies are substantially increased by the inclusion of overlap[28] (cf. Figs. 2,4). Since B_1 and B_2 may now become equal,

---

28 In the SCF method upon which the present semi-empirical treatment is based, the difference between the ground and excited state effective Hamiltonians is allowed for only in a crude approximation.[29] Some preliminary calculations by the authors[30] indicate that, if a more accurate correction were applied in the semi-empirical method, the calculated energy of the state would be lowered relative to the ground state (i.e., in opposition to the effect of inclusion of overlap) and the energies of the other three BA states would be increased. A corresponding correction for CT transitions would probably be especially large.

29 P. O. Lowdin, Advances in Physics 5, 1 (1956).

30 E. G. McRae and L. Goodman, unpublished.

---

there exists the possibility of the $\bar{0} \longrightarrow \bar{1}$ transitions being accidentally forbidden throughout the range of θ. In any case, with overlap included, the predicted intensity is smaller than with overlap neglected.

Charge - Transfer Transitions:—The lowest energy CT configurations, together with the corresponding singlet configurational functions, are as follows:

$$s)^1\ 0)^2\ \bar{1})^2\ 1)^2\ 2)^1;\quad x_{s\bar{2}},\qquad B$$

$$s)^1\ 0)^2\ \bar{1})^2\ 1)^2\ 2)^1;\quad x_{s2}.\qquad A$$

Although the $n \rightarrow \pi^*$ and $\pi \rightarrow \pi^*$ classification of electronic transitions is not strictly applicable in the cases we are discussing here (C_2 symmetry), it is helpful and not too inaccurate to think of the CT transition changing from the $\pi \rightarrow \pi^*$ to the

$n \rightarrow \pi^*$ type as θ runs from 0 to $\pi/2$. Since $n \rightarrow \pi^*$ transitions are generally weak as compared with those of the $\pi \rightarrow \pi^*$ type, it is to be expected that the CT oscillator strengths should decrease upon twisting. By analogy with $n \rightarrow \pi^*$ transition intensities in substituted benzenes (not heterocyclics), an upper limit for the CT oscillator strength at $\theta = \pi/2$ may be set at 0.001.

As for CT transition intensities at $\theta < \pi/2$, we may be guided to some extent by the values of the one-configuration transition moments such as

$$\mathbb{m}_{s\bar{2}} = \sqrt{2} \int \Phi_s \, \mathbb{m} \, \Phi_{\bar{2}} \, d\tau,$$

which are given in Table 5. It must be kept in mind, however, that the CT intensities could be greatly increased through interaction between BA and CT configurations.[31] As the relevant

---

31 Conversely, the BA transition energies and intensities could be affected by low-energy CT configurations. A possible case of this is discussed in Sec. 6.

CI integrals all tend to zero (or to very small values) as θ approaches $\pi/2$, there is no need to revise our conclusion concerning the limiting CT intensity as θ approaches $\pi/2$.

6. APPLICATION TO N,N-DIMETHYLANILINE AND RELATED MOLECULES.

Assignment of Transitions:--The effects of intramolecular twisting on the spectra of N,N-dimethylaniline and related molecules have been studied experimentally by Wepster,[4,5] by

Klevens and Platt[6] and by Remington.[7] A representative selection of the experimental data is reproduced in Table 6. The structures of the less familiar molecules figuring in Table 6 are shown below.

In the molecules listed in Table 5, ortho-substitution or intramolecular bridge formation leads to twisting of the amino group about the bond joining the nitrogen atom to the adjacent ring carbon atom. There is little doubt that the observed intensity changes may be attributed primarily to intramolecular twisting perturbations, since in the absence of intramolecular twisting, alkyl-, chloro- or bromo- substitution has a relatively small effect on band intensities. In order approximately to eliminate the direct effects of substitution on the band frequencies, the observed frequencies are corrected by adding the difference between the corresponding band frequencies

for benzene and for an appropriate substituted benzene.[32] The corrected band frequencies are given in Table 6. The corrections actually depend in part on the band assignments indicated below. The nine molecules appearing in the table are designed numerically in what is thought to be the order of increasing twist angle, the twist angle being defined, following Klevens and Platt,[6]

32 The ortho substituent correction of the $\bar{0} \longrightarrow 1$ and $\bar{0} \longrightarrow \bar{1}$ transitions in Table 6 represent the difference between the $\bar{0} \longrightarrow 1$ and $0 \longrightarrow \bar{1}$ o-o band energies of benzene and the corresponding alkyl or halo benzene applied to the band maxima of the dimethylaniline derivative. For the $0 \longrightarrow 2,2$ transitions band maxima are used throughout.

This procedure is justified on the following grounds: The calculations reported in this paper assume the same molecular dimensions in the ground and excited states and therefore apply to vertical transitions. On first thought, this would imply that an experimental band maximum is to be used for comparison with a theoretical excitation energy. However, the problem is complicated by the $\bar{0} \longrightarrow 1$ and $\bar{0} \longrightarrow \bar{1}$ transitions becoming forbidden, or nearly forbidden as θ runs to $\pi/2$. (The presence of an inductive effect will remove the formal forbiddeness at $\theta = \pi/2$, but will in general not change the sense of the following argument.) A weakly perturbed transition may be regarded as retaining "memory" of the forbiddeness and therefore possesses a weak o-o band.[33] In the following series of substituted benzenes of increasing substituent perturbation (benzene, toluene, chlorobenzene, fluorobenzene), the o-o band in the vapor spectrum increases in strength until the band maximum occurs at the o-o transition. For these cases the vertical transition is likely the o-o one. Since our corrections are for the alkyl and halogen groups it seems clear that the substituent correction should be the difference in the o-o band energies of benzene and the substituted benzene for the $\bar{0} \longrightarrow 1$ and $\bar{0} \longrightarrow \bar{1}$ transitions; but for the allowed $\bar{0} \longrightarrow 2,\bar{2}$ transitions the difference in band maxima. These corrections are applied to the band maxima of the Dimethylanilines since o-o forbiddeness is believed to be sufficiently removed for the maximum to be the vertical transition. This procedure may be open to some question in VII, where the $\bar{0} \longrightarrow 1$ transitions show benzene structure and the vertical transition is not completely unambiguous. We note that this implies a small error in our empirical parameters since benzene band maxima were used throughout.

33 W. W. Robertson and F. A. Matsen, J. Am. Chem. Soc. 72, 5252 (1950).

as the angle of inclination to the ring plane of the line joining the amino carbon atoms. Except for VII and possibly IIc, it is not possible to specify actual values of θ because the molecular geometries are not known. On the basis of symmetry, we can say fairly certainly that the twist angle in VII (benzoquinuclidine) is 90°, and that in IIc (Troger's base) it probably lies close to 45°.[5] The upper and lower limits for the twist angles are reproduced in Table 7. The figures quoted there provide the basis for the ordering of molecules in Table 6.

The parameter θ cannot be identified with the twist angle, because at a given twist angle θ depends on the type of hybridization of the nitrogen valence orbitals. The values of θ corresponding to the limiting twist angles are shown in Table 7. From this table, we conclude that θ increases monotonically with twist angle.

The trends in the observed absorption energies and intensities are illustrated in Figs. 4a and 5a respectively. The trends in the spectra as the twist angle approaches $\pi/2$ suggest definite assignments for each of the observed absorptions. Thus the lowest-frequency transition, which in I appears weakly ($f = 0.04$) at 4.2 e.v., shifts sharply to the blue with pronounced diminution in intensity. In VII, the band has a frequency very close to that of the $A_{1g} \longrightarrow B_{2u}$ band in benzene, and has similar vibrational structure. Accordingly the band may be attributed to the BA transition $\bar{0} \longrightarrow 1$.[34,35] We should not be surprised

---

[34] This is contrary to an assignment made by Klevens and Platt.[6]

[35] See also the similar assignments of Goodman and Shull.[15]

---

that the $\bar{0} \longrightarrow 1$ band intensity in VII is considerably larger (by a factor of four) than that of the benzene $A_{1g} \longrightarrow B_{2u}$ band, since this effect is predicted theoretically (see below). However, the intensities of the other BA bands are expected to revert to those of the corresponding benzene bands as θ approaches $\pi/2$.

The next band is fairly strong ($f = 0.28$) in I. It loses intensity upon twisting and disappears altogether in VII ($f < 0.001$). The band frequency suffers relatively little change upon twisting, remaining close to 5.0 e.v. The transition must be of the CT type; otherwise, its intensity would approach that of one or other of the benzene transitions, all of which have oscillator strengths in excess of 0.001. By similar reasoning, the band at 6.2 e.v. in I ($f = 0.54$) may be attributed to the BA transition $\bar{0} \longrightarrow \bar{1}$. As the twist angle increases, the band shifts to the red with a fairly pronounced drop in intensity.

Finally, the absorption at 7.0 e.v. in I ($f = 0.79$) may be attributed to the remaining two BA transitions, $\bar{0} \longrightarrow 2$ and $\bar{0} \longrightarrow \bar{2}$, which presumably lie so close together that they appear as one.[15] Its behavior is different from that of the other three bands, in that its intensity undergoes only a small fractional change as a result of intramolecular twisting. Thus, its intensity in VI is twenty per cent less than in I while the intensities of each of the other three bands are diminished by a factor of three or more.

Empirical Parameters:--In order to apply the theory described in Sec. 3, we choose values of δ which, for $\theta = 0$, lead to

approximately the correct intensity for the $\bar{0} \longrightarrow 1$ transitions in I. With overlap neglected, we adopt $\delta = 1.5$,[36] and with overlap included $\delta = 1.0$. Where the inductive effect is included, we adopt $\delta_1 = 0.2\delta$. Throughout, we choose $\rho_0 = 1$. This means that, where overlap is included, the 7-1 overlap integral at $\theta = 0$ is taken equal to the C-C overlap integral. These values are appropriate to a substituent which interacts rather strongly with the ring. In particular, it is considered to represent with reasonable accuracy the strength of the 7-1 π-bond in N,N-dimethylaniline. We note that setting $\rho_0 = 1$ (implying $\beta_{17} = \beta$ at $\theta = 0$) does not imply equality between the 7-1 and C-C π-bond strengths, because β is diminished in magnitude by the term involving MO electron repulsion integrals while β_{17} does not contain a term of this type. Since in substituted benzenes the 7-1 bonds are somewhat weaker than the bonds between ring carbon atoms, the adopted 7-1 overlap integral value may be viewed as an upper limit. In conformity with the above assumptions about the overlap integrals, we assume all bond lengths equal, and equal to the carbon-carbon bond length in benzene (1.4 Å). For purely conjugative substituents, the MO

---

36 In Ref. 15 we have estimated $\delta \sim 1.0$ for I by fitting the energy of the $\bar{0} \longrightarrow 1$ transition. Our conclusions are rather insensitive to the particular numerical values assigned to the parameters, except where otherwise noted, and are therefore considered to be fairly generally applicable. We note that the intensity of the $\bar{0} \longrightarrow 1$ transition should be highly sensitive to assymmetry of charge,[37] and thus valid for conjugative parameter correlation.

37 L. Goodman, I. G. Ross and H. Shull, J. Chem. Phys. 26, 474 (1957).

secular equation was solved by the method of Goodman and Shull, as described in Sec. 3. The inductive effect was treated by first-order perturbation theory,[38] adopting the MO's for the purely conjugative case as zeroth-order functions. All solutions were obtained subject to conditions (5) and (8). The results of the calculations are given in Tables 3 and 4. To illustrate an intermediate stage of calculation, the MO's and MO energies are given in Table 2.

[38] H. Eyring, J. Walter, and G. E. Kimball, "Quantum Chemistry", Wiley and Sons, New York, 1944, p. 95.

Benzene-analogue Transitions:--The behavior of the observed A → A transition energies is on the borderline between Types ii and iii while the A → B transition energies exhibit Type ii behavior (Fig. 4a). The trends predicted by the theory with overlap neglected belong to Type i, and thus conflict with experiment. The inclusion of overlap leads to a better agreement with experiment, Type iii behavior being predicted for the A → A, and Type ii for the A → B transition energies (Fig. 4b). Actually, the predicted trends tend to be too much like Type iii. However, we have probably overestimated the 7-1 overlap integral in adopting $\rho_0 = 1$, and a smaller estimate of the 7-1 overlap integral at $\theta = 0$ would lead to an improved agreement with observation. In comparing the calculated and observed trends in transition energies, it should be kept in mind that, in the $\bar{0} \rightarrow 1$ transition, the error incurred through neglect of overlap tends to be cancelled out by the Hamiltonian approximation inherent in the MO method.[28]

The highest-energy absorption shows a definite red shift in the series I, IV, VI. It is natural to expect that, if the observations were extended to VII, the absorption energy would revert approximately to that for the corresponding absorption in benzene. The implied non-monotonic behavior is correctly predicted by the theory with overlap included, according to which both the $\bar{0} \rightarrow 2$ and $\bar{0} \rightarrow \bar{2}$ transition energies pass through minima at intermediate values of θ. The theory predicts deviations from monotonic behavior for the other band energies, but these are relatively slight and are not observed experimentally.

We draw attention to the predicted θ-dependence of the lowest-energy singlet-triplet transition energy given in Table 3. In order to carry out the calculation, the $^3E_{1u}$ state in benzene was assumed to lie at 4.8 e.v., and the lowest-energy triplet state was assumed to be $^3B_{1u}$ (3.8 e.v.). Generally speaking, the trends in corresponding singlet-singlet transitions under intramolecular twisting. However, in each case some differences are expected because of the changed magnitudes of the relevant CI integral. The parallelism between the calculated variations of corresponding triplet and singlet state energies is not greatly disturbed either by the inclusion of overlap or by the choice of different limiting values for the benzene $^3E_{1u}$ state energy.

As far as transition energies are concerned, qualitative conclusions drawn from the calculations for a purely conjugative substituent are not altered by inclusion of the inductive effect.

The highest-energy absorption shows a definite red shift in the series I, IV, VI. It is natural to expect that, if the observations were extended to VII, the absorption energy would revert approximately to that for the corresponding absorption in benzene. The implied non-monotonic behavior is correctly predicted by the theory with overlap included, according to which both the $\bar{0} \rightarrow 2$ and $\bar{0} \rightarrow \bar{2}$ transition energies pass through minima at intermediate values of θ. The theory predicts deviations from monotonic behavior for the other band energies, but these are relatively slight and are not observed experimentally.

We draw attention to the predicted θ-dependence of the lowest-energy singlet-triplet transition energy given in Table 3. In order to carry out the calculation, the $^3E_{1u}$ state in benzene was assumed to lie at 4.8 e.v., and the lowest-energy triplet state was assumed to be $^3B_{1u}$ (3.8 e.v.). Generally speaking, the trends in corresponding singlet-singlet transitions under intramolecular twisting. However, in each case some differences are expected because of the changed magnitudes of the relevant CI integral. The parallelism between the calculated variations of corresponding triplet and singlet state energies is not greatly disturbed either by the inclusion of overlap or by the choice of different limiting values for the benzene $^3E_{1u}$ state energy.

As far as transition energies are concerned, qualitative conclusions drawn from the calculations for a purely conjugative substituent are not altered by inclusion of the inductive effect.

The trends in the observed band intensities are shown, in Fig. 5, in indirect comparison with those predicted theoretically. As predicted, the $\bar{0} \rightarrow 1$ and $\bar{0} \rightarrow \bar{1}$ transition intensities decrease upon twisting, while the $\bar{0} \rightarrow 2$ and $\bar{0} \rightarrow \bar{2}$ intensity sum is relatively insensitive to twisting perturbations.

The fact that the $\bar{0} \rightarrow 1$ intensity in VII ($\theta = \pi/2$) is substantially greater than that of the $A_{1g} \rightarrow B_{2u}$ transition in benzene may be attributed to the inductive effect of the substituent. For the $\bar{0} \rightarrow 1$ transition, the accidental forbiddeness predicted at an intermediate twist angle cannot be discerned with certainty in the experimental results. However, the relationship between the observed transition intensities and energies, which is shown in Fig. 6a, indicates indirectly that it does occur in fact (see below).

The theory fails to account for the high intensity of the $\bar{0} \rightarrow \bar{1}$ transition at small twist angles. With overlap neglected, the calculated oscillator strength ($\theta = 0$) is less than half that observed in the spectrum of I, and a still smaller intensity is predicted with overlap included.[39] In agreement with observation,

---

[39] The condition of "accidental forbiddeness", which was mentioned in Sec. 5 with reference to the $\bar{0} \rightarrow 1$ transition, is approached closely with the present set of parameters. This is a fortuitous circumstance, however, and is not an essential implication of the theory as applied here. To illustrate this, we point out that the consideration of the inductive effect, with overlap included, could lead to a considerable increase of the predicted intensity.

---

the observed intensities in the series I, II(b), III, IV, V, VI are related linearly to the corresponding transition energies (Fig. 6a). The points for II(a) and II(c) depart somewhat from

the main trend, while the point for VII lies well above the straight line passing through the points for I and V. The shapes of the corresponding theoretical curves are shown in Fig. 6b. At low energies, the observed linear relationship is reproduced in all three curves. This comes about from the approximate $\cos^2 \theta$ dependence of both the intensity and excitation energy for small and moderate θ values. For larger twist angles the intensity, in particular, deviates markedly from $\cos^2 \theta$ behavior. At higher energies, the observed behavior appears to conform qualitatively to that predicted with the inductive effect included. The probable trend followed by the experimental points, including that for VII, is indicated by the broken line in Fig. 6a. From the figure, it is seen that the available information definitely suggests that the intensity of the $\bar{0} \rightarrow 1$ transition should pass through a minimum value at an intermediate value of θ, as predicted theoretically. We note that the data for II(a), II(b) and II(c) implies that the nitrogen - atom valence states for those molecules may be different from the unbridged cases.

The Oscillator Strength Sum:—Klevens and Platt have pointed out that the sum of the oscillator strengths for the observed transitions decreases upon twisting, from 1.7 in I to 0.9 in VI. In qualitative accord with that result, the sum of squares of the transition moments listed in Table 5 decreases with increasing θ. The predicted trend is not so pronounced as that observed. However, the agreement between theory and experiment would be improved by taking more transition moments

into account, and by allowing appropriately for changes in the transition energies.

Previous Work:--The theory of twisting effects on the spectra of ortho-substituted N,N-dimethylanilines has been discussed recently by Murrell.[40] Although Murrell's method of

---

[40] J. W. Murrell, J. Chem. Soc. 1956, 3779.

---

treatment is quite different from that adopted in the present work, it is gratifying that his conclusions are almost identical with some of those of the present study.

Acknowledgments:--We thank Professor M. Kasha for providing the opportunity to undertake this study. We thank Professors M. Kasha and H. Shull for many helpful discussions; and Dr. P. O. Lowdin for some helpful suggestions, which have been followed in this paper.

Table 1

EMPIRICAL PARAMETERS

Overlap Approximation	Excited State	β(e.v.)	CI Integral
Overlap Neglected	^1A	-3.30	0.121β
	^1B	-2.98	0.353β
	^3A	-2.15	0.233β
Overlap Included	^1A	-3.09	0.129β
	^1B	-2.79	0.377β
	^3A	-2.02	0.248β

Table 2

MO'S AND MO ENERGY FACTORS[a]

		Overlap neglected						Overlap included					
θ (°)	i	a_{io}	a_{is}	a_{il}	a_{i2}	a_{i3}	n_i	a_{io}	a_{is}	a_{il}	a_{i2}	a_{i3}	n_i
0	0	0.7219	0.6264	0.2671	0.1078	0.0588	2.3543	0.7027	0.5554	0.2570	0.0819	0.0389	1.4961
	s	-0.6748	0.5490	0.4747	0.1188	0.0611	1.6678	-0.6857	0.4937	0.4979	0.0935	0.0392	1.1631
	1	-0.1501	0.4929	-0.8363	0.1714	0.0756	0.6597	-0.1982	0.5733	-0.8306	0.1845	0.0648	0.4870
	2	-0.0280	0.2146	-0.0582	-0.9694	0.1005	-1.1278	-0.0548	0.3483	-0.1033	-0.9820	0.1223	-1.6683
30	0	0.7706	0.5852	0.2307	0.0895	0.0485	2.2685	0.7605	0.5188	0.2238	0.0682	0.0302	1.4584
	s	-0.6227	0.6123	0.4615	0.1155	0.0593	1.6523	-0.6262	0.5564	0.5056	0.0921	0.0385	1.1506
	1	-0.1332	0.4840	-0.8510	0.1411	0.0630	0.7156	-0.1799	0.5751	-0.8362	0.1541	0.0550	0.5335
	2	-0.0217	0.1899	-0.0433	-0.9777	0.0743	-1.0971	-0.0429	0.3103	-0.0811	-0.9880	0.0899	-1.5865
60	0	0.9127	0.3930	0.0367	0.0196	0.0196	2.0879	0.9185	0.3367	0.0996	0.0272	0.0119	1.3734
	s	-0.4021	0.8161	0.4023	0.0912	0.0464	1.5856	-0.3814	0.7580	0.4864	0.0757	0.0313	1.0925
	1	-0.0731	0.4038	-0.9093	0.0623	0.0287	0.8718	-0.1107	0.5300	-0.8698	0.0735	0.0273	0.6690
	2	-0.0076	0.1135	-0.0162	-0.9931	0.0240	-1.0330	-0.0153	0.1873	-0.0296	-0.9970	0.0283	-1.4181
90	0	1	0	0	0	0	-1.0000	1	0	0	0	0	1.3333
	s	0	1	0	0	0	1.0000	0	1	0	0	0	1.0000
	1	0	0	1	0	0	1.5000	0	0	1	0	0	0.8000
	2	0	0	0	1	0	1.0000	0	0	0	1	0	-1.3333

(a) Inductive effect neglected.

Table 3

CALCULATED TRANSITION ENERGIES AND INTENSITIES

θ (°)	Upper State	Overlap neglected Inductive effect neglected		Overlap neglected Inductive effect included		Overlap included Inductive effect neglected	
		E(e.v.)	f	E(e.v.)	f	E(e.v.)	f
0	$^3A_1$	3.61	-	3.54	-	3.91	-
	1	4.53	0.041	4.60	0.018	4.74	0.058
	1	5.77	0.139	5.65	0.156	6.31	0.022
	2	6.73	0.447	6.54	0.468	7.23	0.462
	2	6.73	0.537	6.71	0.507	6.96	0.769
30	$^3A_1$	3.64	-	3.58	-	3.86	-
	1	4.63	0.028	4.69	0.008	4.80	0.041
	1	5.84	0.109	5.73	0.130	6.25	0.014
	2	6.71	0.472	6.54	0.491	7.06	0.486
	2	6.75	0.548	6.72	0.516	6.91	0.743
60	$^3A_1$	3.74	-	3.70	-	3.82	-
	1	4.83	0.004	4.83	0.002	4.93	0.006
	1	6.05	0.029	5.97	0.046	6.18	0.014
	2	6.79	0.597	6.68	0.528	6.84	0.547
	2	6.84	0.590	6.80	0.558	6.88	0.646
90	$^3A_1$	3.80	-	3.80	-	3.80	-
	1	4.90	0	4.86	0.012	4.90	0
	1	6.20	0	6.20	0	6.20	0
	2	7.00	0.600	6.03	0.581	7.00	0.600
	2	7.00	0.600	7.00	0.600	7.00	0.600

Table 4

STATE FUNCTIONS

θ (°)	Overlap neglected Inductive effect neglected Λ_A (o)	Λ_B (o)	Overlap neglected Inductive effect included Λ_A (o)	Λ_B (o)	Overlap included Inductive effect neglected Λ_A (o)	Λ_B (o)
0	24.0	19.7	26.3	14.8	-3.0	23.3
30	21.3	16.7	24.5	10.7	1.8	20.0
60	11.7	7.1	10.5	-0.2	5.8	9.2
90	0	0	0[a]	-8.0	0	0

(a) Higher order approximations than first-order perturbation theory will cause Λ_A to be slightly different from zero in the presence of an inductive perturbation.

Table 5

TRANSITION MOMENTS [a-c]

θ (°)	M_1^1	M_2^1	M_1^1	M_2^1	m_{s_2}	m_{13}	m_{s_3}	Σ
0	.007	.937	.095	1.095	.383	.239	.166	2.32
30	.003	.944	.078	1.078	.382	.198	.162	2.27
60	.016	.966	.029	1.029	.334	.062	.128	2.12
90	0	1.0000	0	1.000	0	0	0	2.00

(a) Both overlap and inductive effect neglected.

(b) The magnitudes of the transition moments are given in units of ϵR, where ϵ denotes the electronic charge and R denotes the C-C bond length. The m's denote one-configuration transition moments, and Σ denotes the sum of squares of the transition moments in columns 2-8.

(c) The following were found to be less than 0.1 ϵR at θ = 0: m_{s_2}, m_{o_2}, m_{o_2}.

Table 6

SPECTRA OF N,N-DIMETHYLANILINE AND RELATED MOLECULES[a]

Substance	$\epsilon_{max} \times 10^{-3}$	f	E_{obs} (e.v.)	E_{corr} (e.v.)[b]	f sum
I. N,N-Dimethylaniline	2.39	0.036	4.14	--	1.66
	15.50	0.29	4.92	--	
	22.2	0.54	6.18	--	
	36.6	0.79	7.02	--	
IIa. N-Methylindoline	2.9	0.041	4.07	4.13	
	10.0	0.21	4.87	--	
b. N-Methyl-homo-tetrahydro-quinoline	2.0	0.021	4.34	4.37	
	8.5	0.17	4.88	--	
c. Troger's Base	2 x 1.11	2 x 0.017	4.24	4.32	
	2 x 4.25	2 x 0.08	4.99	--	
III. o-Chloro-N,N-dimethylaniline	1.8	0.026	4.20	4.34	1.28
	7.6	0.14	4.84	--	
	18.5	0.39	5.82	6.18	
	36.10	0.72	6.54	6.76	
IV. N,N-Dimethyl-o-toluidine	1.30	0.014	4.45	4.52	1.07
	6.36	0.128	4.98	--	
	11.4	0.23	5.96	6.17	
	30.8	0.69	6.66	6.84	
V. o-Isopropyl-N,N-dimethylaniline	1.17	0.013	4.48	4.54	
	4.30	0.089	4.98	--	
	(12.0)	--	5.95	6.16	
VI. 2,6-N,N-Tetramethylaniline	--	(< 0.002)	4.61	4.76	0.86
	2.09	--	4.76	--	
	8.6	0.15	5.84	6.18	
	36.1	0.66	6.37	6.70	
VII. Benzoquinuclidine	0.5	0.005	4.78	4.82	
	(0.4)	(0.004)	(4.88)	--	

(Table 6, continued)

(a) Molar extinction coefficients, ϵ max, at absorption maxima, oscillator strengths f and observed transition energies E_{obs} (absorption maxima): data of Wepster,[4,5] Klevens and Platt,[6] and Remington.[7] Where oscillator strengths were not given in the literature, they were estimated from the published absorption curves. In some cases oscillator strengths could not be estimated because of overlapping by adjacent bands. Uncertain results are given in parentheses.

(b) Transition energies corrected on the assumption that alkyl substitution has the same effect as alkyl substitution in benzene.[32] Spectra of benzene and alkyl benzenes (4.9 e.v. band) from API tables and far ultraviolet spectra of benzene, alkyl benzenes from Platt and Klevens (J. R. Platt and H. B. Klevens, Chem. Revs. 41, 301 (1947); and of chlorobenzene from Klevens and Platt Survey of Vacuum Ultraviolet Spectra of Organic Compounds in Solution, Report of Laboratory of Molecular Structure and Spectra, University of Chicago (1953-1954).

Table 7

LIMITING TWIST ANGLES[a] AND θ-VALUES[b]

Substance	Twist Angle (°) Planar	Twist Angle (°) Pyramidal	θ (°) Pyramidal
I.	0	0	35
IIa.	0	30	45
IIc.	-	45	55
III.	58	44	54
IV.	75	56	63
VI.	75	90	90
VII.	-	90	90

(a) Twist angles estimated by Klevens and Platt[6] (III, IV, VI) and by Wepster[5] (IIc), for limiting substituent shapes.

(b) sp^2 hybridization assumed for planar substituent (θ then equals twist angle), and sp^3 for pyramidal substituent.

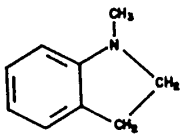

IIa

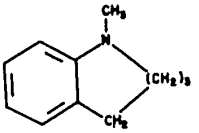

IIb

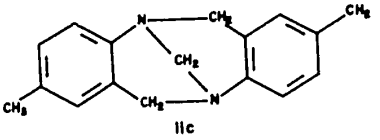

IIc

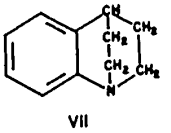

VII

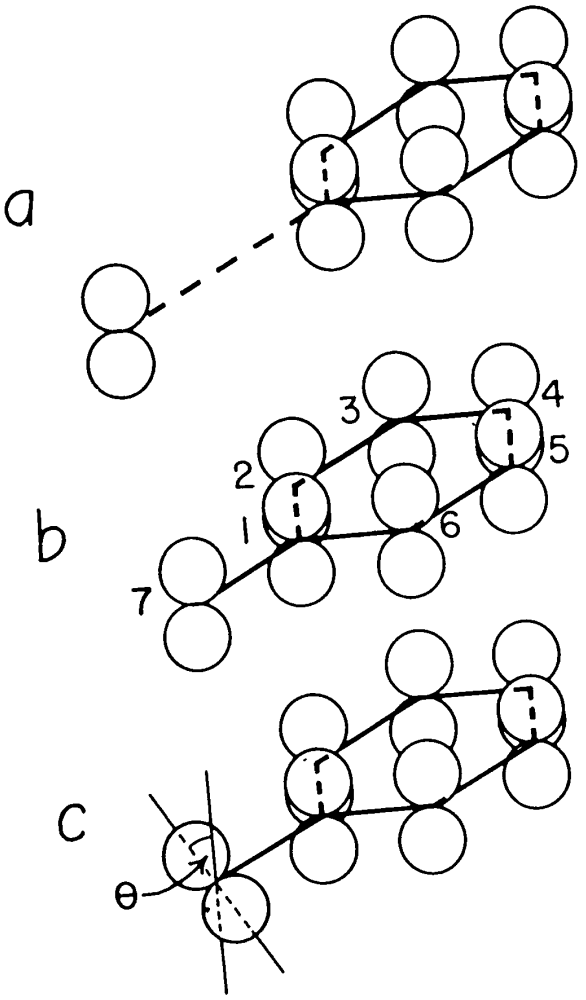

Fig. 1. - AO's in substituted benzenes.

(a) Zeroth-order case.
(b) Substituent not twisted.
(c) Substituent twisted.

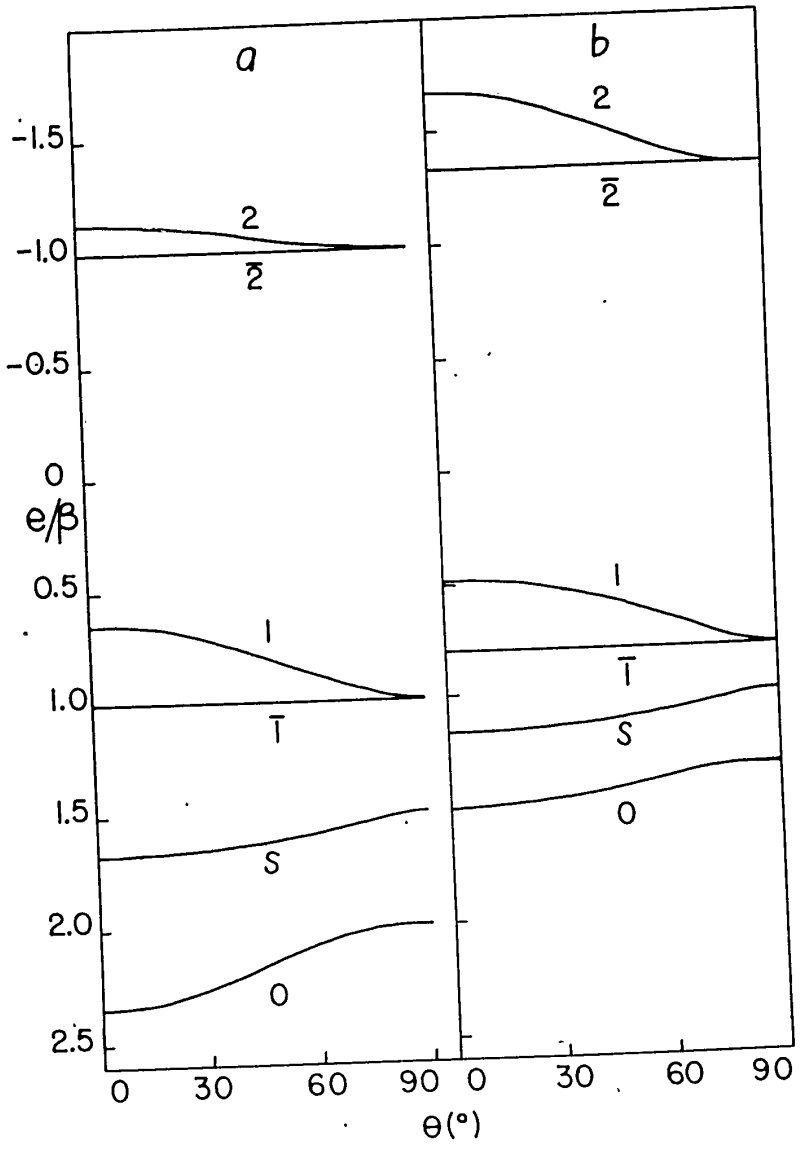

Fig. 2. - The effect of overlap on the MO energies.

(a) Overlap neglected.
(b) Overlap included.

The inductive effect is neglected for both (a) and (b).

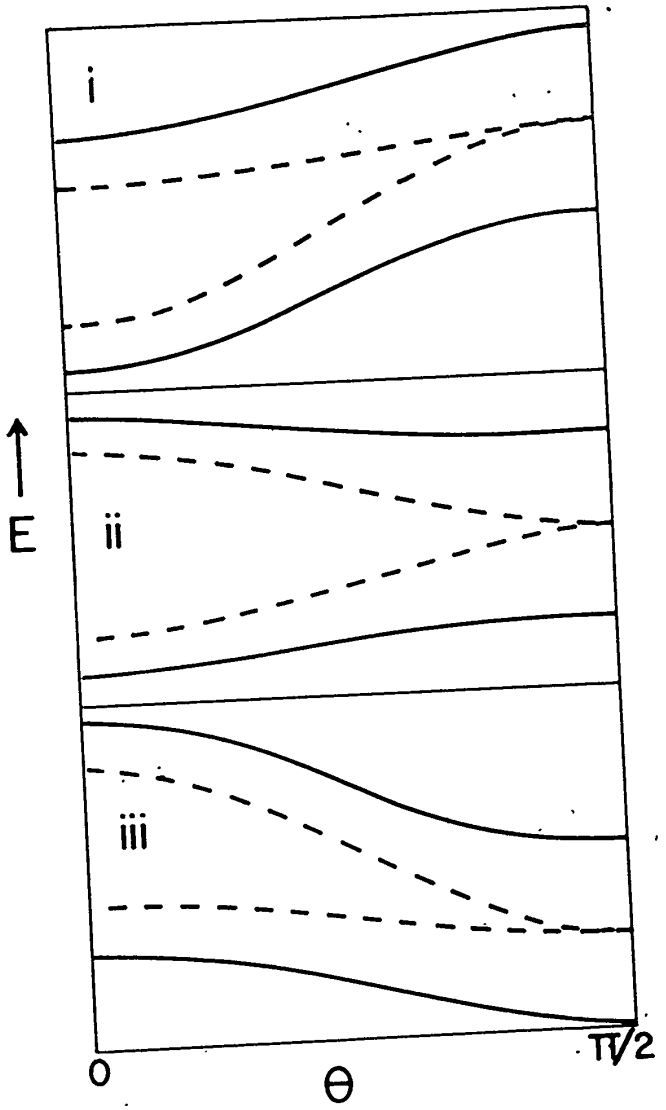

Fig. 3. - Trends in configurational energies (broken lines) and state energies (full lines). Types i - iii (schematic).

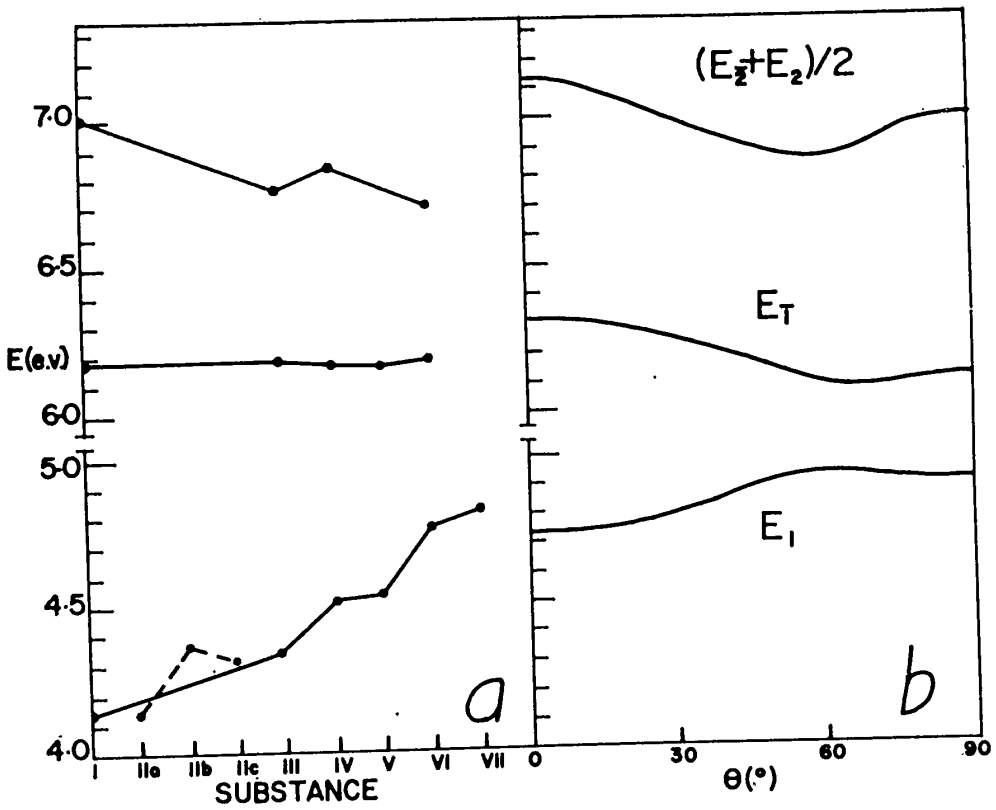

Fig. 4. - (a) Observed BA transition energies (corrected). The points for II a-c appear not to follow the main trend, and are connected by a broken line.

(b) Calculated transition energies; overlap included, inductive effect neglected.

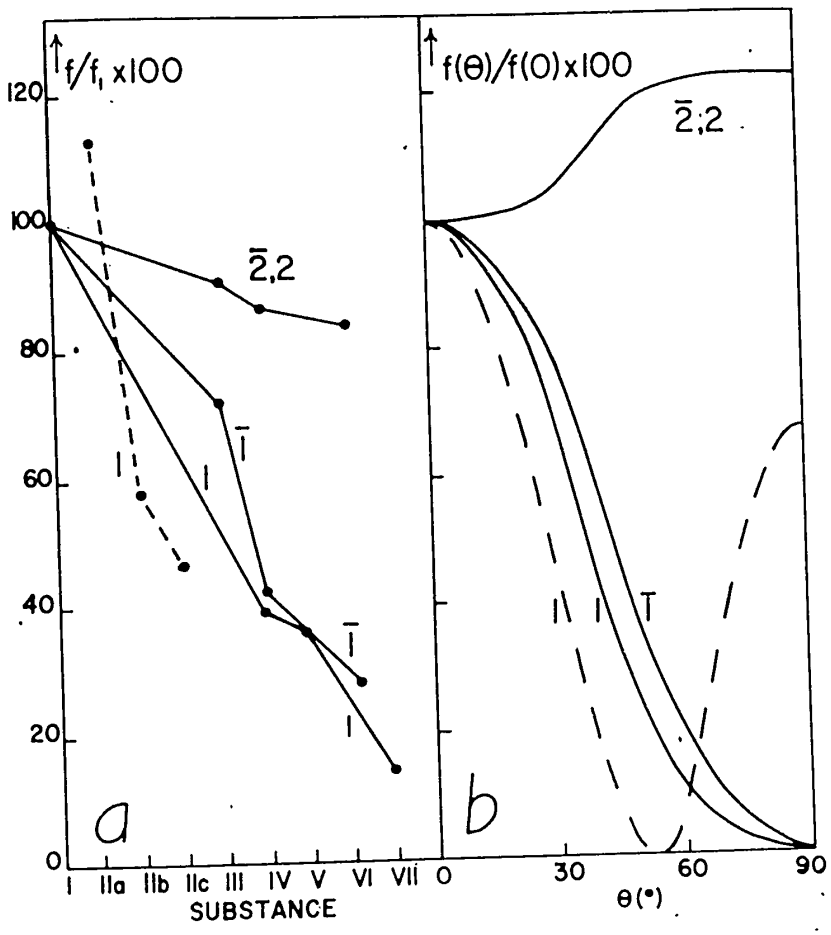

Fig. 5. - (a) Observed BA transition intensities, each expressed as a percentage of the corresponding intensity for I. The points for II a-c appear not to follow the main trend, and are connected by a broken line.

(b) Calculated transition intensities, each expressed as a percentage of the corresponding intensity for $\theta = 0$.

Full Lines - overlap neglected, inductive effect neglected.

Broken Line - overlap neglected, inductive effect included.

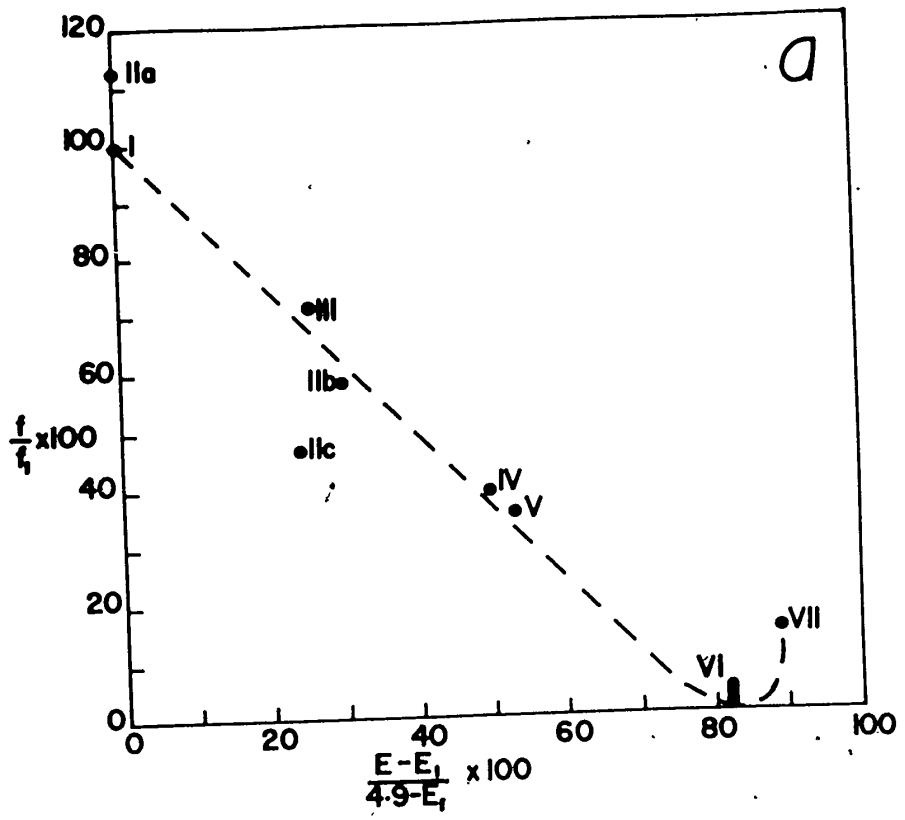

Fig. 6. - The relationship between transition intensity and transition energy for the $\bar{0} \rightarrow 1$ transition.

Experimental:
(a) relative intensity (as in Fig. 5a) vs. percentage frequency shift (corrected transition energies).

(b) Theoretical; relative intensity (as in Fig. 5b) vs. percentage frequency shift.

Dot - dash line - both overlap and inductive effect neglected.

Dashed line - overlap neglected, inductive effect included.

Full line - overlap included, inductive effect neglected.

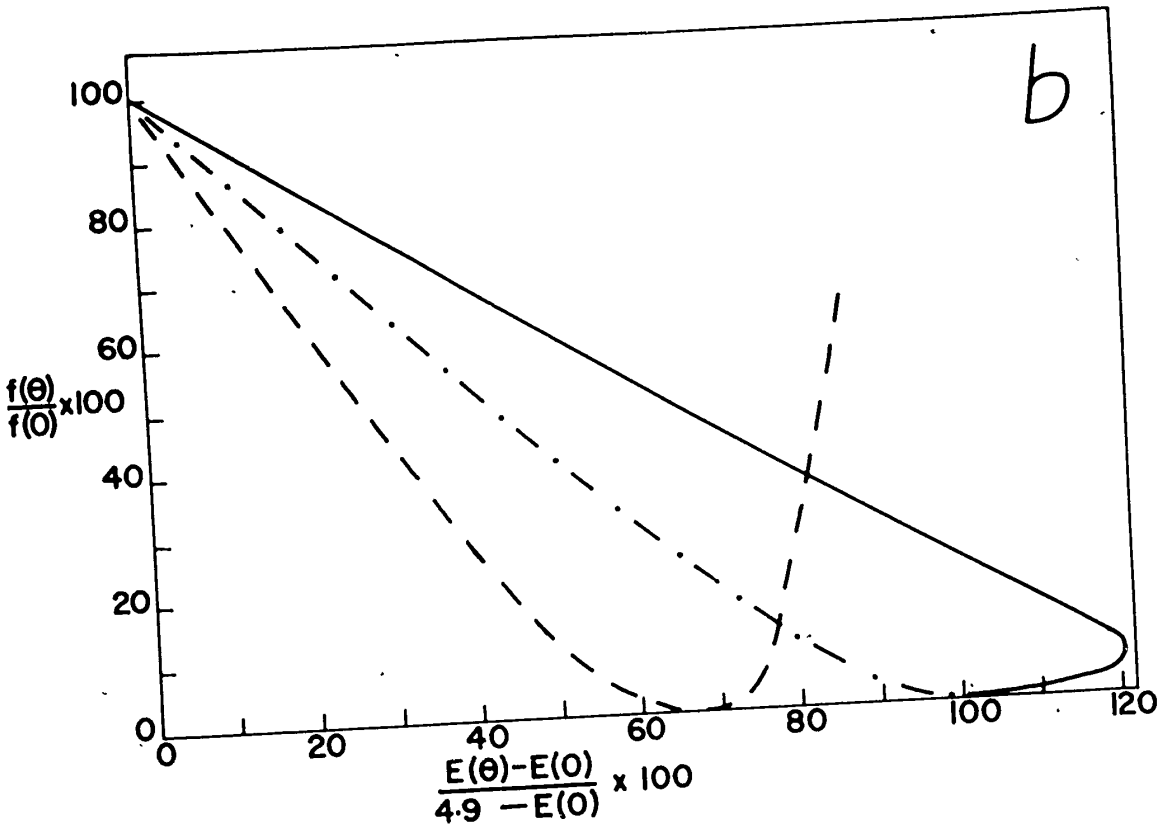

INTRAMOLECULAR TWISTING EFFECTS IN SUBSTITUTED BENZENES. II. GROUND-STATE PROPERTIES.[1,2]

By Eion G. McRae and Lionel Goodman[3]

Department of Chemistry, Florida State University,

Tallahassee, Florida

---

[1] Taken in part from a dissertation submitted by E. G. McRae for the degree of Ph.D. at Florida State University, 1957.

[2] The work was carried out under a contract between the U. S. Air Force, Office of Scientific Research, ARDC, and the Florida State University.

[3] Present addresses: E. G. M. - Chemical Physics Section, C.S.I.R.O., Melbourne, Australia; L. G. (to whom reprint requests should be addressed) - Department of Chemistry, Pennsylvania State University, University Park, Pennsylvania.

(Abstract)

The effects on ground-state properties of twisting a substituent group about the substituent-ring bond in substituted benzenes are discussed from the viewpoint of semi-empirical MO theory. The ground-state properties are discussed with reference to a parameter, θ, which generally increases as the substituent is twisted. The substituent-ring bond order varies approximately as $\cos\theta$, and the following vary approximately as $\cos^2\theta$: the resonance energy, charge densities, ring C-C bond orders and the π-electronic dipole moment. The θ-dependence of the total dipole moment is discussed. Numerical applications to N,N-dimethylaniline and related molecules are described, including a detailed treatment of the dipole moments of N,N-dimethylaniline and some of its ortho-substituted derivatives. A brief discussion of the valence state of the dimethylamino group is included.

I. INTRODUCTION

This is the second of two papers dealing with the effects of intramolecular twisting in substituted benzenes. In the preceding paper,[4] which will be referred to as I, we discussed twisting effects on electronic spectra. The present paper is devoted to a corresponding treatment of some ground-state properties, specifically resonance energies, charge densities, bond orders, π-electronic and total dipole moments.

[4] E. G. McRae and L. Goodman, ~~J. Chem. Phys. 28, 0000 (1958).~~ in Press.

We adopt the same notation and nomenclature as in I. Also, insofar as they apply to the ground state, the general approach and method of treatment are the same as in I, and numerical applications are based on the same sets of MO's and MO energy factors.

In I, the values of the parameters δ, δ_1 (where non-zero) and ρ_o were chosen so as to secure a reasonably close correspondence between the calculated spectra and the observed spectra of N,N-dimethylaniline and related molecules. In the present paper we assume that this correspondence extends to ground-state properties. The assumption is justified to some extent by the moderately good agreement between the total dipole moment calculated for low values of θ, and the observed dipole moment of N,N-dimethylaniline (Sec. 4).

II. RESONANCE ENERGIES

The excess resonance energy of a substituted benzene, as compared with that of benzene, is given in the semi-empirical method by

$$E^o - E = 2 \sum_{occ} (e_i^o - e_i) = 2\beta \sum_{occ} (n_i - n^o_i), \quad (1)$$

where E denotes the ground-state energy calculated with the inductive effect neglected, E^o denotes the corresponding zeroth-order energy, the summations are carried over orbitals occupied in the ground state.

Excess resonance energies calculated from (1) are given in Table 1. The adopted values of β (Table 1) conform to the resonance energy of benzene, which is taken to be 36 K cal mole^{-1}. When overlap is neglected, the calculated excess resonance energy varies as $\underline{\cos}\ ^2\theta$. This is in accord with second order perturbation theory (see I, Eq. 17). The inclusion of overlap leads to the prediction of a smaller value at $\theta = 0$, and a somewhat sharper initial decrease of excess resonance energy.

III. CHARGE DENSITIES AND BOND ORDERS

The π-electronic charge densities, q_μ, and bond orders, $P_{\mu\nu}$, are calculated with overlap neglected from the formulas

$$q_\mu = \sum_{occ} \left(\sum_{j=s,\,o}^{3} a_{ij}\, c_{j\mu} \right)^2 \quad \text{and} \quad (2)$$

$$P_{\mu\nu} = \sum_{occ} \left(\sum_{j=s,\,o}^{3} a_{ij}\, c_{j\mu} \right) \left(\sum_{j=s,\,o}^{3} a_{ij}\, c_{j\nu} \right). \quad (3)$$

The θ-dependence of the charge densities and bond orders thus calculated may be represented, with errors not greater than 5 per cent of the total variation of each quantity in question, by the formulas:

$$q_\mu(\theta) = q_\mu(\pi/2) + Q_\mu \underline{\cos}^2\theta , \tag{4}$$

$$P_{17}(\theta) = P_{17}(0)\ \underline{\cos}\ \theta, \text{ and} \tag{5}$$

$$P_{\mu\nu}(\theta) = P_{\mu\nu}(\pi/2) + P_{\mu\nu}\ \underline{\cos}^2\theta. \tag{6}$$

Here, Q_μ and $P_{\mu\nu}$ are constants, and (6) does not apply to the 7-1 bond.

The predicted effects of intramolecular twisting on the π-electron charge densities and bond orders are illustrated in A and B, where we have made use of (4) - (6). In A and B, c means $\underline{\cos}\ \theta$. A applies to a purely conjugative substituent, and B to a substituent exerting both conjugative and inductive effects.

A

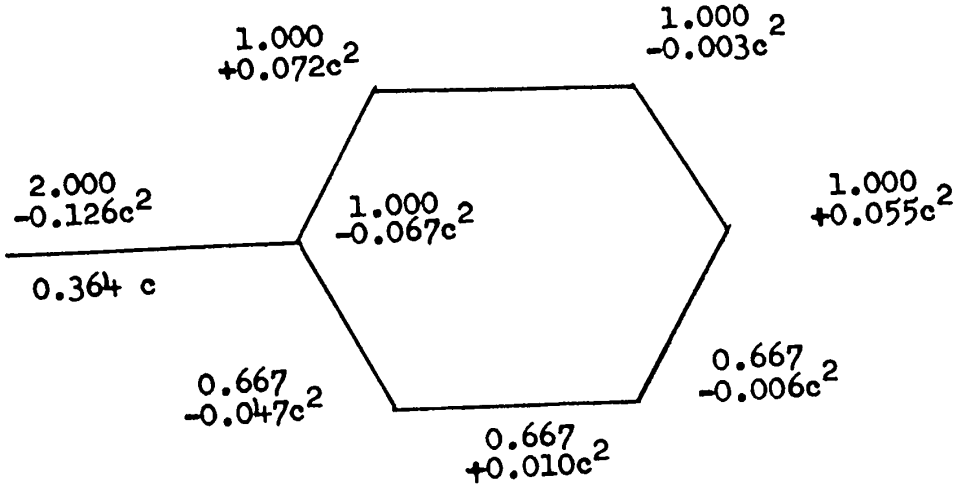

B

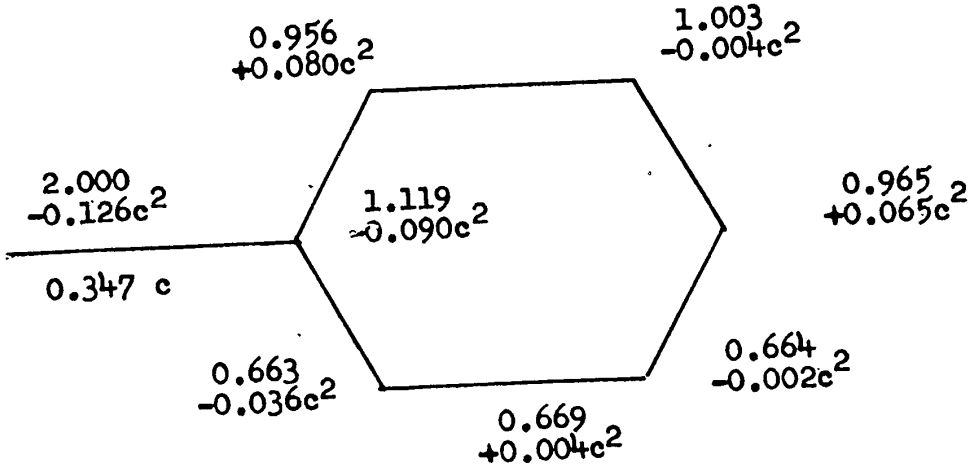

IV. DIPOLE MOMENTS

The π-electronic dipole moments are calculated by a method analogous to that described in I for the transition moments (see I, Eq. 13). The results are shown in Table 2. The results belonging to each of the three series shown in Table 2 may be represented with moderate accuracy ($\pm$ 0.1 Debye) by the formula

$$m_{\pi}(\theta) = m_{\pi}(\pi/2) + M_{\pi} \cos^2\theta, \qquad (7)$$

where m denotes the component of the π-electronic dipole moment in the $1 \rightarrow 4$ direction,[5] and M_{π} is a constant.

[5] The sign convention for dipole moments is such that, if a dipole consisted of a positive charge at atom 1 and a negative charge at atom 4, the positive direction of the moment would be the $1 \rightarrow 4$ direction.

In order to discuss the effect of twisting on the total dipole moment, m, we assume that it is given approximately by

$$\underset{\sim}{m} = \underset{\sim}{m}_{\pi} + \underset{\sim}{m}_{\sigma}, \qquad (8)$$

where $\underset{\sim}{m}_{\pi}$ and $\underset{\sim}{m}_{\sigma}$ respectively denote the π-electronic and σ-electronic dipole moments.[6] We confine our attention to the

[6] Even if there were considerable departure from additivity in (8), it is probable that the resulting error in (8) could be represented by a vector whose magnitude varied approximately as $\cos^2\theta$. In that case, much or all of the error could be absorbed into $\underset{\sim}{m}_{\pi}$, and (8) could still be approximately correct, at least in a formal sense.

case in which $\underset{\sim}{m}_{\sigma}$ has constant magnitude and is inclined at a fixed angle to the 1-4 line. This case is particularly simple,

and is frequently approached in practice. From (8), we infer that the magnitude of the total dipole moment may pass through a minimum value at an intermediate value of θ. Let Ω denote the (fixed) angle of inclination of $\underset{\sim}{m}_\sigma$ to the $1 \rightarrow 4$ direction. The condition for a minimum dipole moment is that the component of the total dipole moment along the $1 \rightarrow 4$ axis be zero, i.e.

$$m_\pi + m_\sigma \cos \Omega = 0. \tag{9}$$

This condition being satisfied, the value of θ at which the minimum should occur is from (7) and (9),

$$\theta_{\widehat{min.}} = \text{Arc cos} \left\{ -\left[m_\pi (\pi/2) + m_\sigma \cos\Omega \right] / M_\pi \right\}^{1/2} \tag{10}$$

and the minimum magnitude of the dipole moment is

$$m_{\widehat{min.}} = m_\sigma \sin \Omega . \tag{11}$$

The inductive effect, as represented by a negative value for $m_\pi (\pi/2)$, causes the minimum to occur at a lower value of θ (see Eq. 10). The qualitative conclusions of the theory are not altered by the inclusion of overlap, since the π-electronic dipole moments calculated with overlap included fit the cos 2θ formula (Eq. 7) quite as well as those calculated with overlap neglected. As shown by (11), the minimum value of the dipole moment depends only on the σ-electronic dipole moment.

Application to N,N-Dimethylaniline and Related Molecules:

The dipole moments of the following molecules, each appropriately corrected for the effect of methyl substitution at the ring, are

shown in Fig. 1a: Ia, N,N-dimethylaniline; Ib, N,N-dimethyl-p-toluidine; IVa, N,N-dimethyl-o-toluidine; IVb, 2,4,N,N-tetramethylaniline; VI, 2,6,N,N-tetramethylaniline. The numbering conforms as closely as possible to that adopted in I. The dipole moment of 2,4,6-tribromo-N,N-dimethylaniline is also of interest; it is given in the caption to Fig. 1a. For each molecule, the observed dipole moment is corrected on the assumption that the effect of methyl or bromo substitution is the same as in the corresponding aniline derivative. The data are those reported by Fischer[7] and by Few and Smith.[8]

7 I. Fischer, Nature 165, 239 (1950).

8 A. V. Few and J. W. Smith, J. Chem. Soc. 1949, 2663.

The trends predicted theoretically are shown in Fig. 1b, in indirect comparison with the observed trend. The two curves shown in Fig. 1b represent limiting trends, which correspond respectively to rigid planar and rigid pyramidal N-C bond configurations, with tetrahedral bond angles in the pyramidal case.

In order to calculate the dipole moment on the assumption of a rigid planar configuration, the σ-electronic dipole moment was set equal to zero.[9] For the rigid pyramidal configuration,

9 This assumption of course is not quite correct since there should be a small positive moment due to the different electronegativities of carbon atoms in the sp^3 and sp^2 valence states. The assumption of zero moment for the planar configuration will cause error in θ_{min}; however the minimum magnitude of the dipole moment will still be zero.

the σ-electronic dipole moment was assigned a fixed value of 0.8 Debye,[10] and $\angle$ was assigned a fixed value of 110°.

[10] This value was chosen to correspond to the dipole moment of an aliphatic tertiary amine.

Throughout, the π-electronic dipole moment was taken to be that calculated with inclusion of the inductive effect (Table 2, column 3).

The theory accounts well for the comparatively sharp decrease of the dipole moment on going from I to IV, and for the fact that the corrected dipole moments of IV and VI are of about the same magnitude. The dipole moments calculated for low values of θ are in quite good agreement with those observed for Ia and Ib, and would have been improved had the values of m_π been taken from column 4 rather than column 3 of Table 2. The significance of this has been pointed out in Sec. I.

The comparison between theory and experiment makes possible some discussion of the shape of the N,N-dimethylamino group in IVa and IVb. Assuming a pyramidal configuration of N-C bonds, with tetrahedral bond angles, θ for these molecules is 63° on the basis of Van der Waals radii. If a planar configuration is assumed, θ is 75° (I Table 7). Now these values of θ do not differ greatly from those at which minima of the dipole moment are predicted theoretically (cf. Fig. 1b). Therefore, if the shape were pyramidal with tetrahedral bond angles, we would expect a dipole moment somewhat greater than the minimum value

given by (11) -- in the present case, 0.7 Debye. On the other hand, if the shape were planar, the dipole moment ought certainly to be less than 0.7 Debye. The observed dipole moment of 0.9 Debye implies a pyramidal shape, with bond angles approaching the tetrahedral. This conclusion is by no means unexpected; in a careful discussion of the structure of Ia, Wepster[11] has

---

11 B. M. Wepster, Rec. Trav. Chim. 72, 661 (1953). Wepster's argument is supported by the rather low estimate of the excess resonance energy arrived at in the present work, where overlap was included (Sec. II).

---

concluded from other considerations that the C-N-C bond angles are close to the tetrahedral angle.

Table 1

EXCESS RESONANCE ENERGIES

θ (^{o})	Excess Resonance Energy (K cal mole^{-1}) Overlap neglected[a]	Overlap included[b]
0	6.5	1.0
30	4.9	0.6
60	1.6	0.1
90	0	0

(a) β = -18 K cal mole^{-1}.

(b) β = -34 K cal mole^{-1}.

Table 2

π-ELECTRONIC DIPOLE MOMENTS

θ (°)	π-Electronic Dipole Moment (Debye)[a]		
	Overlap and inductive effect neglected	Inductive effect included	Overlap included
0	+ 2.02	+ 1.46	+ 2.84
30	+ 1.55	+ 0.99	+ 2.19
60	+ 0.54	- 0.12	+ 0.79
90	0	- 0.72	0

(a) For sign convention, see footnote 5.

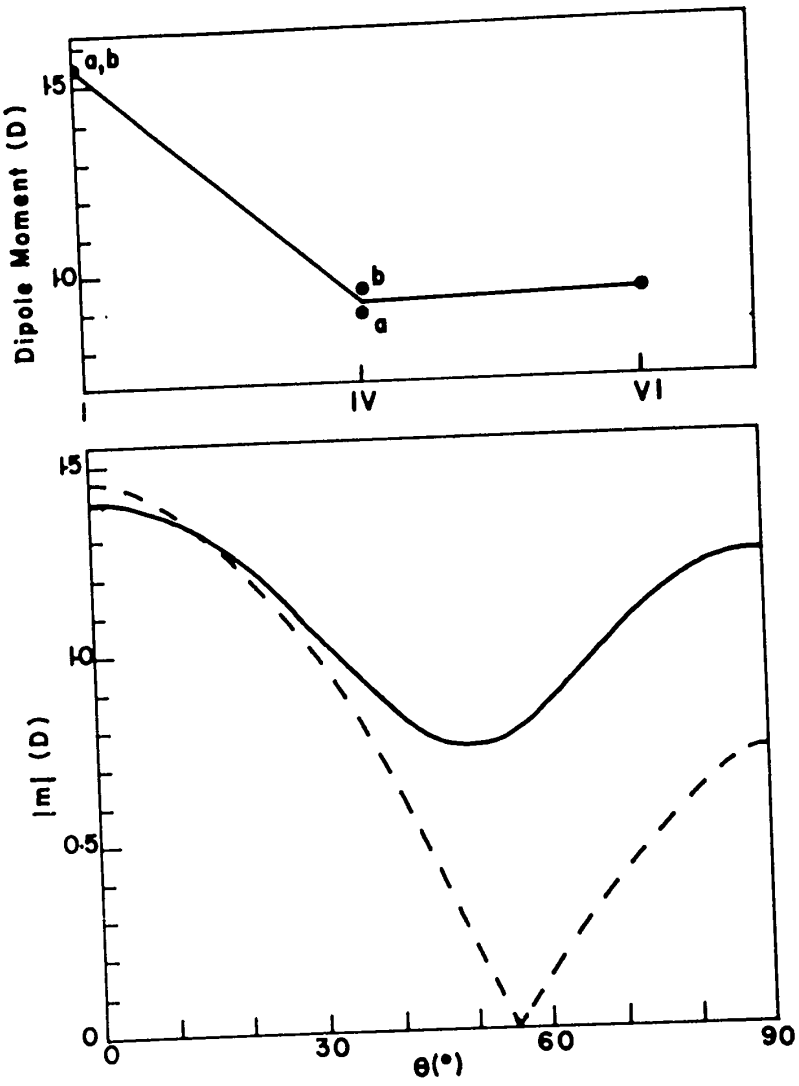

Fig. 1 - (a, top) Observed dipole moments corrected for methyl substitution. The corrected dipole moment for 2,4,6-tribromo-N,N-dimethylaniline (not shown) is 0.86 D; the angle of twist in this case is probably slightly less than for VI.

(b, bottom) Calculated dipole moments. Full line, substituent assumed pyramidal with tetrahedral bond angles. Broken line, substituent assumed planar.

ENERGY TRANSFER IN MOLECULAR COMPLEXES OF SYM-TRINITROBENZENE WITH POLYACENES

I. GENERAL CONSIDERATIONS*

by

S. P. McGlynn**

Coates Chemical Laboratories, Louisiana State University

and

Department of Chemistry, The Florida State University

and

J. D. Boggus

Department of Chemistry, The Florida State University

ABSTRACT

The emission spectra of π-complexes of aromatics with sym-trinitrobenzene have been studied. It is shown that after irradiation in the charge-transfer band, two emissions occur; one the reverse of the charge-transfer absorption, the other from a triplet level of the uncomplexed aromatic. Absorption spectra of complexes, their total emission spectra and delayed emissions are described.

Theoretical considerations of the processes involved lead us to presume that after excitation in the charge-transfer band, some intersystem crossing occurs to a dissociative triplet level of the complex. The resultant production of uncomplexed aromatic in its lowest triplet state then gives rise to the observed phosphorescence. State correlation diagrams and plots of ionisation potential of aromatic versus the energy of the charge-transfer absorption are also described.

---

*Portions of this research are taken from S. P. McGlynn, Ph.D. Dissertation, The Florida State University, Jan., 1956 and J. D. Boggus, M.S. Thesis, The Florida State University, Jan., 1956. The research was done under Contract AF-18(600)-678 between the Office of Scientific Research, U.S. Air Force, and the Florida State University.

**Reprints available from SPM, Coates Chemical Laboratories, Louisiana State University, Baton Rouge 3, La.

ENERGY TRANSFER IN MOLECULAR COMPLEXES OF SYM-TRINITROBENZENE WITH POLYACENES

I. GENERAL CONSIDERATIONS

by

S. P. McGlynn

Coates Chemical Laboratories, Louisiana State University

and

Department of Chemistry, The Florida State University

and

J. D. Boggus

Department of Chemistry, The Florida State University

INTRODUCTION

The origin of the emission spectrum characteristic of many π-complexes of sym-trinitrobenzene (TNB) with aromatics is to a large extent uncertain. Reid[1] observed a general parallelism of the emission spectra of such complexes with the T $\rightarrow$ S luminescence of the free uncomplexed aromatic component; since the anthracene - TNB complex had an emission

1) C. Reid, J. Chem. Phys., 20, 1212, 1214 (1952).

extending from 5200Å into the infrared, he assigned, on the basis of the above parallelism, an energy of 19000 cm^{-1} to the lowest triplet state of anthracene. An energy of 14700 cm^{-1} had already been assigned to this state by Lewis and Kasha,[2] and this value was later affirmed[3] by

---

2) G. N. Lewis and M. Kasha, J. Am. Chem. Soc., 66, 2100 (1944).

3) S. P. McGlynn, M. R. Padhye and M. Kasha, J. Chem. Phys., 23, 593 (1955).

M. R. Padhye, S. P. McGlynn and M. Kasha, J. Chem. Phys., 24, 588 (1956).

---

vibrational analyses of the phosphorescence spectra of anthracene and its derivatives. Despite this exception of the anthracene-TNB complex, the great majority of the other complexes studied[4] did have emissions corresponding almost

---

4) M. M. Moodie and C. Reid, J. Chem. Phys., 22, 252 (1954).

---

exactly to the T⟶S luminescence of the aromatic components. Indeed the remarkable spectral coincidence was interpreted as meaning that the triplet level of the aromatic was almost unaffected energy-wise in the complexing process.[5,6]

---

5) L. E. Orgel, Quarterly Rev. (London), 8, 442 (1954).

6) It was assumed, of course, that emission occurred from a triplet level of the complex which was approximately described as a product of the ground state wave function($^1A_{1g}$) of TNB and the first excited triplet state ($^3B_{2u}$) of anthracene. The energy of this level of the complex was supposed to be only slightly different from its energy at infinite separation of the components.

Bier and Ketelaar[7] noted that the emission and

7) A. Bier and J. A. A. Ketelaar, Rec. trav. chim., 73, 264 (1954).
A. Bier, Rec. trav. chim., 75, 866 (1956).

absorption spectra of both anthracene-TNB and phenanthrene-TNB were approximate "mirror images." They concluded that both processes involved the same two levels, that is that the emission process was the reverse (E ⟶ N) of the charge-transfer absorption (E ⟵ N). This suggestion, however, did not meet with a general acceptance.[8] More

8) H. Sponer, Ann. Rev. Phys. Chem., 6, 193 (1955).

recently Czekalla, Briegleb and collaborators[9] have extended

9) J. Czekalla, G. Briegleb, W. Herre and R. Glier, Z. Elektrochem., 61, 537 (1957).

the work of Bier and Ketelaar. These authors investigated the molecular compounds of hexamethylbenzene with each of eight different acceptor molecules ("acceptor" in the Lewis acid-base sense). The charge-transfer absorption of the complex shifted to the red as the electron affinity of the acceptor component increased; and the emission spectrum red-shifted similarly so that in each case the "mirror-image"

relation was maintained. There remains then but little doubt that, at least for complexes of hexamethylbenzene, the emission is a charge-transfer (E ⟶ N) emission.

For the particular complex tetrachlorophthalicanhydride-naphthalene it was possible[9] because of a large spectral separation, to distinguish two emissions after excitation with Hg 3650: one the reverse of the charge-transfer absorption with half life $\tau = 10^{-9}$ sec, and the other corresponding to the phosphorescence of naphthalene with an unchanged half-life of a few seconds.[10,11]

---

10) J. Czekalla, Naturwissenschaften, 43, 467 (1956).

11) J. Czekalla, Physik. Verh., 6, 104 (1955).

G. Briegleb and J. Czekalla, Z. Electrochem., 59, 184 (1955).

J. Czekalla, A. Schmillen and K. J. Mager, ibid., 61, 1053 (1957).

In view of these experimental results the following interpretation seems reasonable: absorption in the charge-transfer band is followed either by the converse emission, or by intersystem crossing[12] to a dissociative level of the

---

12) M. Kasha, Faraday Soc. Discussions, No. 9, 14 (1950).

---

complex which yields the aromatic in its first excited triplet state. The aromatic hydrocarbon then phosphoresces.

We have arrived at virtually the same conclusions from a study of complexes of TNB with naphthalene, anthracene, phenanthrene and carbazole. This study was both experimental and theoretical.

EXPERIMENTAL RESULTS

It is not our intention of reporting detailed experimental data here.[13] Rather we will give a brief resume of the more important experimental facts and then elaborate on these on the basis of the Mulliken charge-transfer theory of π-complexing.[14] The results are presented for the anthracene-TNB complex, which is fairly typical of the other complexes studied. The observations made on this system were:

13) Paper II in this series. In preparation for publication.

14) R. S. Mulliken, J. Am. Chem. Soc., 72, 600 (1950); ibid., 74, 811 (1952); J. Chem. Phys., 19, 514 (1951); J. Phys. Chem., 56, 801 (1952); J. chim. phys. (France), 51, 341 (1954).

(a) The charge-transfer absorption band of the complex occurs at 4,600Å with $\epsilon_{max} = 1500$.

(b) The complex was dissolved in a 1:1 V/V ethyl ether-isopentane solution, cooled to -190°C and irradiated with filtered light of band pass 4000-4800 Å ($\lambda_{max} = 4358$ Å) from a 1 KW. AH-6 water-cooled mercury lamp. Photography of the resultant emission required 15 minutes. The emission was a broad continuum extending from 5400 to 8200 Å and similar in most respects to that obtained by Reid.[1] An over-lying fine banded structure was observable in the longer

wavelength region of the continuum. The spectrograph used was a Steinheil instrument in a Raman setting.

(c) Excitation of the complex under similar conditions to (b) above, but with a phosphoroscope interposed between light source and spectrograph, yielded an emission which required two hours to photograph. This phosphorescence was very slightly blue shifted from that of pure anthracene,[3] but even though slightly more diffuse it corresponded accurately in vibrational detail to that of the anthracene.

(d) Excitation of pure anthracene dissolved alone in the ether-isopentane glass, and under the same conditions as (b) and (c) above, produced no observable emission, even with exposure times of 24 hours and wide slit (1 mm). Similar excitation of an ether-isopentane glass containing only TNB, and exposure for 20 hours, produced no trace of a photographic image.

(e) Subtraction of the phosphorescence (c) appropriately corrected, from the total emission (b), gave a resultant fluorescence which was a good "mirror-image" of the charge-transfer absorption.

(f) The lifetime of the phosphorescence (c), was of the same order of magnitude as that of pure anthracene, and certainly not less than 10^{-3} sec. as evidenced by its observation in a phosphoroscope of 10^{-4} sec. resolving time. The lifetime of the total emission (b), on the other hand, is 10^{-9} sec.[11]

THEORETICAL RESULTS

The most complete consideration of nitro-complexes thus far,[11] suggests that charge-transfer interaction is responsible for some 50% of the stabilization energy of the ground state.[15] The wavefunction (WF) of the ground or

---

15) In this respect see, however, earlier papers of Briegleb, for example: G. Briegleb, and J. Kambeitz, Naturwissenschaften, 22, 105 (1934), and the more recent work of H. Murakami, Bull. Chem. Soc. Japan, 26, 441 (1953); 27, 268 (1954) and 28, 577 (1955).

---

normal state of a donor-acceptor complex may be approximately written[14]

$$\Phi_N = a\Phi_o + b\Phi_1$$

where Φ_o is the no-bond WF $\Phi(A,B)$ and may be presumed descriptive of such dipole-induced dipole effects, closed shell repulsions and such perturbation effects of higher order (i.e., London Forces) as occur when the two components are brought together, each in its singlet ground state, to the equilibrium internuclear distance r_{AB}. A is the Lewis Acid and B the Lewis Base. Φ_1 is the singlet dative WF, $\Phi(A^- - B^+)$, which includes the effect of attractive ionic forces, chemical bonding between the odd electrons, etc. We choose to ignore other structures such as $A^{*+}\!\!-\!\!B^-$ or $A^{+}\!\!-\!\!B^{*-}$, where the star implies excited states of either

A^+ or B^-, which may contribute to Φ_N or Φ_E, also.[16]

---

16) However, in the future in expanding Φ_0 or Φ_1 in terms of MO's we will consider these MO's as the one electron eigenfunctions of the Hamiltonian for either TNB alone or anthracene alone. This is done to facilitate symmetry considerations, and is not expected to introduce any error.

The WF of the charge-transfer excited state is now

$$\Phi_E = a^*\Phi_1 - b^*\Phi_0$$

where $a^* \simeq a \simeq 1$, and where $b^* \simeq b$ is very nearly zero.

The existence of a new absorption band characteristic of the complex alone and corresponding to the transition $\Phi_E \leftarrow \Phi_N$ (or E ← N absorption) can now be predicted. This absorption, despite the small resonance effect, can be expected to be intense because of the large transition moment lengths associated with it.

The no-bond WF may be written

$$\Phi_0 = (n!)^{-1/2} \left| \varphi_B(1)\,\bar{\varphi}_B(2)\,\varphi_3(3) \cdots \bar{\varphi}_n(n) \right|$$

where n is the total number of electrons in the complex, and the φ's are the MO's, separately normalised. φ_B is the highest energy filled MO of the base and $\varphi_3, \cdots, \varphi_n$ are those MO's of either A or B which are unaffected by the excitation $\Phi_1 \leftarrow \Phi_0$. The bar denotes spin β ; no bar denotes spin α. The dative WF may be written

$$\Phi_1 = (\Phi_I + \Phi_{II}) / (2 + 2S_{AB}^2)^{1/2}$$

where $S_{AB} = \int \varphi_A^* \varphi_B \, d\tau$ and

$$\Phi_I = (n!)^{-1/2} \left| \varphi_B(1) \bar{\varphi}_A(2) \varphi_3(3) \cdots \bar{\varphi}_n(n) \right|$$

Φ_I differs from Φ_0 only in that an electron has been transferred from φ_B to the lowest energy unfilled MO of the acid, φ_A. Φ_{II} differs from Φ_I only in the orbital interchange of φ_A and φ_B.

A triplet state also derives from the charge-transfer process, again describable approximately as

$$\Phi_2(M_S = 0) = (\Phi_I - \Phi_{II}) / (2 - 2S_{AB}^2)^{1/2}$$

where M_S=0 indicates this to be the component of the triplet state with spin component zero. In the cases we consider, the three components will be approximately degenerate. Φ_2 will not interact with Φ_0 because of spin-orthogonality.

A certain similarity between the formalism used here to describe the charge-transfer state and the simple Heitler-London treatment of Li_2 is to be noted. Our basis is MO's rather than AO's, yet the neglect of the core interactions in Li_2 is comparable to the neglect of all electron interactions in the complex except those in φ_A or φ_B. In the case of weak interactions this neglect is expected to be quite valid, and it is on this basis that the triplet state (^3E) is drawn higher in energy than the ^1E state in Figure 2.

Let us consider anthracene-TNB in particular. The three components of the presumed no-bond state of the complex which arises from the $^3B_{2u}(D_{2h})$ state of anthracene and the $^1A_{1g}(D_{3h})$ ground state of TNB may be written

$$\Phi_3(M_S=0) = (\Phi_{III} - \Phi_{IV}) \Big/ (2 - 2S^2_{BB'})^{1/2}$$

where $S_{BB'} = \int \varphi_B^* \varphi_{B'} d\tau$ and

$$\Phi_{III} = (n!)^{-1/2} \left| \varphi_B(1)\, \overline{\varphi}_{B'}(2)\, \varphi_3(3) \cdots \overline{\varphi}_n(n) \right|$$

and differs from Φ_{IV} only in the orbital interchange of φ_B and $\varphi_{B'}$. φ_B and $\varphi_{B'}$ are the two unfilled MO's of that configuration of anthracene which gives rise to the $^3B_{2u}$ state. A knowledge of the geometry of the complex is necessary before we can say what symmetry species Φ_3 belongs to. In any case Φ_2 will not interact with Φ_3 unless Φ_3 is totally symmetric with respect to the point group of the complex.[17] It is expected that these two

---

17) This assertion is true only if we presume the ionic — no-bond resonance necessary for complex formation.

---

triplet states will be important in considerations of energy degradation. There is a corresponding singlet state of the complex given by

$$\Phi_4 = (\Phi_{III} + \Phi_{IV}) \Big/ (2 + 2S^2_{BB'})^{1/2}$$

It is of energy 26700 cm^{-1} when the complexing co-ordinate is infinity.[18] It should be noted that there is no a priori

18) E. Clar and Ch. Marschalk, Memoires Presentes a la Societe Chimique, 17, 434 (1950).

reason why the WF's Φ_3 and Φ_4 should be of no-bond type. They are such only because we assume no unpairing of the TNB electrons. This assumption is probably not quite true.

The energies of the combinations A,B , A,B ($^3B_{2u}$) and A,B ($^1B_{2u}$) at $\gamma_{AB}=\infty$ are known experimentally. Thus, if the minimum in the potential energy curve of the ground state of the complex is designated the zero of energy, the energy of A,B is[11] 1540 cm^{-1}, of A,B ($^3B_{2u}$) 16470 cm^{-1} and A,B ($^1B_{2u}$) 28240 cm^{-1}. The energy of the A^-,B^+ combination at $\gamma_{AB}=\infty$ is approximately 55500 cm^{-1}, a value which may be arrived at in two ways. Thus from the ionisation potential[19] of 7.83 ev., and an estimate of 1.1 ev. for

19) N. S. Hush and J. A. Pople, Trans. Faraday Soc., 51, 600 (1955).

the electron affinity of TNB (see appendix) we obtain a value of 55640 cm^{-1}. Conversely, we may work backward. The position of the charge-transfer state, ^1E, is 22300 cm^{-1}; the electrovalent attractive force between the two ionic species in the ^1E state as estimated from the orbital charge

distributions in TNB^- and in the anthracene cation is 3.4 ev. (γ_{AB} = 3.5 Å); the overlap[20] of two $2p_z$ orbitals at a distance of centers of 3.5 Å is $S(2p_z, 2p_z) = 0.09$, leading to a covalent binding energy for six such orbital pairs of about 0.5 ev.; in this manner a value of 54000 cm^{-1} is obtained for the energy of A^-, B^+.

20) R. S. Mulliken, C. A. Rieke, D. Orloff and H. Orloff, J. Chem. Phys., 17, 1248 (1949). Self-consistent-field $2p_z$ AO overlap integrals were used. These SCF AO's give quite different, and presumably better S values than the corresponding Slater AO's, at large γ_{AB} distances.

It now remains to introduce symmetry considerations. Two possible highest symmetry structures are envisaged for the complex. These are of sandwich type with the planes of the both partners parallel because of the dipole—induced-dipole orientation effects. They belong to point groups C_{1h} and C'_{1h}, respectively (see Table I.). The axes are defined in Figure 1. The ground state of TNB^- (see appendix) is $^2E''$ in D_{3h}, and that of the anthracene cation is $^2B_{2g}$ in D_{2h}. These transform as follows:

$^2E''$ (D_{3h}); $^2A'$, $^2A''$ $(C_{1h}$ or $C'_{1h})$

$^2B_{2g}$ (D_{2h}); $^2A'(C_{1h})$, $^2A''$ (C'_{1h})

in the point group defined by the complex. The lowest excited states of anthracene $^{1,3}B_{2u}$ (D_{2h}) transform as $^{1,3}A''$ (C'_{1h}). The lowest excited singlet state of TNB of n,π^* type is either $^1A'$ or $^1A''$ (C'_{1h}).

TABLE I

Point Groups Defined

C_{1h}	E	z,x	axes	C'_{1h}	E	z,x	axes
A′	1	1	z,x	A′	1	1	z,y
A″	1	-1	y	A″	1	-1	x

Using the above energy and symmetry considerations we have plotted Figure 2 for the anthracene-TNB complex belonging to point group C'_{1h}. A number of points are to be noted. Potential crossing occurs between the $^3N^*$ ($^3A''$) state which correlates with $^3B_{2u}$ of anthracene, and the ^1E state which is shown correlating with $^2B_{2g}$ of B^+. Thus immediately following the charge-transfer ($E \leftarrow N$) absorption, process (i), energy should revert by intersystem crossing from the ^1E ($^1A'$) state of the complex to the $^3N^*$($^3A''$) state. The vibrational energy of this state is now greater than its dissociation energy; accordingly production of free anthracene in its $^3B_{2u}$ state and of free TNB in its ground state should occur rather rapidly after crossover. The phosphorescence emission of anthracene, $^3B_{2u} \rightarrow {}^1A_{1g}$, should then occur with practically the same lifetime as that of pure anthracene. This is denoted process (iii) in Figure 2. This intersystem conversion of energy competes of course with the emission process (ii), which is a charge-transfer fluorescence. We thus conclude that immediately following excitation in the $E \leftarrow N$ band, there should occur not only a strongly allowed fluorescence (ii), but also the lowest energy $T \rightarrow S$ emission (iii) of the uncomplexed anthracene. These conclusions accord well with experiment. The slight diffuseness of the phosphorescence may be due to some vibrational inactivation of the $^3N^*$ ($^3A''$) state of the complex, and consequent emission before dissociation.

It is perhaps appropriate to make the following point here. If ionic—no-bond resonance is a primary stabilizing effect in the ground state of the complex, the charge-transfer state must be of the totally symmetric species. This condition can be fulfilled for any 1:1 complex of anthracene since the maximal geometric symmetry is so low. It will not, however, be generally the case for complexes where higher geometric symmetries are possible (cf. benzene-Cl_2). In this particular instance the maximal geometric symmetry will be limited by the necessity of resonance. However, any configuration of lesser symmetry, where permitted, can exist. All that the resonance condition implies is a knowledge of the higher geometries possible. All other appropriate geometric configurations will exist to some extent in thermodynamic equilibrium.

Benzene-TNB Complex. - The maximal geometric symmetry is C_{3v}. The ground states of TNB^- and the benzene cation transform as

$$^2E''\ (D_{3h});\ ^2E(C_{3v})$$

$$^2E_{1g}\ (D_{6h});\ ^2E(C_{3v})$$

Geometry C_{3v} is thus quite allowed by the ionic—no-bond resonance condition. The lowest triplet state of benzene, $^3B_{1u}(D_{6h})$ or $^3A_1(C_{3v})$, lies at 30574 cm^{-1}. The $E \leftarrow N$ transition is of energy 33300 cm^{-1}. The lowest singlet state of TNB (n,π^* type) is at energy higher than 25000 cm^{-1} and can

be of species E, A_1 or A_2 in C_{3v}. Consequently, since incipient crossing of either of the potential curves correllating with $A^*(^1E)$,B or $A^*(^1A_2)$,B can occur with the charge-transfer potential curve, energy transfer should occur to some extent to yield TNB in an excited singlet state. However, TNB does not fluoresce or phosphoresce, this probably being due to energy localisation in, and subsequent disruption of, the aryl-NO_2 bond[21] (for which $D_E \simeq 58$ Kcal/mole).

---

21) Th. Förster, "Fluoreszenz Organischer Verbindungen," Vandenhoeck and Ruprecht, Göttingen (Germany), 1951, p. 117f.

Th. Förster, Z. Electrochem., 56, 716 (1952).

E. Lippert, Z. Physik. Chem. (Neue Folge), 2, 5, 328 (1954), J. phys. radium, 15, 627 (1954).

The emission properties of benzene-TNB have not thus far been investigated. It should prove valuable, since if any emission is observed it will be explicable only by competition of processes (ii) or (iii) with the aryl NO_2-bond dissociative process.

Naphthalene-TNB, Naphthacene-TNB and Phenanthrene-TNB Complexes. - These complexes can belong to point groups C_{1h}, C'_{1h}, or lower. Since the E ⟵ N absorption of the naphthalene-TNB complex is at 27600 cm^{-1}, energy localisation in the aryl-NO_2 bond may compete with the E ⟶ N and T ⟶ S processes. However, we have observed both of these latter emissions.[22]

22) R. V. Nauman and C. Garrett, in this laboratory, have observed two emissions from thianaphthene-TNB complex. One is a fluorescence (presumably E⟶N), the other a phosphorescence probably of the thianaphthene. Excitation was selective, but the phosphorescence was not photographed.

The E⟵N absorption of naphthacene-TNB should occur at 17500 cm^{-1}, somewhat lower in energy than the 2nd excited triplet state of naphthacene at 19600 cm^{-1}. Accordingly, excitation in the charge-transfer band might afford a means of excitation of the lowest triplet state of naphthacene which has been observed in absorption at 10250 cm^{-1} but which has not yet been detected in emission.[3,23]

23) S. P. McGlynn and M. Kasha, in preparation for publication

ACKNOWLEDGMENT

Much of the work reported here was initiated by Michael Kasha. We are grateful for his advice and criticism. We also thank Professor R. S. Mulliken and Professor W. T. Simpson for many helpful suggestions and comments.

APPENDIX

(A) ENERGIES OF CATACONDENSED CATIONS.-- This question may be approached by the perimeter method of Mofitt.[24] We consider a cyclic polyene of general formula $C_{4\nu+2}H_{4\nu+2}$. The carbon atoms are numbered serially from 0 to $4\nu+1$ on going around the ring, with carbon zero on the y axis. The MC's may be specified immediately as linear combinations of $2p\pi$ carbon AO's X_k

$$\varphi_j = \sigma_j \sum_{k=0}^{4\nu+1} e^{2\pi i jk/4\nu+2} X_k \quad , \quad j = 0, \pm 1, \cdots, \pm 2\nu, 2\nu+1$$

The one electron energy ϵ_j associated with φ_j is a monotonically increasing function of j with $\epsilon_j = \epsilon_{-j}$. We may thus specify two isoenergetic electron configurations for the cyclic polyene $C_{4\nu+2}H^+_{4\nu+2}$. These are $^2\Theta_1$ and $^2\Theta_2$, two of the interacting components of which are

$$^2\Theta_1^{\alpha} = |\cdots \varphi_{+\nu}(1)\,\bar{\varphi}_{+\nu}(2)\,\varphi_{-\nu}(3)|$$

$$^2\Theta_2^{\alpha} = |\cdots \varphi_{-\nu}(1)\,\bar{\varphi}_{-\nu}(2)\,\varphi_{+\nu}(3)|$$

To complete the distortion of the $D_{(4\nu+2)h}$ polyenic cation to the point group of the cation of interest we make use of the one electron Hermitian operators

$$P = \sum_{j=1}^{4\nu+1} h_j$$

The first order interaction matrix is

$$\begin{vmatrix} {}^2\Theta_1 & q - h_{-\nu,-\nu} & -h_{\nu,-\nu} \\ {}^2\Theta_2 & -h_{-\nu,\nu} & q - h_{\nu,\nu} \end{vmatrix} = 0$$

The configurational splitting is then $2|h_{\nu,-\nu}|$, where q is the diagonal element corresponding to the first order ground state of the non-ionized polyacene in the matrix representing the perturbation

$$P' = \sum_{j=1}^{4\nu+2} h_j$$

The ground state WF is given by

$${}^2\Theta_G = 1/\sqrt{2}\left({}^2\Theta_1 - (-1)^{\nu}\,{}^2\Theta_2\right)$$

and the excited state by

$${}^2\Theta_E = 1/\sqrt{2}\left({}^2\Theta_1 + (-1)^{\nu}\,{}^2\Theta_2\right)$$

The transformation properties of these states of the cations are easily derived from those in the $D_{(4\nu+2)h}$ point group. These are given in Table II for appropriate operations.

On this basis the cations of naphthalene, anthracene, naphthacene and phenanthrene have ground states of species ${}^2A_{1u}(D_{2h})$, ${}^2B_{2g}(D_{2h})$, ${}^2A_{1u}(D_{2h})$ and ${}^2B_2(C_{2v})$, respectively. The configurational splitting in the case of the linear polyacenes is given by $(2\nu-2)\beta/(2\nu+1)$, and for

phenanthrene is 0.127 β , where β is the resonance integral.

The following quantities are defined:

$$h_{\nu,\nu} = \frac{\beta}{2\nu+1} \sum_{m} \sum_{n>m} \cos\left[\pi(n-m)\nu/(2\nu+1)\right] = h_{-\nu,-\nu}$$

$$h_{\nu,-\nu} = \frac{\beta}{2\nu+1} \sum_{m} \sum_{n>m} e^{-\left[\pi i(n+m)\nu/(2\nu+1)\right]} = h^{*}_{-\nu,\nu}$$

The summation extends in each case over pairs of serial numbers between which bonds are formed in the distortion process. Thus for anthracene (Figure 1), there are two terms in the summation: $m = 1$, $n = 6$ and $m = 8$, $n = 13$.

(B) THE RELATION OF E←N TRANSITION ENERGY TO IONIZATION POTENTIAL FOR AROMATIC — TNB COMPLEXES.-- A linear relation between the ionisation potential of the base and $\overline{\nu}_{max}$ of the E←N transition is a general characteristic of charge-transfer complexes of the same acid with different bases.[25] It is to be noted that this linearity has very little basis in theory[26] and that many experimental deviations

25) S. H. Hastings, J. L. Franklin, J. C. Schiller and F. A. Matsen, J. Am. Chem. Soc., 75, 2900 (1953).

26) R. S. Mulliken, Rec. trav. chim., 75, 845 (1956).

TABLE II

Transformation Properties of Configurational and State WF's

	Θ_1	Θ_2	Θ_N	Θ_E
σ_{yz}	Θ_2	Θ_1	$-\Theta_N$	$(-1)^{\nu}\Theta_E$
σ_{xz}	$(-1)^{\nu}\Theta_2$	$(-1)^{\nu}\Theta_1$	$(-1)^{\nu+1}\Theta_N$	$(-1)^{\nu}\Theta_E$
σ_{xy}	$-\Theta_1$	$-\Theta_2$	$-\Theta_N$	$(-1)^{\nu+1}\Theta_E$

from it have been noted.[27] However, within a group of

27) C. Reid and R. S. Mulliken, J. Am. Chem. Soc., 76, 3869 (1954); S. Nagakura, ibid., 80, 524 (1958).

closely related donors, especially when the ionisation potential (I_p) range spanned is relatively small, linearity is not entirely unexpected.

Unfortunately experimental values of I_p are not known for many aromatics. They may be evaluated readily in terms of the discussion of (a); however we choose to use the "better theoretical" values of Hush and Pople.[19] These are plotted against $\bar{\nu}_{max}$ in Figure 3. The excellent linearity obtaining, affords good confirmatory support of the charge-transfer origins of this absorption band.

(C) SYM-TRINITROBENZENE AND ITS CONJUGATE ANION. -- The π-group orbitals (GO's) of the hexagonal carbon skeleton of TNB are just the π-MO's of benzene. The NO_2 groups are each replaced by a negative carbon atom C^- as the initial step in the calculations. In the sense of the skeletal carbon atoms these C^- atoms are not nearest neighbours, and the two GO's embracing these centers are energy degenerate. The GO's embracing the skeleton and those of the C^- system are symmetrically disposed energy-wise with respect to the group theoretic species (in D_{3h} only) and energy. Interaction will then be to a first approximation also symmetric.

Efforts were made to take account of the inductive effect due to the difference in field of NO_2 as compared to C^-, and of the resonance effect due to the π-orbital extension. Constants involved were evaluated from a postulated spectroscopic assignment of the electronic transitions of TNB and an ionization potential. This assignment was itself tenuous, and the value of 2.1 ev. for the electron affinity of TNB can be questioned.

The ground configurations of TNB and TNB^- are believed accurately given by

$$\ldots\ldots (a_2'')^2 (e'')^4 (a_2'')^2 (e'')^4, \; {}^1A_1 \text{ and}$$

$$\ldots\ldots (a_2'')^2 (e'')^4 (a_2'')^2 (e'')^4 (e'')^1, \; {}^2E'',$$

respectively.

Figure 1.- The two highest geometrically symmetric forms of the anthracene-TNB complex are depicted in (a) and (b). The heavy lines in the case of (a) merely indicate the positioning of TNB directly above, the central hexagon of anthracene. The choice of axes in (c) is that of McClure, Craig, Ross and Sponer, and is to be distinguished from that of Moffitt and Platt.

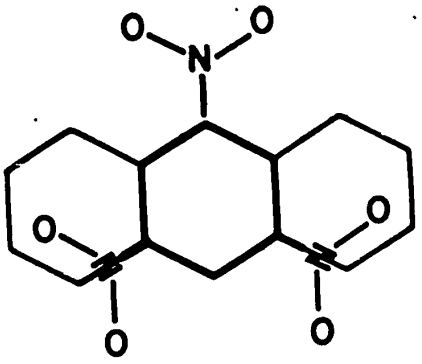

(a) C'_{1h}

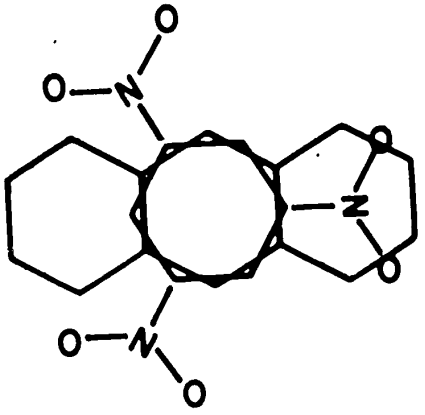

(b) C_{1h}

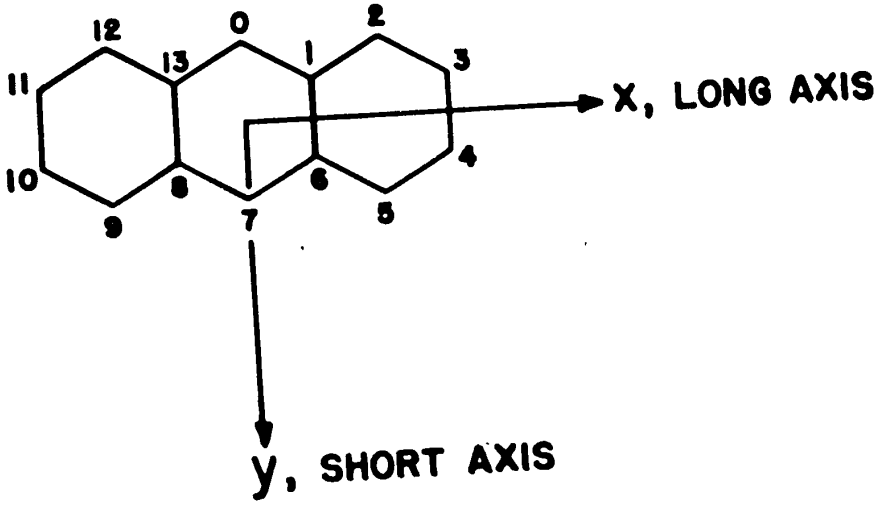

(C) AXES AND NUMBERING

Figure 2.- A correlation diagram for the electronic states of the anthracene-TNB complex - for which geometry C_{1h}' is assumed. A refers to Lewis acid, B to Lewis base. Symmetries of the excited states for each of the three species present are shown in columnar form under the appropriate point group symbol. Text should be consulted for more detail.

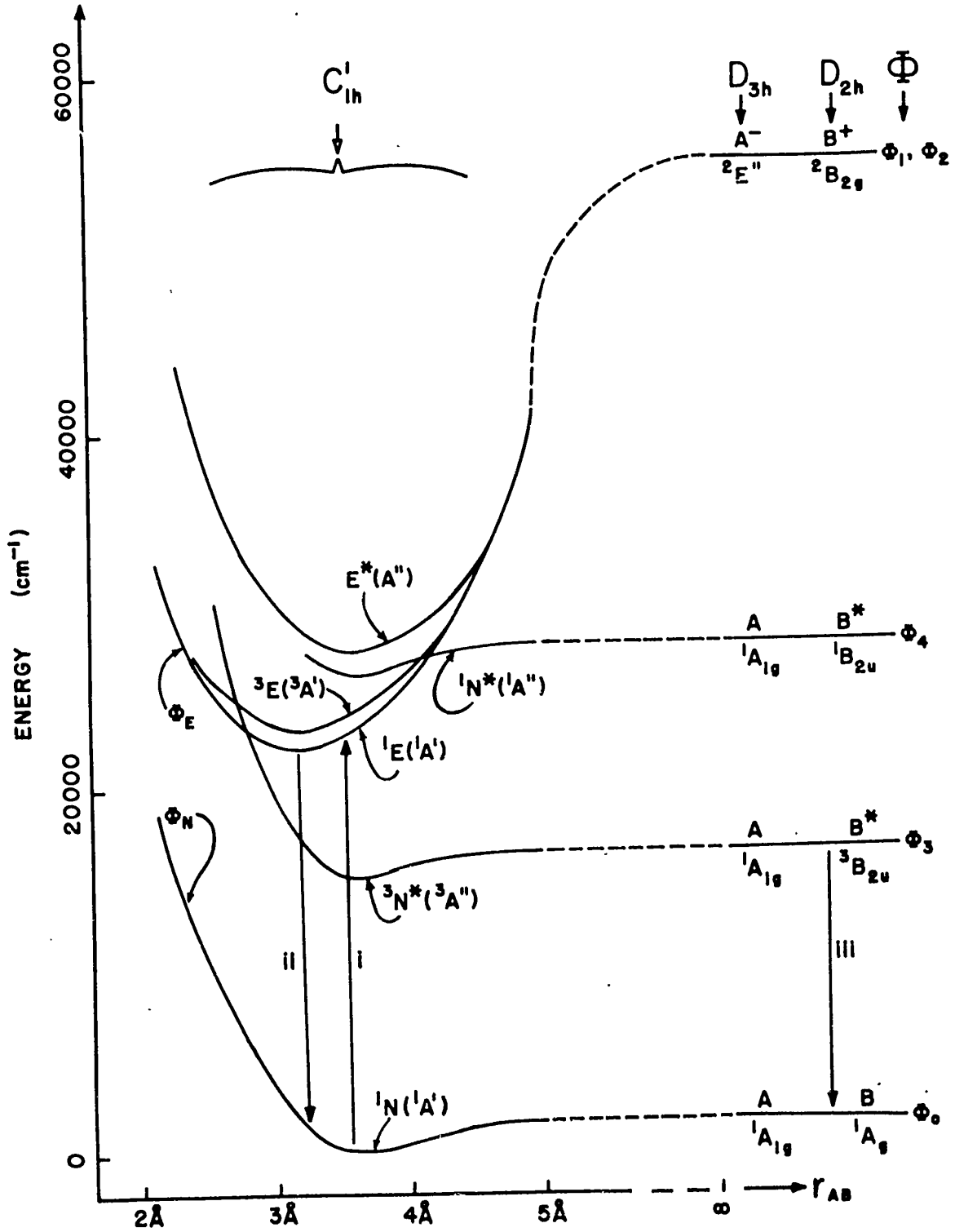

Figure 3 - A plot of $\overline{\nu}_{max}$ of the E←N absorption band of the complex versus the ionisation potential of the base. The values of $\overline{\nu}_{max}$ used are from the present work except that for benzene-TNB, which is taken from D. M. G. Lowrey and H. McConnell, J. Am. Chem. Soc., 74, 6175 (1952).

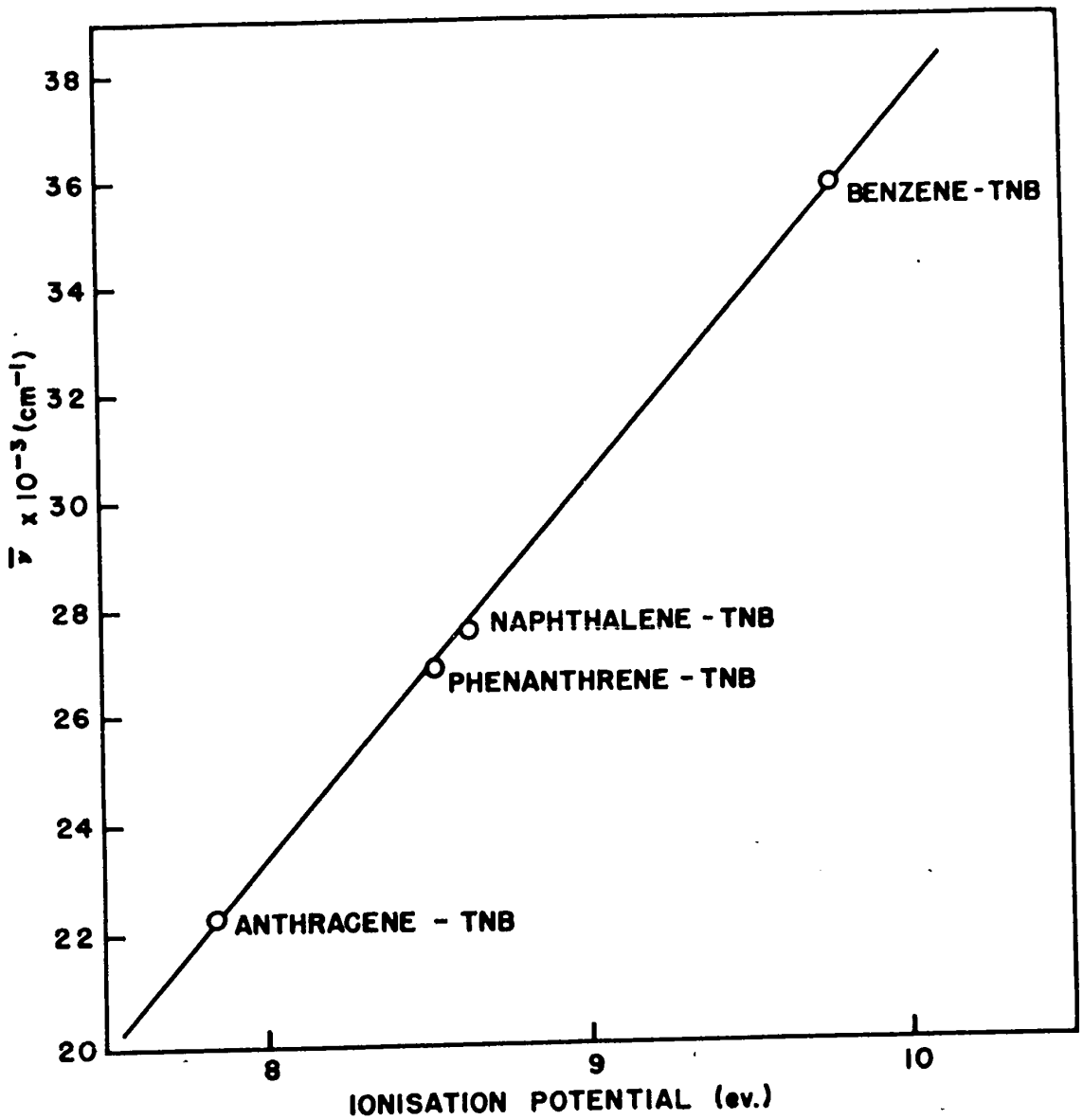

STAT

Next 5 Page(s) In Document Denied